ISTANBUL TECHNICAL UNIVERSITY ★ GRADUATE SCHOOL OF SCIENCE ENGINEERING AND TECHNOLOGY

EFFECTS OF GRADATION, FINES CONTENT AND SILT SHAPE CHARACTERISTICS ON STATIC LIQUEFACTION OF LOOSE SANDS

Ph.D. THESIS

Ehsan ETMINAN

Department of Civil Engineering

Soil Mechanics and Geotechnical Engineering Programme

AUGUST 2016

ISTANBUL TECHNICAL UNIVERSITY ★ GRADUATE SCHOOL OF SCIENCE ENGINEERING AND TECHNOLOGY

EFFECTS OF GRADATION, FINES CONTENT AND SILT SHAPE CHARACTERISTICS ON STATIC LIQUEFACTION OF LOOSE SANDS

Ph.D. THESIS

Ehsan ETMINAN
(501122301)

Department of Civil Engineering

Soil Mechanics and Geotechnical Engineering Programme

Thesis Advisor: Assoc.Prof. Aykut ŞENOL
Thesis Co-Advisor: Assoc.Prof. M. Murat MONKUL

AUGUST 2016

İSTANBUL TEKNİK ÜNİVERSİTESİ ★ FEN BİLİMLERİ ENSTİTÜSÜ

DANE DAĞILIMI, İNCE DANE ORANI VE SİLT DANE ŞEKİL ÖZELLİKLERİNİN KUMDAKİ STATİK SIVILAŞMA DAVRANIŞINA ETKİSİ

DOKTORA TEZİ

Ehsan ETMINAN
(501122301)

İnşaat Mühendisliği Anabilim Dalı

Zemin Mekaniği ve Geoteknik Mühendisliği Programı

Tez Danışmanı: Doç. Dr. Aykut ŞENOL
Eş Danışman: Doç. Dr. M. Murat MONKUL

AĞUSTOS 2016

Ehsan ETMINAN, a Ph.D. student of ITU Graduate school of Science Engineering and Technology student ID 501122301, successfully defended the thesis entitled “EFFECTS OF GRADATION, FINES CONTENT AND SILT SHAPE CHARACTERISTICS ON STATIC LIQUEFACTION OF LOOSE SANDS”, which he prepared after fulfilling the requirements specified in the associated legislations, before the jury whose signatures are below.

Thesis Advisor :	**Assoc.Prof. Aykut ŞENOL** Istanbul Technical University	....
Co-advisor :	**Assoc.Prof. M.Murat Monkul** Yeditepe University	....
Jury Members :	**Prof. Dr. Musaffa Ayşen Lav** Istanbul Technical University	....
	Assoc.Prof. M. Kubilay Keleşoğlu Istanbul University	....
	Assis.Prof. Berrak Teymür Istanbul Technical University	....
	Assis.Prof. Esra Ece Bayat Istanbul Technical University	....
	Assis.Prof. Zehra Nil Taylan Kutlu Maltepe University	....

Date of Submission : 02 August 2016
Date of Defense : 12 August 2016

To my parents,

FOREWORD

First and foremost, I wish to thank to the respectful members of Geotechnical Department of Istanbul Technical University and Civil Engineering Department of Yeditepe University for giving me the opportunity to study and work on my Ph.D. thesis. Also, it was my honor to conduct this research under the guidence of my advisors, Dr. Aykut ŞENOL and Dr. Mehmet Murat MONKUL who were great mentors and spent their valuable time on my thesis, guided me throughout my study and shared their knowledge with me. I have achieved so much in so little time with their support, for which I am very grateful.

I also would like to thank my committee members Dr. Musaffa Ayşen Lav, Dr. Ece Eseller-Bayat and Dr. Mustafa Kubilay Keleşoğlu for their guidence and suggestions during my thesis.

Moreover, experimental programme of this study was supported by European Union's 7th Research Framework Programme (FP7) under project number 303974. Grateful appreciation is expressed for this support. I also want to thank to Dr. Mustafa Çulha from Nanobiotechnology Center of Yeditepe University for his help in providing the Optical Microscope and SEM images.

I want to extend my thanks to Res. Assist. Feyzullah GÜLŞEN, Res. Assist. Mehmet ADA, Dr. Tolga Y. ÖZÜDOĞRU, Dr. Mustafa HATIPOĞLU and Res. Assist. Sinan SARGIN for their valuable advices and also friendship during my long PhD journey.

Finally, I want to thank to my beloved parents for their moral support and I would like to dedicate this thesis to them. They, more than anyone else, have been the best role models I could have hoped for. Any accomplishments of mine are due to their support. They are the joy of my life.

August 2016

Ehsan ETMINAN
(Civil Engineer)

TABLE OF CONTENTS

Page

ABBREVIATIONS

1-D	**:** One dimesional
2-D	**:** Two dimesional
3-D	**:** Three dimesional
CU	**:** Consolidated undrained triaxial compression test
D_r	**:** Relative density
FC	**:** Fines content
FC_t	**:** Transition fines content
G_s	**:** Specific gravity
MT	**:** Moist tamping method
R	**:** Roundness
S	**:** Sphericity
SD	**:** Slurry deposition method
SEM	**:** Scanning electron microscopes
SSL	**:** Steady state line
WP	**:** water pluviation method
WS	**:** water sedimentation method

SYMBOLS

μ	: micron
$C_{U\text{-}sand}$	: Coefficient of uniformity of sand
$C_{U\text{-}silt}$	: Coefficient of uniformity of silt
$D_{50\text{-}sand}$	: Mean grain diameter of sand
$d_{50\text{-}silt}$	: Mean grain diameter of silt
e_{max}	: Maximum void ratio
e_{min}	: Minimum void ratio
e_s	: Intergranular void ratio
m_v	: Volumetric compressibility
p'	: Mean effective stress
q	: Deviator stress
q_{peak}	: Peak deviator stress
ε_a	: Axial strain
ε_v	: Volumetric strain
σ'_{3c}	: Effective Confining stress
ϕ_{cs}	: Critical state friction angle

LIST OF TABLES

Page

LIST OF FIGURES

Page

FFECTS OF GRADATION, FINES CONTENT AND SILT SHAPE CHARACTERISTICS ON STATIC LIQUEFACTION OF LOOSE SANDS

SUMMARY

Static liquefaction remains to be a challenging problem of geotechnical engineering as its consequences are generally catastrophic when occurred on site. Previous laboratory studies focused on various factors that could influence the static liquefaction potential of silty sands. Most popular of those investigated factors are stress conditions, deposition method and fines content. Regarding the behavior of clean sands, possible influence of grain size distribution or sand grain shape on liquefaction response had also attracted the attention of a limited number of researchers. However, very little is known about how gradation influences the liquefaction response of sands involving silt fractions. Furthermore, the possible effects of shape characteristics of silt grain matrix within sand, during undrianed monotonic loading, were unknown. The purpose of present study is to investigate the influence of several factors including fines content, base sand gradation, silt gradation, overall gradation and silt grain shape on static liquefaction of sands and finally volumetric compressibility, as an indicator of liquefaction potential of silty sands. Three base sands with same geologic origin but with different gradations (Sile Sands 20/30, 50/55 and 80/100) and three different non-plastic silts (TT, SI and IZ silts) with different gradations and shape characteristics were mixed and tested at four fines contents (i.e. FC=0, 5, 15, 25%). The experimental results revealed that each of the mentioned factors had their own influence on static liquefaction behavior of sands. Results of undrained monotonic triaxial compression tests showed that liquefaction potentials of Sile Sands have systematically increased with increasing fines content within the studied range (for FC≤25%). At low fines contents (i.e. FC≤ 15%), the greater and more uniform IZ silt made three base sands more liquefiable compared to other two silts. Therefore, the general trend was that the liquefaction potential of silty sands increased as the mean grain diameter ratio ($D_{50\text{-}sand}/d_{50\text{-}silt}$) decreased (when D_r, FC, initial stress conditions, base sand gradation and mineralogy were kept the same). However, there was an exception for the specimens involving TT silt versus SI silt. After the grain shape characterization of three silt types, it was discovered that the angular nature of TT silt and the resulting meta-stable grain contacts were responsible for that exception. It was also found that the impact of gradation parameters ($C_{U\text{-}silt}$, $d_{50\text{-}silt}$) and shape characteristics (roundness, sphericity) of silt grain matrix on liquefaction potential of Sile Sands was found to be dependent on the amount of fines content. In another words, their impact gradually diminished for FC≥15%. When clean Sile Sands were tested, it was observed that the liquefaction resistance of base sands slightly decreased as the sand became finer and relatively uniform (e.g. Sile Sand 80/100 had the lowest liquefaction resistance). However, when silts were added to the sands the order of liquefaction resistance had been reversed (i.e. specimens with the larger and relatively well graded Sile Sand 20/30 suddenly had the least liquefaction resistance for all three silt types). Possible reason was expressed to be the different levels of gap gradations in specimens induced by the base sand

gradation. It was shown that soils with similar C_U could have very different liquefaction resistances, whereas soils with very different C_U could have similar liquefaction potentials. Therefore, C_U by itself cannot be an indicator of liquefaction behavior because of the many factors investigated in this study.

In other part of the study, the relationship between the normalized peak deviator stress (q_{peak}/σ'_{3c}) and coefficient of uniformity (C_U) is discussed. With respect to outcomes, intrestingly, it was shown that unlike clean sands, for which liquefaction potential decreases with increasing C_U, the liquefaction potential of sand-silt mixtures reconstituted in the laboratory increases with increasing coefficient of uniformity (i.e. technically as they became more well graded). Two equations were proposed to represent the discussed relationship between q_{peak}/σ'_{3c} and C_U; one for stable and temporarily liquefied specimens, the other for liquefied specimens. Then, the applicability of these equations to other types of silty sands in literature was illustrated.

As the last part of experiments, volumetric compressibilty of three used base sands and mixtures of Sile Sand 80/100 with TT silt and IZ silt has been investigated. In fact, to evaluate the liquefaction potential for silty sands, a quantity that may be used as an indicator and can be measured in-situ is the volume compressibility. The more compressible the easier the soil will liquefy. Analysis of performed experiments have shown that volumetric compressibilities increase with increasing fines content for silt types, which is similar to the observation of increasing liquefaction potential with fines content. Approximate boundaries for stable response, transition stage, and liquefaction region are determined. Accordingly, specimens with volumetric compressibility values smaller than 0.17 (1/MPa) were stable, while all specimens with volumetric compressibility values greater than 0.23 (1/MPa) liquefied. It should be noted that further laboratory and in-situ tests on different sand and silt types are still needed to verify and tune those boundaries, which could potentially serve as indicators of liquefaction potential via in-situ compressibility tests.

The dissertation includes literarure review on the liquefaction and specially static type of liquefaction phenomena which includes basic theoris of them. Then, index properties of the soils used during experimental program, and experimental programs are discussed in details. The following two chapters refers to evaluation of tests' outcomes from different aspects. Finally, all of conducted tests' results and suggestions for future studies have discussed in conclusion chapter.

DANE DAĞILIMI, İNCE DANE ORANI VE SİLT DANE ŞEKİL ÖZELLİKLERİNİN KUMDAKİ STATİK SIVILAŞMA DAVRANIŞINA ETKİSİ

ÖZET

Zemin sıvılaşması, geoteknik mühendisliğinin en önemli olgularından biri olup, çeşitli dinamik veya statik yükler neticesinde, özellikle kumlu zeminlerde, çeşitli problemlere yol açabilmektedir. Zemin sıvılaşması modern geoteknik mühendisliğinin son elli yılı gözönüne alındığında en çok merak edilen ve araştırılan konulardan birisi olma özelliğini halen korumaktadır. Bunun en önemli sebebi; ister statik ister dinamik yükler etkisinde gerçekleşsin, sıvılaşmanın sonuçlarının çoğu zaman, ekonomik ve sosyal anlamda önemli kayıplara neden olmasıdır. Bu sebeple, özellikle silt ve kil gibi ince dane içeren kumlu zeminlerin, sıvılaşma davranışı laboratuvar ortamında, ince dane içeriği, plastisite vb... gibi çeşitli parametreler kontrol altında tutularak incelenmeye devam edilmektedir. Her ne kadar SPT, CPT ve kuyu yöntemi kullanarak, kayma dalgası hızı belirleme gibi arazi deneyleri ile sismik yükler altında sıvılaşma potansiyeli tahmini yapılabilse de, statik yükler altında sıvılaşma potansiyelinin belirlenmesi için benzer arazi deneylerine dayanan bir yöntem bulunmamaktadır. Bu sebeple kumlu zeminlerden oluşan setler, dolgular, kıyı ve liman zeminleri, sualtı şevleri ve hidrolik dolgular vb... gibi mühendislik yapılarının statik yükler altında sıvılaşma potansiyellerinin belirlenmesi için drenajsız üç eksenli basınç deneyi yapılması gerekmektedir.

Başlangıçta sıvılaşma vakalarının, kumlu zeminde meydana geldiğini kabul ederek, araştırmacılar laboratuvarda bu tür zeminlerin davranışlarını belirlemek üzere çeşitli deneyler yapmışlardır. Ancak, saha çalışmaları ve vaka analizleri, sıvılaşabilen suya doygun gevşek kumlu zeminin bir çoğunun çeşitli oranlarda silt muhteva ettiğini göstermiştir. Bu gözlemler sonucu, çeşitli parametrelerin kontrol edilmesine dayanan laboratuvar çalışmaları hız kazanmış ve geoteknik literatüründe, özellikle gerilme koşulları, numunelerin hazırlanması ve ince dane oranının sıvılaşma davranışına nasıl etki ettiği sorgulanmıştır.

Araştırmacıların amacı, söz konusu gerçek arazi gerilme koşullarını, laboratuvar ortamında gerçekleştirmek olmuştur. Ayrıca, kohezyonsuz zeminlerden örselenmemiş numune almak çok kolay olmadığından dolayı, laboratuvarlarda hazırlanan numunelerin, arazi koşullarını ne derece temsil ettiği diğer bir araştırma konusudur. Farklı araştırmacılar tarafından önerilen numune hazırlama yöntemlerinin avantaj ve dezavantajlarını gözönüne alarak, siltli-kum zemin için kuru huni yöntemi ile hazırlanmıştır. Geotenik literatüründe, temiz kumun dane dağılımının ve şekil özellikerinin, sıvlaşma davranışına etkileri, çok az sayıda bilimadamı tarafından araştırılmıştır. Buna rağmen, kumun içinde bir miktar silt olduğunda, dane dağılımının, sıvılaşma sırasında nasıl etkilendiği çok az bilinmekteydi. Ayrıca siltin dane şekil özelliklerinin siltli kumun drenajsız kayma mukavemetine ve sıvılaşma davranışına etkileri bilinemiyordu.

Bu araştırmanın amacı, çeşitli faktörlerin, siltli kumun statik yükler altında sıvılaşma potansiyeline etkilerini incelemektir. Bu faktörler; ince dane oranı, ana kum dane dağılımı, siltin dane dağılımı, siltli kumun dane dağılımı, siltin şekil özellikleri ve zeminin hacimsel sıkışma katsayısıdır.

Çalışma kapsamında, İstanbul'un Şile bölgesinden alınmış, aynı jeolojiye sahip olan fakat farklı dane dağılımlı üç ana kum (Sile Sand 20/30, 50/55 ve 80/100), üç farklı dane dağılım ve şekil özelliklerine sahip, plastik olmayan silt (TT, SI ve İZ silt), çeşitli ince dane yüzdelerinde (%0, %5, %15 ve %25) karıştırılmış ve elde edilen numuneler deney programında kullanılmıştır. Deney programının sonuçlarına göre yukarıdaki faktörlerin hepsi, statik yükler altında sıvılaşma davranışlarına etkili olmuştur. Drenajsız üç eksenli basınç deneyleri sonucunda, tüm numunelerde, ince dane oranın artışı ile, zeminlerin sıvılaşma potansiyelinin sistematik olarak arttığı görülmektedir (ince dane oranın %0 ile %25 arası). Düşük yüzdeli ince dane oranlarında (≤%15) en kaba daneli ve en üniform numune olan İZ silti, diğer siltlere göre, her üç ana kumun daha çok sıvılaşmasına sebep olmuştur.

Bu sebeple, relatif sıkılık, ince dane oranı, gerilme koşulları, kumun dane dağılımı ve minerolojik koşullarının değişmediği deney ortamlarında, ortalama dane çap oranının (D50-kum / d50-silt) azalması ile zeminlerin sıvılaşma potansiyelinin arttığı görülmektedir. Sadece TT silt ile SI silti karşılaştırıldığında, bir farklılık görüldü. Bu sonucu açıklamak amacı ile, SEM ve optik mikroskopları kullanılarak, siltlerin dane şekil özellikleri saptanmıştır. Sonuçlara göre, TT siltinin çok köşeli danelere sahip olduğu ortaya çıkmış ve dolayısıyla TT siltlerinin kum daneleri ile temas noktalarında yarı dengeli (meta-stable) bir yapı oluşturduğu gözlenmiş ve bunun diğer iki silt karışımlarına benzemeyen bir davranış göstermiştir. Bu araştırmanın devamında, siltlerin dane parametreleri ($C_{u\text{-silt}}$ ve $d_{50\text{-silt}}$) ve dane şekil özellikleri (yuvarlaklık ve küresellik) incelenmiştir ve buradan ince dane oranının %15 ve üzeri olduğunda, ince dane üzerindeki etkisinin olmadığı gözlenmiştir. Temiz kumların (%0 ince dane oranı) deney sonuçlarını incelediğimizde, Sile kum 80/100 diğer temiz kumlara göre sıvılaşma direncinin en düşük olduğu ve sistematik olarak Sile kum 50/55 ve 20 / 30 kumlarının sıvılaşma dirençlerinin arttığı gözlenmiştir. Başka ifade ile temiz kumlarda, dane çapları küçüldükçe ve daha üniform hale geldiğinde sıvılaşma potansiyelinin artabilmektedir fakat temiz kuma silti ilave ettiğimizde, bu eğilim tam tersi bir davranış göstermektedir. Deneylerde kullanılan siltler, en kaba daneli olan Sile kum 20/30 a ilave ettiğimizde, bu karışımların hepsisinin sıvılaşma dirençlerinin, diğer karışımlara göre en düşük olduğu görülmektedir. Görülen bu ters davranışın nedenini bulmak için süreksiz bir dane dağılıma sahip olan bir numune hazırlanıp, deneylere tabii tutulmuştur ve bu sonuç kanıtlanmıştır.

Bütün siltli kum karışımları için, dane dağılımları gözönüne aldığında, üniformlük katsayı artışı ile, sıvılaşma direncinin azaldığı görülmektedir. Üniformlük katsayıları çok yakın olan numunelerin de, farklı sıvılaşma direncini gösterdiğini gözlenmiştir. Bu sebeple, sadece üniformlük katsayısı (C_u) sıvılaşma belirticisi etkin bir parametre olarak kullanılamaz.

Çalışmanın diğer bir kısmında, üniformlük katsayısı (C_u) ve normalize edilmis deviatör gerilme arasındaki ilişki incelenmiştir. Bu ilişkiler için iki farklı denklem önerilmiştir. İlki, dengeli ve geçici sıvılaşma davranışı gösteren numuneler için, diğeri ise sıvılaşmış numuneleri kapsamaktadır.

Araştırmanın son kısmında ise tam 6 grup deney numunesi bulunmaktadır. Bunlar üç temiz kum ve Sile kum 80 / 100 numnunesinin 3 faklı silt ile karışımlarıdır. Bunların hacimsel sıkışabilirlikleri incelenmiştir. Siltli kumların arazide sıvılaşma potansiyeli tahmin etmek için hacimsel sıkışma katsayısını kullanmak yeni bir yöntem olarak kabul edilmektedir. Zemin ne kadar sıkışabilirlirse, o kadar sıvılaşma potansiyele sahip olduğu görülmüştür. Araştırmanın sonucunda, hacimsel sıkışma katsayısının, 0.17 (1/MPa) dan düşük olduğunda zeminin sıvılaşmaya karşı dengeli olduğu ve 0.23 (1/MPa) dan büyük olduğunda ise zeminin sıvılaşmış olduğu belirlenmiştir. Gelecekte numune çeşidi ve sayısı arttırılarak bu sonuç daha da irdelenebilir.

1. INTRODUCTION

The concept of liquefaction phenomenon has been an important research area for many years and goes on to be studied by many researchers. In fact, the reason behind this ongoing research is that liquefaction take place very often and when occurred on site, its consequences are generally catastrophic. With respect to previous researchers' efforts, it can be inferred that, many theories have been developed to explain the fundamental causes of why cohesionless soils liquefy. In spite of the fact that there is a general agreement between researchers about general mechanism triggering liquefaction, but there seems to be many contrary opinions about the factors that make certain soils more liquefiable than others. Nowadays, it is well known that liquefaction is the consequence of large excess pore pressure development in loose saturated cohesionless soils, result in lack of effective stress condition that decreases the available shear strength in significant way. The mentioned disagreement among researchers originate in variations of laboratory testing methods such as sample preparation techniques, data interpretations and even terminologies used to explain observed behaviors. It is obvious that each of these variations may have a noticeable influence on end outcomes.

When reviewing previous literature on liquefaction phenomenon, it can be inferred that there is significant variation in terminologies used to define the soil behaviors. Among them, the term liquefaction seems to show the greatest conflicts among researchers when used to express soil behavior, especially for the laboratory experiments. In other words, there have been numerous definitions suggested from different researchers for liquefaction over the years. Then, Youd (1973) distinguished the apparent difference among the existent definitions and tried to present a definition to eliminate this confusion. According to his definition for liquefaction phenomenon, it is the transformation of granular materials from solid state into a liquefied state as a result of increased pore water pressure. Although this definition adequately describes the main concept, but it is not specific enough to distinguish between different types of liquefaction behavior observed in the field or in the laboratory, as a consequence of either monotonic or cyclic loadings conditions. According to the all literature available now, it can be derived that there is no single definition existing which is accurate and versatile enough to explain each type of liquefaction phenomenon, whether it can be complete static liquefaction, temporary or limited liquefaction or cyclic mobility. On the other hand, it seems that by defining each type of liquefaction behaviors individually and completely, the mentioned confusion can be eliminated. With respect to the fact that this thesis mainly concentrates on static liquefaction, hence, definitions of this type of liquefaction will be discussed.

In fact, when discussing static liquefaction, which is a liquefaction as a result of monotonic loading, researchers mainly consider the undrained stress-strain response exhibited in curve A in figure 1-1 to constitute a liquefied condition. In this type of liquefaction, a loss in load carrying capacity of tested sample accompanied by large development of excess pore water pressure. It should be noted that this is not a complete static liquefaction because the deviator stress (q) do not reach the zero value.

Curve B of figure 1-1 represents the response of a complete liquefied specimen. According to the mentioned figure, it can be seen that the principle stress difference (σ_1-σ_3) and effective confining pressure (σ_3') are equal to zero.

Finally, curve C illustrate the response of a specimen which is called either limited liquefaction (Castro 1969, Reimer & Seed 1997) or temporary liquefaction (Yamamoro & Lade 1997). Since most recent researchers use the temporary term for this type of liquefaction, it has been decided to use this term during rest of the thesis. According to this response, specimen first shows contractive tendency, but strength is regained at higher strains.

According to what mentioned above, it can be inferred that the response exhibited in curve A of figure 1-1 is a special case of the temporary liquefaction in which, the residual strength of specimen remained constant. Accordingly, a slightly looser specimen may have shown complete liquefaction behavior, and on the other hand, a slightly denser specimen may have shown true temporary liquefaction response as curve C.

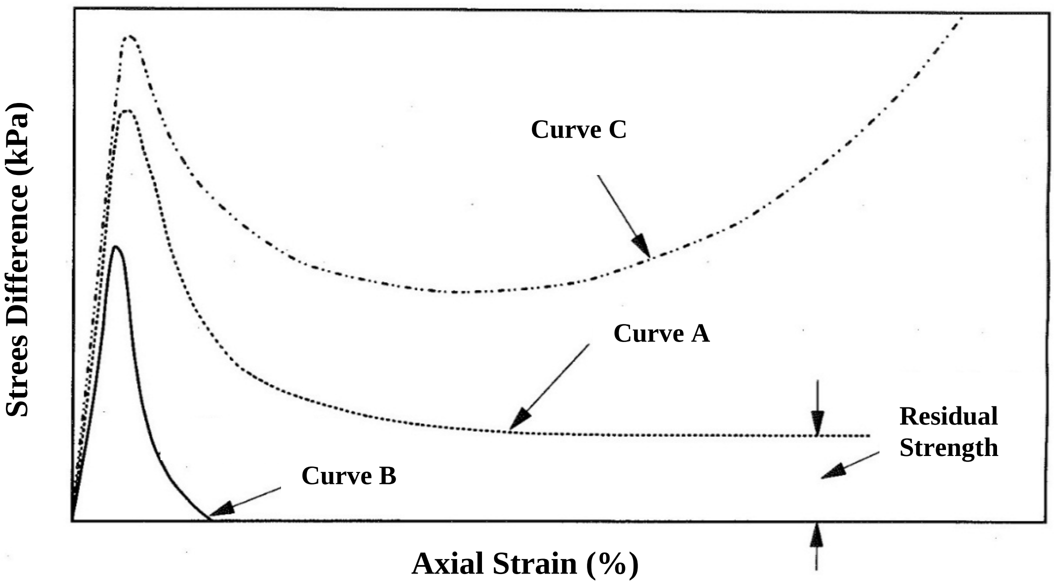

Figure 1.1 : Undrained compression tests' three possible outcomes.

1.1 Statement of problem

As mentioned above, liquefaction of sandy soils is still among the most popular, yet challenging research areas of geotechnical engineering. Many people in civil engineering practice often subconsciously link the word "liquefaction" with a source of dynamic loading such as earthquakes. Even though liquefaction due to cyclic mobility is an important aspect, liquefaction can occur under static loading conditions as well, which is called static liquefaction or flow liquefaction. When occurred on site, static liquefaction could be quite catastrophic as it occurs in a sudden manner accompanied by large displacements. Even though liquefaction due to cyclic mobility could occur in a wider range of soil and site conditions, consequences of static liquefaction are generally more severe (Kramer, 1996). Lade and Yamamuro (2011) presented a summary of twenty cases, in which submarine slopes, earth dams, various types of fills and embankments were subjected to static liquefaction. These static liquefaction cases revealed that the predominant soil type was generally silty sands.

Laboratory studies are still quite important to understand the role of various factors on liquefaction behavior. Several factors including fines content (FC)(Pitman et al., 1994; Lade and Yamauro, 1997; Monkul and Yamamuro, 2011), confining stress (Yamamuro and Lade, 1997; Thevanayagam, 1998) and deposition method (Brandon et al., 1991; Høeg et al., 2000; Yamamuro and Wood, 2004) were shown to influence the static liquefaction or undrained behavior of sands through laboratory research. The effect of fines content (FC) was perhaps the relatively most studied one among those factors. But still, it is difficult to say that there is consensus about whether the silt content increases or decreases the liquefaction resistance of a sand. According to the results of some studies increasing non-plastic silt content had increased the static liquefaction resistance of sands (Kuerbis et al., 1988; Pitman et al., 1994; Ni et al, 2004), while others showed a decrease of static liquefaction resistance with increasing non-plastic silt content (Zlatovic and Ishihara, 1995; Lade and Yamamuro, 1997; Monkul and Yamamuro, 2011; Belkhatir et al., 2013). In fact, both conclusions are valid considering that different comparison bases (i.e. same void ratio, relative density, loosest possible density after deposition etc.) and initial conditions (i.e. depositional methods influencing initial soil fabric) were employed for different studies.

Among the other factors that could influence the static liquefaction behavior of sands is initial stress conditions. Yamamuro and Lade (1997) run monotonic undrained triaxial compression tests on Nevada Sand with silt and clean Ottawa sand at various confining stresses and for both soils static liquefaction potential was shown to increase with decreasing confining stress. More explicitly, static liquefaction is a low-stress phenomenon; therefore, both clean and silty sands are more liquefiable at considerably low confining stress (e.g. σ_{3c}=30 kPa). Thevanayagam (1998) also conducted monotonic undrained triaxial tests and stated that undrained shear strength of silty sands became sensitive to the magnitude of the initial confining stress especially when the intergranular void ratio (void ratio of the sand matrix alone) of the specimens were greater than or equal to the maximum void ratio of the base sand.

The complexity of the liquefaction problem is not limited to the effect of above mentioned factors only. Grain size distribution had also attracted attention for its possible influence on the shear strength of sands. Koerner (1970) performed drained triaxial compression tests on clean quartz sand in both saturated and dry states to look at the influence of gradation on the internal friction angle. He found that varying the coefficient of uniformity (C_U) had negligible effect on the value of the effective friction angle for quartz sands at a given relative density. Kuerbis et al. (1988) compared two different gradations of clean Brenda mine tailings sand, and concluded that undrained triaxial compression behavior is similar for both well graded and uniform versions of Brenda mine tailings sands. In a later study, Pitman et al. (1994) added clean 70/140 silica sand to clean Ottawa sand in order to change the sand gradation. Similar to

Kuerbis et al. (1988), Pitman et al. (1994) also concluded that monotonic undrained triaxial compression behavior of various samples prepared at similar initial void ratios are not influenced by the gradation of the sand (i.e. uniform or relatively well graded).

Some researchers on the other hand have reported that grain size distribution could be important for the undrained response of sands. Kokusho et al. (2004) performed both monotonic and cyclic undrained triaxial tests on clean river sand of different gradations. Accordingly, influence of sand gradation had negligible effect on cyclic liquefaction resistance at a given relative density. However, static liquefaction resistance increased as the river sand became well graded (i.e. the coefficient of uniformity increased) at a given relative density. Kokusho et al. (2004) also reported that effective stress internal friction angles (ϕ') of the sands have increased with increasing C_U. Igwe et al. (2007) conducted stress controlled undrained ring shear tests on clean industrial quartz sand with different gradations. Similar to Kokusho et al. (2004), Igwe et al. (2007) also concluded that as the sand gradation is changed so that the coefficient of uniformity is increased, its static liquefaction resistance is also increased at a given relative density.

So far, the vast majority of the previous literature focused on the possible influence of gradation on the liquefaction behavior of clean sands. However, it seems that similar to the effect of FC, conclusions regarding the influence of grain size distribution on static liquefaction behavior of clean sands are somewhat conflicting. Furthermore, when silty sands are of interest, the number of previous studies investigating the influence of gradation is very limited. Belkhatir et al. (2011) conducted undrained triaxial compression tests on mixtures of Chlef sand and silt, and stated that peak undrained strengths decreased linearly with increasing C_U of the mixtures due to increased fines content up to 50% for the specimens prepared at the same relative density. Maleki et al. (2011) run undrained triaxial compression tests on different gradations of Shooshab sand mixed with 15% silt, and observed that as the sand matrix became smaller, undrianed shear strength of specimens increased when prepared at the same void ratio. Monkul (2013) performed drained direct shear tests on mixtures of two base sands and two non-plastic silts, and observed that drained shear strengths of mixtures were not significantly influenced by either the gradations of base sand or silt or the value of fines content (≤25%). However, the amount of volumetric contraction was found to be influenced by the gradation of specimens.

When shape characteristics is considered as another factor that could have an influence on the static liquefaction behavior, previous studies once again focused on shape effects of sand grains (i.e. influence of grain shape on drained/undrained clean sand response). Cho et al. (2006) investigated the influence of grain shape effects on extreme void ratios (e_{max}, e_{min}), small strain stiffness and critical state parameters. They conducted oedometer, bender element and drained triaxial compression tests on 33 different sands, and found that increasing angularity and/or decreasing sphericity of sand grains caused an increase in extreme void ratios, compression index (Cc), and critical state friction angle (ϕ_{cs}) of sands. Rouse et al. (2008) also depicted that increasing angularity of sand grains resulted an increase in extreme void ratios and internal friction angle based on the data of various sands in literature. Guo and Su (2007) did drained triaxial compression tests on two clean sands with different grain shapes and mentioned that increasing angularity tends to increase the shear strength and influences the dilatancy of sands. Georgiannou and Tsomokos (2010) discussed the influence of grain shape effects on undrained behavior of sands. They performed torsional hollow cylinder and undrained triaxial compression tests on four uniform clean sands with similar grading curves but having different shape characteristics. In that study, angular sands had shown a stronger undrained response compared to rounded sands at similar relative densities, and angularity of sand grains were shown to be as influential as gradation on the undrained behavior of clean sands. Yang and Wei (2012) conducted an important study regarding the influence of particle shape on the instability of loose sands via undrained triaxial compression tests on two base sands (Toyoura and Fujian) mixed with two different fine types: crushed silica fines (angular) and glass beads (rounded). Similar to Cho et al. (2006), Yang and Wei (2012) also observed an increase in ϕ_{cs} of clean sands as they become more angular. But more importantly, Yang and Wei (2012) reported that at a particular fines content a sand involving rounded glass beads had more susceptibility to static liquefaction than a sand involving angular crushed silica fines.

1.2 Scope of the research

According to the studies mentioned above, it can be inferred that fines content, grain size distribution and grain shape characteristics are among the major factors which could play considerable role on the shear strength and liquefaction response of sands.

However, many of the previous studies have focused on the properties and characteristics of sand grain matrix. This was perhaps a reasonable approach with the assumption that it is the dominating matrix for both clean and silty sands. Nevertheless, relatively little is known about how and to what extent the gradation and shape characteristics of silt grain matrix (e.g. mean size, coefficient of uniformity, angularity) in a silty sand influence the static liquefaction behavior of those soils. Furthermore, it is unclear whether some effects of the mentioned factors are independent of each other or coupled, as most of the previous studies investigated the effects of mentioned factors individually. In this study, monotonic undrained triaxial compression tests were performed on three base sands with same geologic origin and on twenty seven silty sands obtained by mixing the base sands with three different non-plastic silts at various fines contents (i.e. FC≤25%). The results were analysed based on several aspects including the effects of content, grain size distribution and shape characteristics of the silts on static liquefaction of silty sands.

2. LITERATURE REVIEW

Over the years, there have been many researchers who investigated various aspects of liquefaction phenomena. The aim of this chapter to outline the conclusions of researchers so that exhaustive discussion on topics relating to thesis can be presented.

The term “liquefaction” was initially used by Hazen in 1920 with the aim of behavior characterization of Calaveras Dam in California (Castro & Poulos 1997, after Hazen 1920). Then, Karl Terzaghi used this term in 1925 to depict submarine slop failures which took place in the fjords of Norway and also around coastal regions of Netherlands (Terzaghi 1956). In fact, Terzaghi assigned mentioned slope failures to the collapse of very weak metastable particle structures formed in alluvial deposits of fine sands. He also states that slope failures for coarser soils take place at much steeper angles. Besides, he concluded that sands with high percentage of fine particles ranges between 6 and 20 μ (fine silts) are more sensitive to shock loads than either coarser or looser sands and that these soils show a significant decrease in void ratio upon shearing.

With the scope of investigating the slope failures observed in the Norwegian fjords and also along the banks of Mississippi river, Bjerrum et al. (1961) conducted strain controlled drained and undrained triaxial compression tests on very loose fine silty sands. Even though their experiments did not resemble a complete static liquefaction, due to the moist tamping (MT) technique they used for specimen preparation, but they were able to make some key observations of the soil behavior. For instance, they discovered that for specimens that were sheared on undrained conditions, effective stress and friction angle decrease quickly as porosity increased above 44 percent. It should be noted that they use an initial confining pressure of 100 kPa during experiments, which may be too great for static liquefaction to happen.

Later, Anderson and Bjerrum (1968) investigated the submarine slope failures of very loose sands and silts of Scandinavia. In that study, the authors use the term, metastable particle structure -suggested by Terzaghi- to describe potential failure mechanism.

They also accepted that a complete understanding of the real mechanism of the slope failures was not accomplished at the time. Besides, they claimed that metastable particle structures are difficult to reconstruct after experiencing the flow slide due to the re-sedimentation. According to their investigations, relatively uniform fine sands and coarse silts are the common type of soils that vulnerable to flow failures. They also stated that the tested sample’s high porosities may be due to presence of small amount of fine particles. In accordance with Terzaghi and Peck (1948), they claimed that the capacity of soils to form an abnormally porous aggregate can be eliminated by removing either the finest or coarsest components of them. With respect to all mentioned above, it can be inferred that the degree of sensitivity of the structure of fine sands to flow failures depend not only on the deposition method, but also on minor details of their grain size characteristics.

Then, Youd (1973) provided literature review of many case histories of failures due to liquefaction. Besides, he gathered existent definitions for the liquefaction phenomena which was suggested by previous researchers (Terzaghi and Peck (1948), Seed and Lee (1967), Castro (1969) and etc.) He also investigated experimental outcomes of Seed and Lee (1967), Seed et al. (1969) and Castro (1969), whom preformed monotonic and cyclic loadings. The experiments by Castro (1969) comprised of stress controlled, undrained monotonic and cyclic triaxial compression tests conducted on Ottawa sand specimens, which prepared at various relative densities. According to the results of monotonic loading experiments, it was found that as initial relative density increases, the liquefaction potential of specimen decreases. In spite of the fact that, complete static liquefaction (i.e. reaching zero value of deviator stress) was not accomplished in any of the experiments that he conducted, but the specimen prepared at loosest density (sample with the relative density of 37 percent) reached what Youd denoted to as the “unlimited flow” after achieving point of stability, which corresponds to the initial peak of the deviator stress versus axial strain curves.

With the scope of finding a general definition for liquefaction phenomena, Youd also studied the behavior of specimens under cyclic loading from researchers mentioned above. According to the data obtained by Castro (1969) from the undrained cyclic triaxial compression experiments, it was found that excess pore pressure develop during cyclically compression loadings until liquefaction and unlimited flow were reached. Besides, Seed and Lee (1967) decided to perform cyclic triaxial tests which consisted of both compression and extension loadings on clean Sacramento river sand. Outcomes of the mentioned experiment revealed that repeated episodes of unstable soil behavior was possible as long as stress reversals were provided. Then, additional cyclic triaxial compression-extension experiments conducted by Seed et al. (1969) and it was found that the strains recorded during this type of cyclic loadings are much greater for samples which subjected to stress reversal compare to samples that subjected to cyclic compression.

While undrained cyclic triaxial experiments of cohesionless soils became more constituted, Casagrande (1975) distinguished the essential need for distinction between the concepts of cyclic liquefaction and flow liquefaction. He recognized that flow type liquefaction can not take place in monotonic loadings of dense sands, while this type of sand can liquefy under cyclic loadings. Besides, he talked about the concept of flow structure term which he employed to explicate the Fort Peck dam's failure due to liquefaction. According to Casagrande, flow structure is a accumulation of soil particles that rotating constantly in relation to surrounding grains which result in creation of very low frictional resistance among them. He also claimed that mentioned flow structure spreads by chain reaction and only existent when soil is liquefied and when the flowing due to liquefaction ended, the particles start to densify as a result of rearrangement.

Lee et al. (1975) studied the flow liquefaction of San Fernando dam that took place as a result of earthquake. The authors investigated the hydraulic fill methods that used to construct mentioned dam. Results of in-situ sampling revealed that the hydraulic fill comprised of various layers of clean sand, silty sands and sandy silts with thickness of approximately 0.3 meters. Experimental program of the mentioned fill demonstrated that the density increases as the mean grain size increases. Drained and undrained monotonic triaxial compression tests were conducted on isotropically consolidated undisturbed samples obtained from the hydraulic fill. Outcomes of the undrained experiments showed quite stable response which was in fact as the result of high relative density (i.e. initial relative density of 55 percent) and also as the consequence of choosing high effective confining stresses which ranged from 96 kPa to 380 kPa. Accordingly, the authors mentioned that no major loss in samples' strength was observed following peak stress differences.

At the same year, Castro (1975) introduced the term “steady state” for both flow liquefaction and cyclic mobility. He described it as the residual strength of sample at relatively large strains after achieving peak strength. He also claimed that when steady state accomplished, the strength of the tested soil is small and become constant. In spite of the fact that outcomes of both monotonic and cyclic undrained triaxial experiments that conducted on loose sands seems to fit well with his suggested theory, but it was still unclear whether the tested samples were sheared up to adequate amount of axial strain or not, to find out the stress strain behavior of them. It should be noted that all tests were stopped when the axial strength of the specimens reached 20 percent. With respect to explanations stated previously by Casagrande, Castro defined the “critical state” term as the state of continuous deformation at constant volume and resistance of the tested specimen. Besides, he claimed that stresses related to the critical state condition are only a function of the void ratio.

Two years later, Castro and Poulos (1977) introduced the Steady State Line (SSL) concept. With respect to their explanation of the concept, it is the boundary between contractive and dilative behavior of soils which can be obtain from effective confining stress versus void ratio graphs of experiments. It should be noted that initial states that are plotted above the steady state line are subject to flow liquefaction, while initial states plotted below the mentioned line are subject to cyclic liquefaction, depending on the value of the deviator stress during shearing. Besides, the authors discuss several factors which influence static and cyclic type of liquefaction phenomena. They claimed that effective confining pressure and initial static shear stress are the key factors for the flow liquefaction. They also conducted monotonic triaxial tests for five different sands with various gradations. With respect to the results of the experiments it was revealed that as the initial principle stress ratio increases the liquefaction potential increases. It was also founded that liquefaction potential of the specimens can not be measured according to the relative density of them and also as the confining stress increases, the liquefaction resistance of the specimen decreases. It can be inferred from the mentioned paper that the authors missed to investigate the effects of gradation and fines content on liquefaction potential of the tested samples.

In the year 1978, Muilis et al. published a paper about the influence of specimen preparation methods and also specimen density on the undrained behavior of isotropically consolidated samples under cyclic loading. According to the experiments' outcomes, samples prepared by using the moist tamping (MT) showed more liquefaction resistance compare to those prepared in similar conditions, but using air pluviation technique. As mentioned above, the authors also investigated the effects of density of behavior of specimens. They stated that small variations in initial relative density of samples can effect the strength of specimen in significant ways.

The term "quick sand" first introduced by Hanzawa et al. (1979) while investigating the behavior of the soil in the Arabian gulf. Determination of index properties of the soils reveal that they were loose silty sands with fines content ranging between 20 to 30 percent. It should be noted that since it was impossible to obtain in-situ undisturbed samples for that case study, the authors developed special method to recover them. Both monotonic and cyclic triaxial testes performed on the recovered specimens. According to the mentioned tests' results, it was found that all samples were extremely contractive and therefore, demonstrated high liquefaction susceptibility. In fact, this was in agreement with previous researchers' (Terzaghi & Peck 1967, Bjerrum et al. 1961 and etc.) observations. The authors hypothesized that this extremely contractive response of the samples may be due to metastable particle structure made between sand and silt grains. The authors also claimed that beside gradation of the soils, particle gradation play an important role on liquefaction susceptibility. They prove it by citing study conducted by Castro (1969) which revealed that soils constituted of angular particles are less liquefiable than those constituted of rounded particles.

The term "collapse surface" first used by Sladen et al. (1985), while investigating slides that took place on an artificial island berm in the Beaufort Sea. The collapse surface consists of three dimensional normal stress – shear stress - void ratio space (i.e. Cambridge p′-q stress path with the added axis of void ratio) and it is used with the aim of evaluation of liquefaction potential of sands. In fact, this collapse surface concept is basically an extension of the steady state concept, and follows the principles of critical state soil mechanics in many aspects. The authors claimed that during undrained triaxial tests, specimens located on or even near the mentioned surface are susceptible to liquefaction phenomena. With the scope of simulating the field conditions, they prepared samples made from Beaufort Sea with 0, 2 and 12 percentages of fines content. It should be noted that the in-situ soil comprises of fines content ranges between 0 to 15%. With respect to the tests' outcomes it was revealed that the position of the steady state line is influenced by the amount of fines content and also, increasing fines content result in decreasing the strength of the soils in a significant way. They assigned the observed various behaviors to increasing compressibility and decreasing the permeability of sands, as the amount of fines content increases.

With the scope of studying the undrianed behavior of sands, Vaid &Chern (1985) performed vast laboratory studies including monotonic and cyclic triaxial tests. They used two different sands with different gradations (i.e. angular tailing sand and rounded Ottawa sand) in order to investigate the shape effects of base sands on liquefaction potential. It should be noted that water pluviation (WP) method were used during sample preparations. According to the monotonic triaxial tests' outcomes it can be inferred that although some of the samples used in experimental program demonstrated limited liquefaction behavior but, none of achieved complete liquefaction. In fact, the reason behind this response is the high level of effective confining pressure used during their experimental programs (i.e. σ´3=100 kPa to 2500 kPa). The authors also conducted cyclic triaxial tests on the same sands, too. Outcomes from cyclic triaxial experiments revealed that the soils' behavior under cyclic loading was connected to their response under monotonic loadings. In other words, for similarly prepared samples, it was shown that for the soils which limited liquefaction observed during monotonic loadings, contractive response occurred under cyclic loadings. This finding indicate the capability of the soil behavior to be independent of the stress path and also confirm the existence of a unique phase transition state line which refers to effective confining stress and void ratio at the point of phase transition of soils.

With the scope of better understanding the behavior of mine tailing dams and also improving design methods of them, Troncoso and Verdugo (1985) performed both monotonic and cyclic triaxial tests on silty sand samples. In fact, they conducted mentioned experiments in order to investigate the effect of silt content on the behavior of silty sands. With respect to the outcomes of both monotonic and cyclic triaxial tests on Chilean copper mine tailings at different amount of fines content, the authors reported following observations. First, drained triaxial compression tests revealed that the friction angle decreased from 44o to 39o and the dilatant volumetric strain decreased from 2.2% to 0.3%, as amount of fines content increased from 0% to 30%. They also stated that increasing fines content result in increasing the compressibility of the soils and therefore, it would cause the soils more liquefiable. The authors associated the observed weakness of mixtures as the fines content increased, to the capability of the fine particles to fill in irregular voids between the sand grains which lead to decreasing favorable interlocking consequences.

Three years later, Kuerbis et al. (1988) conducted undrained monotonic and cyclic triaxial experiments with the aim of investigating the influences of fines content and particle gradation. Vast experimental program performed on the different base sands of Brenda mine tailings which composed of various gradations mixed with different amounts of Kamloopse silt. It should be noted that slurry deposition (SD) technique were used during experimental program. Outcomes of monotonic tests performed on base sands (i.e. 0% of fines content) revealed that decreasing grain size result in increasing dilation tendency of specimens while, outcomes of cyclic tests revcealed reverse behavior (i.e. decreasing grain size lead to increasing contractiveness). Besides, it was found that for all silty sands, increasing fines content result in increasing dilation tendency of the specimens. For the mentioned experiments, keeping the skeletal void ratio (i.e. void ratio of sand grains) effected the outcomes in a significant way. In other words, packing silt particles into the sand grain voids result in denser structures. It can be inferred that, increasing fines content consequences the elimination of existence void spaces reserved for potential densification.

At the same year, Alarcon-Guzman et al. (1988) recognized that the steady state line (SSL) is not unique for type of sands, specially for sands which have high contractive tendencies. They suggested a new diagram which comprised of three regions (strain softening, transition and strain hardening) instead of the conventional diagram introduced by Castro & Poulos (1977) which consisted of two regions (contractive and dilative). According to the authors hypothesize, in undrained triaxial tests, the strain softening region represents the specimen with initial states which demonstrate complete flow liquefaction during shearing phase. On the other hand, the strain hardening region refers to initial states which show dilative response in which stress difference increases continuously during shearing phase. Finally, the transition region refers to initial states that shows limit liquefaction behavior in which, initially a reduction of strength take place and then dilation tendency take over, which result in increasing the strength of tested samples.

Kramer and Seed (1988) conducted stress-controlled monotonic triaxial tests, mainly concentrating on the initiation of liquefaction phenomena. They used Sacramento river clean sand and silty sand comprised of 12% fines during experimental program. Moist tamping (MT) method were used for sample preparation and then specimen sheared under undrained condition. With respect to the test results, it was found that liquefaction potential of both soils decreases as the initial confining stress and relative density of specimen increases.

With the scope of investigating the steady state response of loose sands, Konrad (1993) performed both monotonic and cyclic triaxial tests. He used two different sands, Hoston RF clean sand and Till sand which is consisted of 32% fines content. Samples prepared using the moist tamping (MT) technique, although the author claims that for most cases, mentioned technique does not resemble the actual soil structure in the field. With respect to test outcomes, it can be inferred that for all experiments, testing was ended at low levels of axial strains (i.e. 20% for monotonic and 12% for cyclic experiments). In spite of the fact that 12 to 20% of strains seems to be adequate to cause failures, but it is not correct to say that steady state has been accomplished at these strain levels. It should be noted that the author supports his test results by saying that steady state conditions are obtained at the point where pore pressures of specimens become constant. I can be inferred that what the author called steady state is in fact, the point of phase transition (quasi–steady state) at which specimens' contractive response switches to dilative behavior.

A vast discussion on the behavior of cohesionless soils during liquefaction has provided by Ishihara (1993). He began the paper by admitting that soils that exhibited liquefaction behavior are very loose sands with some amounts of fines, either plastic or non-plastic. Hence, he claimed that it is essential to concentrate on the behavior of silty sands instead of clean sands. He conducted monotonic triaxial tests with two different confining pressure on isotropically consolidated soils obtained from Tia Juana city of Venezuela, with the aim of characterizing the undrained behavior of silty sands. Two different deposition techniques used for specimen preparation, some samples prepared using Water Sedimentation (WS) while the others prepared using dry funnel deposition (DFD) technique. With respect to the results of experiments, it was found that, the all samples became less liquefiable as the effective confining stress increased. In fact, the conventional soil behavior was confirmed by exhibition of unique steady state and quasi steady state lines. It should be noted that the responses observed during experiments, were not consistent for the samples prepared by either of the two mentioned techniques used for deposition. In other words, the samples deposited using the water sedimentation method were more contractive than those prepared using dry funnel depositional method. Another part of this vast investigation is the outcomes of the triaxial compression experiments conducted on very loose Toyoura sand samples deposited using moist placement technique. All the samples exhibited complete static liquefaction behavior at the confining stresses of 100, 300 and also 1000 kPa. Still, it should be noted that this test results may not be useful due to the artificially very loose particle structures created as the result of moist placement used during specimen deposition.

With the scope of investigating the influence of plastic and non-plastic fines content, Pitman et al. (1994) performed undrained monotonic compression tests. The authors used Ottawa sand C-109 as base sand and also Kaolinite as the plastic fines and two non-pastic fines (crushed quartz and 70-140 fine quartz) in their experimental program. They used 350 kPa of effective confining stress for the tests. The experiments outcomes revealed that increasing amount of all fines content, used during experiments, resulted in increasing strength of specimens. It should be noted that since the authors prepared specimens which have initial void ratio variation as much as 20%, the outcomes of the experiments are under question.

Yamamuro and Lade (1997) conducted both drained and undrained tests with the scope of investigating the behavior of loose Ottawa 50/200 and Nevada sands sheared in triaxial compression. Both sands were determined to have angular shape and also have similar grain size distributions. It should be noted that Nevada sand naturally had 6% of non-plastic fines content. For the specimen preparation, two different methods used for the mentioned sands. The Nevada sand specimens prepared using the dry funnel deposition (DFD) technique, while moist tamping (MT) method used for sample preparation of the Ottawa sand. The authors defined complete static liquefaction as zero principle stress difference and zero effective confining pressure. With respect to test results of undrained monotonic tests on the Nevada sand, it was found that complete static liquefaction was achieved at initial confining stresses between 25 and 125 kPa and that the liquefaction potential increased as the initial confining stress decreased. Besides, for the confining stresses higher than 125 kPa, temporary liquefaction behavior was observed. In fact, the authors associated this abnormal behavior to the highly compressibility linked with loosely prepared isotropically consolidated to low initial confining stresses. Besides, they hypothesized that the existence of the small amount of non-plastic fines in the Nevada sand resulted in creation of a weak and also highly compressible particle structures. Their hypothesis was manifested by showing that when samples prepared using both Nevada sand (which contains 6% fines content) and Ottawa 50/200 sand (which contains 0% fines content) at the same initial void ratio and sheared under undrained conditions, complete static liquefaction behavior observed for the Nevada sand, while Ottawa sand showed temporary liquefaction behavior. The authors' claim regarding high compressibility of the loose sand samples was proved by performing drained monotonic triaxial experiments. With respect to the drained compression tests, it was revealed that these samples showed mostly volumetric contractive tendencies and only small dilatant tendencies at relatively high values of axial strain was observed.

At the same year, Lade and Yamamuro (1997) presented another paper, this time mainly focused on the influences of non-plastic fines content on static liquefaction. The authors, used angular Nevada sand and subrounded Ottawa F-95. Specimens prepared using dry funnel deposition (DFD) technique and undrained monotonic compression tests conducted. With respect to the results, it was found that as the amount of fines content increased (studied range was from 0% to 60%), the liquefaction resistance of the specimen decreased systematically even as initial relative density increased. Accordingly, the authors stated that void ratio and relative density factors are not adequate quantities for assessing liquefaction of sands containing various amounts of non-plastic silts. With the scope of verifying the unconventional silty sand behaviors concerning to varying the confining stresses (as discussed in Yamamuro & Lade, 1997), the authors decided to conduct undrained monotonic experiments using Nevada 50/200 sand mixed with 50% of different non-plastic silts as fines content. Totally six different experiments conducted at initial effective confining stresses ranging from 50 kPa to 500 kPa. Outcomes of the mentioned tests confirmed that liquefaction potential of specimens decreases as the initial confining stress increases.

Puzrin et al., (2010), performed a vast investigation on the caisson failure induced by static liquefaction of Barcelona harbor that took place on January 1st 2007. According to the investigations, it was brought out that the static liquefaction of the fill played an important role in the triggering of the caisson slides. It should be noted that fill materials obtained by dredging the natural soil and placing it in designated areas by using new method called rainbowing. In this method, large quantities of dredged soil sprayed from floating vessel on to aimed lands. The authors stated that several reasons may explain high susceptibility of the fill that static liquefaction happened. The main reasons are the silty nature of the fill as described previously by Yamamuro and Lade (1998) and the young age of sediment soil. The authors also claimed that, other factor that lead to errors in investigations is the new rainbowing method which contribute to open soil structures and therefore gas trapped insides the samples.

Monkul (2010) developed a new densification technique for the dry funnel deposition method, which avoids tamping, vibrating and mold tapping. He also stated that this new method of densification is thought to create much consistent soil fabrics than previous specimen densification techniques. He also performed Strain-controlled monotonic undrained triaxial compression experiments on Nevada Sand-B as base sand mixed with three different non-plastic silts (Loch Raven, SilCoSil #125 and Potsdam silts). With the scope of investigating the silt size effects, he mixed Nevada sand-B with 20% of mentioned silts and conducted monotonic trixial tests for isotropically consolidated the samples with initial confining stress equal to 30 kPa. According to the experiment outcomes, the author stated that silt size plays an important role on the liquefaction potential behavior of silty sands. Besides, he declared that liquefaction potential for a silty sand increases, as the mean grain diameter ratio ($D_{50\text{-sand}}/d_{50\text{-silt}}$) decreases. He associated this strange behavior with creation of more meta-stable structures, as the result of increasing fines content.

3. DETERMINATION OF INDEX PROPERTIES OF TESTED SOILS AND EXPERIMENTAL PROGRAM

This chapter mainly covers the details of extensive laboratory investigations that performed to investigate the influence of gradation, fines content and silt shape characteristic on static liquefaction of loose sands. As the first step of experiments, various combinations of clean sands with silt mixtures prepared in the laboratory and the index properties of them defined by relevant experiments. Next, undrained monotonic triaxial tests performed on the mentioned soil mixtures. Finally, SEM (scanning electron microscope) equipment is used for determination of silts' shape used in tests.

3.1 Soils Used in Laboratory Experiments

With respect to previous laboratory studies, it can be seen that most of the previous researchers use one or two base sands and silts with various combinations of them in their experiments. In this experimental program, it is decided to use three silts and three base sands to have more trusted experiment out comes. The reason for selecting three different non-plastic silts is to investigate the possible effects of gradation and shape characteristics of silt grain matrix on the static liquefaction response of silty sands. Besides, the reason for selecting three different base sands is to check the validity of the effects mentioned above for different base sands. Each base sand was thoroughly mixed with available silts on dry weight basis to achieve 5%, 15% and 25% fines content (FC) for the resulting silty sands, in which FC refers to the percentage of soil grains finer than 0.075 mm in total dry weight of solids. At the end of this combination process twenty-seven silty sands were obtained in addition to the three clean sands, and these thirty samples were used in the experimental program.

3.1.1 Sands

Three clean sands, used in studies, were obtained from a sand quarry in Şile region at the city of Istanbul, Turkey and were used in the experimental program as base sand soils. These sands, which have the same geologic origin but different gradations, are named Sile Sand 20/30, Sile Sand 50/55 and Sile Sand 80/100. All of the sands mentioned above have light yellow color and classified as poorly graded sands. With respect to unified soil classification system (USCS) all mentioned sands classified as poorly graded sands (SP). Figure 3.1 exhibits the sands used in experiments.

(a)

(b)

(c)

Figure 3.1 : Sands used in experimental program (a) Sand 20/30, (b) Sand 50/55 and (c) Sand 80/100.

3.1.2 Silts

Three different non-plastic silts: IZ silt, SI silt and TT silt, obtained from three different cities of Turkey and were used in the experimental program as fine grained soils.

TT silt, which is dark gray in color, was obtained from a stone quarry in Şile region of Istanbul. It was produced by wet sieving of stone dust through the No. 200 standard sieve (0.075mm). SI silt, which is white in color, was obtained from a sand quarry in Lüleburgaz region at the city of Kırklareli. IZ silt, which is dark yellow in color, is a naturally formed soil obtained from the city of Izmir. It should be noted that, IZ silt has a natural fines content of 74%, but only the -No 200 portion (<0.075mm), obtained by wet sieving, was used in the experimental program. Since all of the silts have no discernible liquid limit, they all classified as non-plastic silts (ML). Figure 3.2. show the silts used in experiments.

(a)

(b)

(c)

Figure 3.2 : Silts used in experimental program (a) TT Silt, (b) SI Silt and (c) IZ Silt.

3.2 Evaluation of Index Properties

As the first group of experiments aimed at investigating the influence of factors mentioned previously, a complete index determination program was conducted. This program included related tests for evaluation of soils grain size distribution, specific gravity, maximum and minimum void ratios for the used base sands, silts and also various combinations of them.

3.2.1 Particle size analysis

The particle size analysis determines the gradation (the distribution of aggregate particles, by size, within a given sample) with the scope of evaluation of compliance with verification specifications. The gradation data can be used to calculate relationships between various aggregate or aggregate blends, to check compliance with such blends, and even to predict trends during field and laboratory experiments. Used in conjunction with other tests, the particle size analysis is a powerful quality control and quality acceptance tool. All existence six soils' grain size characteristics was determined in the same manner as ASTM D 422. Sieve analysis preformed on available sands while hydrometer tests conducted on three silts. The grain size distribution curves of all used soils are shown in Figure 3.3 The coefficient of uniformity (C_U), the mean grain size (D_{50}) and $D_{50\text{-sand}}$ / $d_{50\text{-silt}}$ ratios are presented in table 3.1.

Table 3.1 : Some properties of the soils used in the experimental program.

	Sile Sand 20/30	Sile Sand 50/55	Sile Sand 80/100	TT Silt	SI Silt	IZ Silt
D_{60}	0.63	0.285	0.184	0.018	0.025	0.057
D_{10}	0.31	0.151	0.131	0.002	0.001	0.007
C_U	2.0	1.9	1.4	10.6	18.5	7.9
$D_{50}/d_{50\text{-TT}}$	52.0	23.6	16.0	-	-	-
$D_{50}/d_{50\text{-SI}}$	33.6	15.3	10.4	-	-	-
$D_{50}/d_{50\text{-IZ}}$	15.5	7.0	4.8	-	-	-

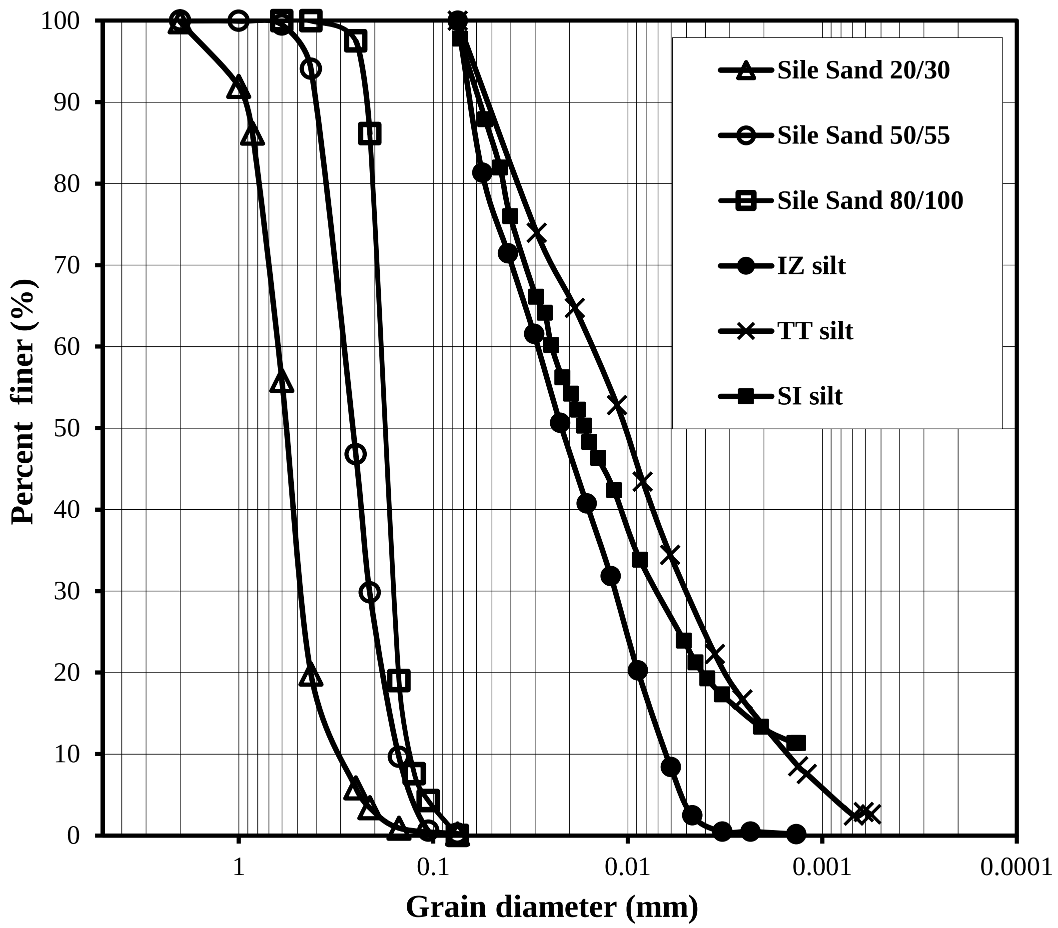

Figure 3.3 : Grain size distribution of the soils used in the experimental program.

3.2.2 Maximum and minimum void ratios

In fact, there is no ASTM procedures which refers to determination of maximum and minimum densities of cohesionless soils with different amounts of silt contents. In other words, vibratory table method which suggested in ASTM D4253 and D4254 for evaluation of extreme densities are limited to soils with maximum fines content of 15%. With respect to the fact that we had soil mixtures more than 15% in our experiments, hence, we can not use these procedures.

Other methods have also employed by some researchers (Kolbuszewski 1948; Mulilis et al. 1977; Vaid and Negussey 1988), and the results shows different values for extreme void ratios than experiments performed by using mentioned ASTM procedures. Hence, the extreme void ratios are not unique, but they depend on the methods used for their determination. Lade et al. 1998, suggested a method which implies well for silty sands, especially for the fine sands, with respect to the fact that their extreme void ratios are sensitive to small variations in methods. One of the most advantages of this method is that it we do not apply any type of surcharge in the densification procedures, in order to avoid any particle breakage during experiments. In order to determine the minimum void ratio of tested soils, 822 gr of soils poured into a 2000-mL graduated cylinder. As the first step, approximately 50 gr of the tested soil poured into the cylinder and it was tapped eight times with the rubber handle of a screwdriver, twice each on opposite sides. This procedure is repeated until the whole sample deposited into the smallest possible volume. Then, height of the deposited sample measured from four different directions and since the diameter of the cylinder is constant, the volume calculated to the nearest cubic centimeters, corresponding to a variation in void ratio of approximately 0.003. The maximum void ratio of tested soils can be measured as following. First, whole sample (822 gr) poured into the cylinder and then, the opening of the graduated cylinder covered using a piece of latex membrane. The cylinder then turned upside down very slowly (approximately 45 to 60 seconds to rotate 180^{o}) until the maximum volume produced and then, the height of the sample measured as mentioned previously. Accordingly, this procedure repeated five times and the average value of them accepted as maximum void ratio. It is estimated that the overall accuracy on evaluation of the both maximum and minimum void ratios are within 0.01 and that is accurate enough for obtaining extreme void ratios of silty sands. It should also be noted that during the mentioned procedures, care was taken to avoid segregation of grains. Table 3.2 exhibits the maximum and minimum values of tested soils using mentioned procedures.

Table 3.2 : Maximum and minimum void ratios of samples.

Soil Type	FC (%)	e_{min}	e_{max}
SAND 20-30	0	0.481	0.769
SAND 50-55	0	0.570	0.870
SAND 80-100	0	0.640	0.959
TT SILT	100	0.513	1.738
IZ SILT	100	0.821	1.366
SI SILT	100	1.553	1.929

Table 3.2 (continued) : Maximum and minimum void ratios of samples.

Soil Type	FC (%)	e_{min}	e_{max}
5% TT SILT + 95% SAND 20-30	5	0.448	0.730
15% TT SILT + 85% SAND 20-30	15	0.421	0.756
25% TT SILT + 75% SAND 20-30	25	0.431	0.784
5% IZ SILT + 95% SAND 20-30	5	0.415	0.700
15% IZ SILT + 85% SAND 20-30	15	0.396	0.664
25% IZ SILT + 75% SAND 20-30	25	0.407	0.703
5% SI SILT + 95% SAND 20-30	5	0.349	0.574
15% SI SILT + 85% SAND 20-30	15	0.254	0.531
25% SI SILT + 75% SAND 20-30	25	0.288	0.521
5% TT SILT + 95% SAND 50-55	5	0.569	0.890
15% TT SILT + 85% SAND 50-55	15	0.553	0.938
25% TT SILT + 75% SAND 50-55	25	0.518	0.982
5% IZ SILT + 95% SAND 50-55	5	0.530	0.861
15% IZ SILT + 85% SAND 50-55	15	0.500	0.872

Table 3.2 (continued) : Maximum and minimum void ratios of samples.

Soil Type	FC (%)	e_{min}	e_{max}
25% IZ SILT + 75% SAND 50-55	25	0.502	0.912
5% SI SILT + 95% SAND 50-55	5	0.549	0.862
15% SI SILT + 85% SAND 50-55	15	0.489	0.853
25% SI SILT + 75% SAND 50-55	25	0.583	0.940
5% TT SILT + 95% SAND 80-100	5	0.630	0.986
15% TT SILT + 85% SAND 80-100	15	0.578	1.033
25% TT SILT + 75% SAND 80-100	25	0.544	1.074
5% IZ SILT + 95% SAND 80-100	5	0.607	0.975
15% IZ SILT + 85% SAND 80-100	15	0.595	0.993
25% IZ SILT + 75% SAND 80-100	25	0.593	1.025
5% SI SILT + 95% SAND 80-100	5	0.606	0.991
15% SI SILT + 85% SAND 80-100	15	0.553	0.994
25% SI SILT + 75% SAND 80-100	25	0.566	1.039

3.2.3 Specific gravity

The specific gravity of a solid substance is the ratio of the weight of a given volume of material to the weight of an equal volume of water. In geotechnical engineering, determination of the specific gravity of soils is essential to compute the soil's void ratio and also for determination of the grain-size distribution in hydrometer test's analysis. All used soils' specific gravities were determined in the same manner as ASTM D 854. It should be noted that the specific gravity of silty sand mixtures calculated with respect to the percentage of consistency of each soil in the whole mixtures. Table 3.3 exhibits the specific gravity of sands and silts used during experimental programs.

Table 3.3 : Specific gravity of the soils used in the experimental program.

Soil Name	Gs
Sile Sand 20/30	2.65
Sile Sand 50/55	2.65
Sile Sand 80/100	2.64
TT Silt	2.75
SI Silt	2.68
IZ Silt	2.70

3.2.4 Atterberg limits

With respect to the standard used for determination of atterberg limits of soils (ASTM D4318), the plasticity index can be evaluate for the soils passed through sieve No. 40. In fact, fine-grained soils can exist in any of several states; which state depends on the amount of water in the soil system. When water is added to a dry soil, each particle is covered with a film of adsorbed water. If the addition of water is continued, the thickness of the water film on a particle increases. Increasing the thickness of the water films permits the particles to slide past one another more easily. A plastic soil can be defined as the one that can be deformed beyond the point of recovery without cracking or change in volume. Therefore, it seems obvious that the behavior of the soils is related to the amount of their atterberg limits in a significant way. With the scope of determination of atterberg limits, plastic limit tests performed on the available silts and it was found that all three silts are non-plastic silts. According to the mentioned ASTM standard, in the case whether the liquid limit or plastic limit of a soil ca not be determined, it is impossible to compute the plasticity index and therefore, should be categorized as non-plastic.

3.3 Triaxial Compression Test

The triaxial test is one of the most common and widely conducted geotechnical laboratory tests which allows the shear strength and stiffness of soils to be measured. This test has significant advantages over simpler procedures, such as the direct shear test, including the capability of controlling specimen drainage and take measurements of pore water pressures. General explanation of the triaxial compression test is that it is a test in which a cylindrical specimen of soil encased in an impervious membrane is subjected to a confining pressure and then loaded axially to failure in compression. Figure 3.4 exhibits the schematic structure of triaxial equipment. It should be noted that all consolidated undrained (CU) triaxial compression tests performed in general accordance with ASTM D4767.

3.3.1 Specimen preparation and experimental program

Soil Mechanics Laboratory of Yeditepe University was used for running the experimental program. It is well known that specimen preparation method can influence the undrained response of sandy soils in significant way (Høeg et al., 2000; Wood et al., 2008), and hence, the same method is consistently used for deposition through the entire experimental program. All soils are deposited in a dry state into a cylindrical triaxial split mold using the dry funnel deposition technique, which had been employed by many researchers in order to reconstitute sandy soil specimens for liquefaction researches (Ishihara, 1993; Zlatovic and Ishihara, 1997; Lade and Yamamuro, 1997; Bahadori et al., 2008; Monkul and Yamamuro, 2011; Monkul et al., 2014). This method, which used in this study, involves a funnel with a tube attached to its spout. Once the tip of the tube is positioned at the bottom of the split mold, soils are poured into the funnel in dry condition. Then, the funnel is raised gently along the axis of symmetry of the specimen. Figure 3.5 schematize the mentioned deposition technique. The resulting specimens were about 7cm in diameter and 17cm in height in the dry stage with height to diameter ratio about 2.4, which is in allowable range of aspect ratio (between 2 and 2.5) determined by relevant ASTM standard. Besides, Wood et al. (2008) had shown that both the base sand gradation and silt distribution remained fairly uniform through the body of specimens reconstituted by the same dry deposition technique employed in this study. Therefore, segregation of silt and sand grain matrix is not a concern in dry funnel deposition method.

After deposition of the specimens, CO_2 gas was flushed through the dry specimens from the bottom to the top for 20 min. Then, de-aired water was percolated in from bottom through the top of specimens for at least three sample volumes. It should be noted that during both deposition and saturation processes special care was taken not to exceeding the effective stress value on the specimen above 20 kPa in order to prevent overconsolidation. During saturation phase, volume and height changes were monitored and considered in the calculations.

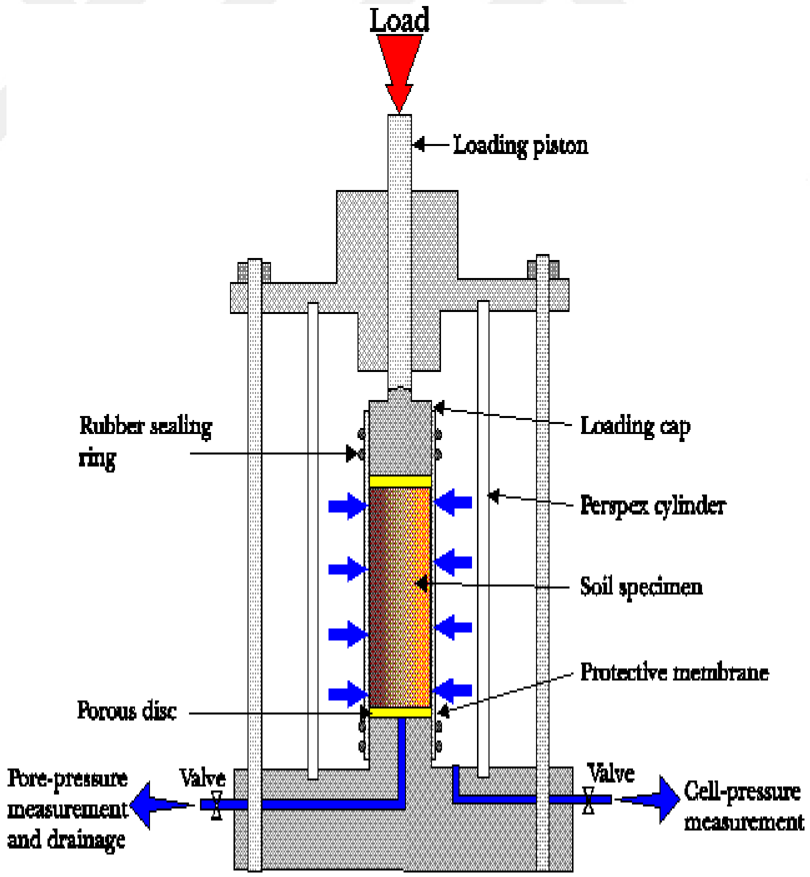

Figure 3.4 : Schematic structure of triaxial equipment (www.geotechdata.info).

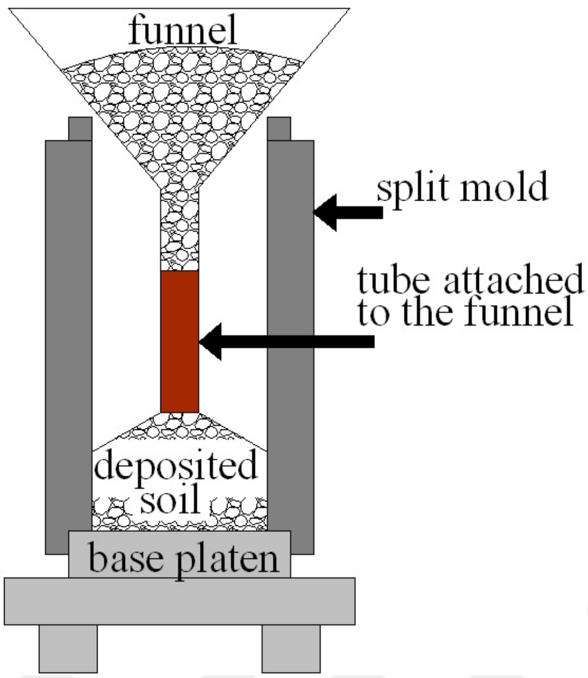

Figure 3.5 : Schematic illustration of dry funnel deposition technique.

A computer controlled Geocomp triaxial testing system was used in the triaxial compression tests. Figure 3.6 exhibits the triaxial equipment used during experiments. This testing system was capable of maintaining the desired pressures within ±0.35 kPa, while monitoring volume changes to within ±0.001 cm^3. A back pressure of 205 kPa was applied prior to the B value check to ensure saturation, and the resulting B-values were at least 0.99 for all tests in this study. In fact, B values above 0.95 are considered to be acceptable according to ASTM D5311. Nevertheless, in this study, specimens with B values smaller than 0.99 were discarded.

After the saturation control phase, specimens were isotropically consolidated to an effective confining stress of 30 kPa with computer controlled cell pressure increments, while maintaining zero excess pore pressure within the samples. In fact, such a low confining pressure is specifically selected, because previous research has shown that silty sands show so-called “reverse behavior” in low confining stress range (Yamamuro and Lade, 1997; Ng et al., 2004; Rahman and Lo, 2014). Consequently, the liquefaction potential of loose silty sands increases with decreasing confining stress at low stress range, which is the reverse of conventional clean sand behavior observed in the literature (i.e. volumetric contractive tendency increases with increasing confining stress). When the consolidation stage ended, the strain controlled undrained triaxial shearing stage was started with an axial strain rate of 0.05%/min. Besides, such a relatively small deformation rate is used because the previous research exhibited that the volumetric contractiveness of silty sands increases with decreasing strain rate and therefore, slow deformation control is recommended for liquefaction testing (Yamamuro and Lade, 1998).

Figure 3.6 : Triaxial equipment used during experiments.

Once the consolidated undrained triaxial compression tests conducted, the data obtained from experiments were corrected for various factors including membrane stiffness, piston friction, piston uplift, buoyancy, and weights of piston with attached LVDT. Since lubricated ends were not used in our experiments, parabolic area correction was applied for slightly barreling specimen. Since the mean grain diameter of the utilized soils were generally small (Table 3.1), membrane penetration effect was considered as negligible and not included in our corrections. (Frydman et al., 1973; Lade and Hernandez, 1977).

3.4 Scanning electron microscopes (SEM)

Scanning Electron Microscopes (SEM) of Nanobiotechnology Center of Yeditepe University is used with the scope of determination of silts' shape used in the previous experimental programs. Scanning electron microscope (SEM) is a type of electron microscope which produces images of sample by scanning it with focused beam of electrons. In fact, the electrons interact with atoms in the sample and produce various signals that comprise information about the sample's surface topography. Mentioned electron beam is scanned in a raster scan pattern and the beam's position is combined with the detected signal to produce an image. It should be noted that SEM equipment have the ability to achieve resolution better than 1 nanometer. Figure 3.5 shows the SEM device of yeditepe university used in this part of study.

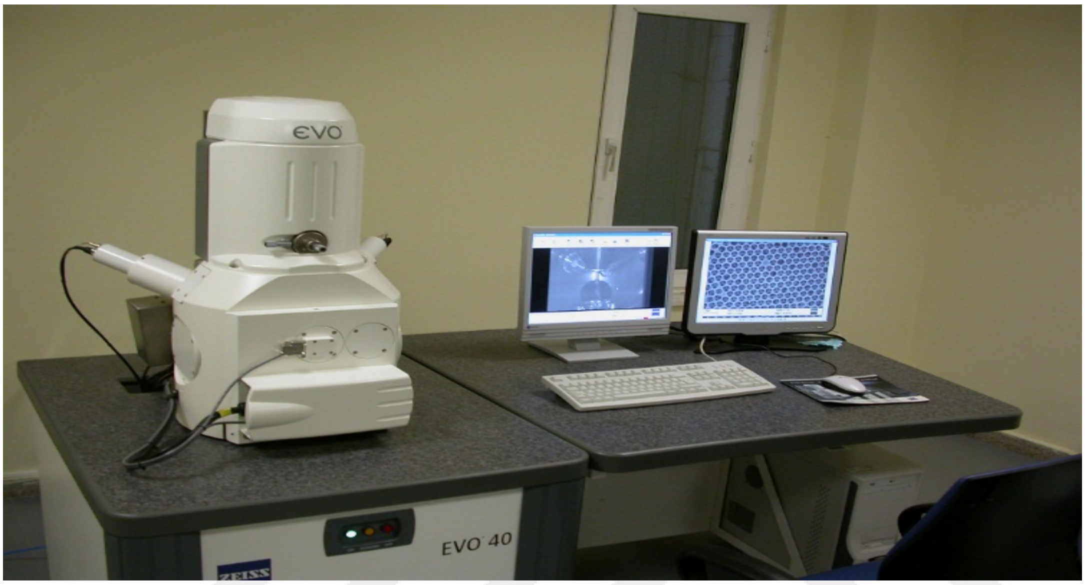

Figure 3.7 : Scanning Electron Microscopes (SEM) of Yeditepe University.

4. INFLUENCE OF CONTENT, GRADATION AND SHAPE CHARACTERISTICS OF SILTS

4.1 Undrained Triaxial Compression Test Results and Effect of Fines Content on Liquefaction Potential of Sile Sands

4.1.1 Undrained triaxial compression tests on sile sand 80/100

Figure 4.1(a) shows the change of deviator stress with axial strain when TT silt was added to the Sile Sand 80/100. Corresponding stress paths are shown in Figure 4.1(b) on a Cambridge p'-q diagram. Accordingly, static liquefaction potential of Sile Sand 80/100 had consistently increased with increasing fines content (FC) for the studied range (FC≤ 25%). In fact, specimens involving 15% and 25% TT silt have both shown static liquefaction, i.e. after the initial peak, the deviator stress was reduced to zero with progressing axial strain due to excess pore pressure generation. The conclusion of increasing liquefaction potential with increasing fines content is valid either the "loosest possible density after deposition (i.e. quasi-natural void ratio achieved by the same deposition technique)" or the same relative density is used as a comparison basis. One can compare the results at Dr = 29%, at which the curves for clean sand and sand with 5% and 15% TT silt would move upwards (i.e. would show relative increase in liquefaction resistance than shown in Figure 4.1). The void ratios of the tested specimens shown in Figure 4.1 indicates a slightly increasing trend with increasing FC, meaning that the base sand matrix has become looser with the addition of TT silt.

When SI silt was added to the Sile Sand 80/100, the resulting stress strain response and the stress paths are shown in Figure 4.2. Once again, liquefaction potential consistently increased with increasing FC. This conclusion is valid either the loosest possible density after deposition or similar relative density or similar void ratio are used as comparison bases. One can compare the results considering Dr=22.8% ± 1.7%, as well as considering e=0.905 ± 0.008 for the specimens in Figure 4.2. Note that for SI silt, only specimen with 25% fines content showed liquefaction, whereas specimens

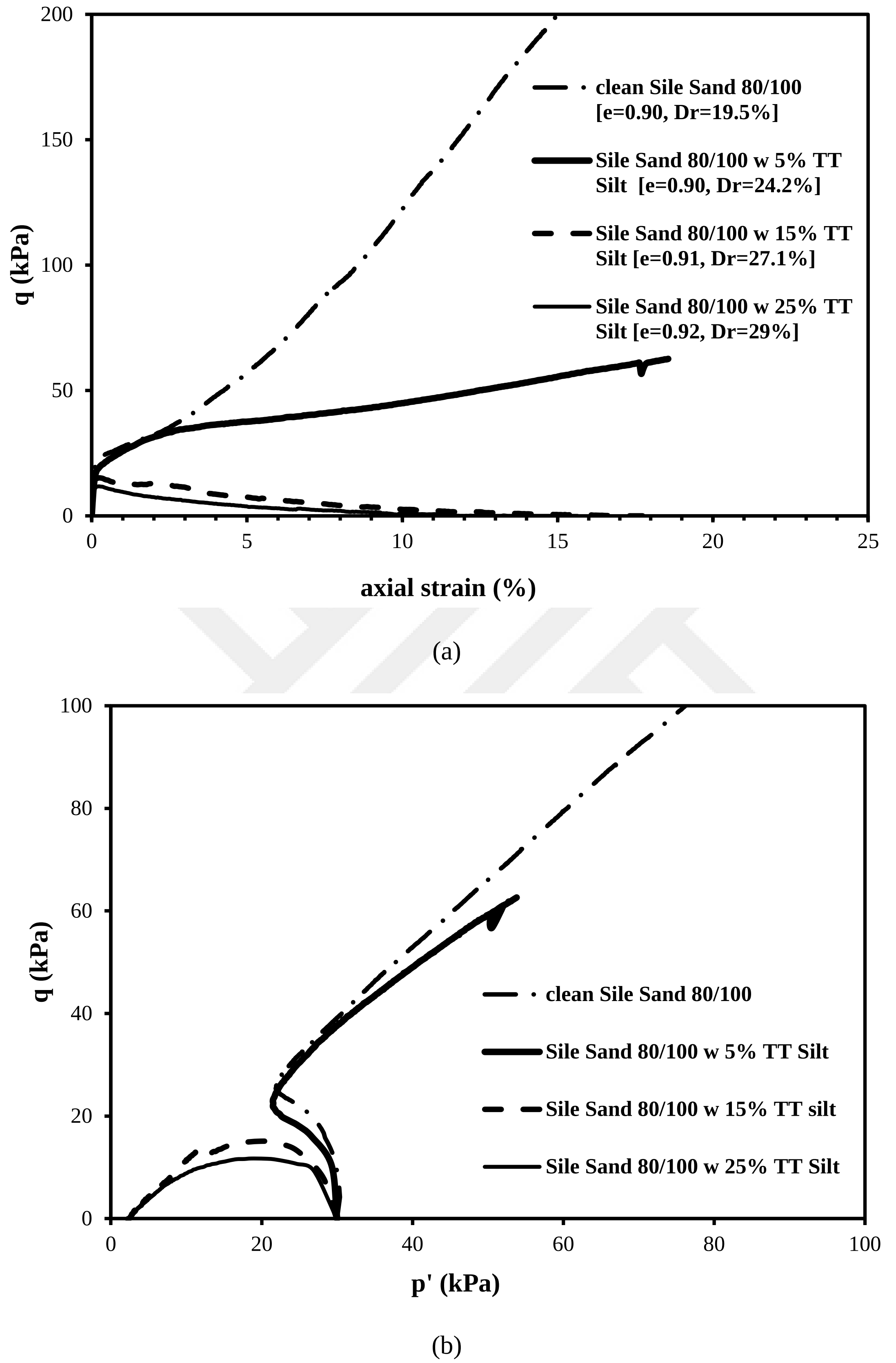

Figure 4.1 : (a) Deviator stress versus axial strain response; (b) Corresponding effective stress paths for Sile Sand 80/100 with different amounts of TT silt.

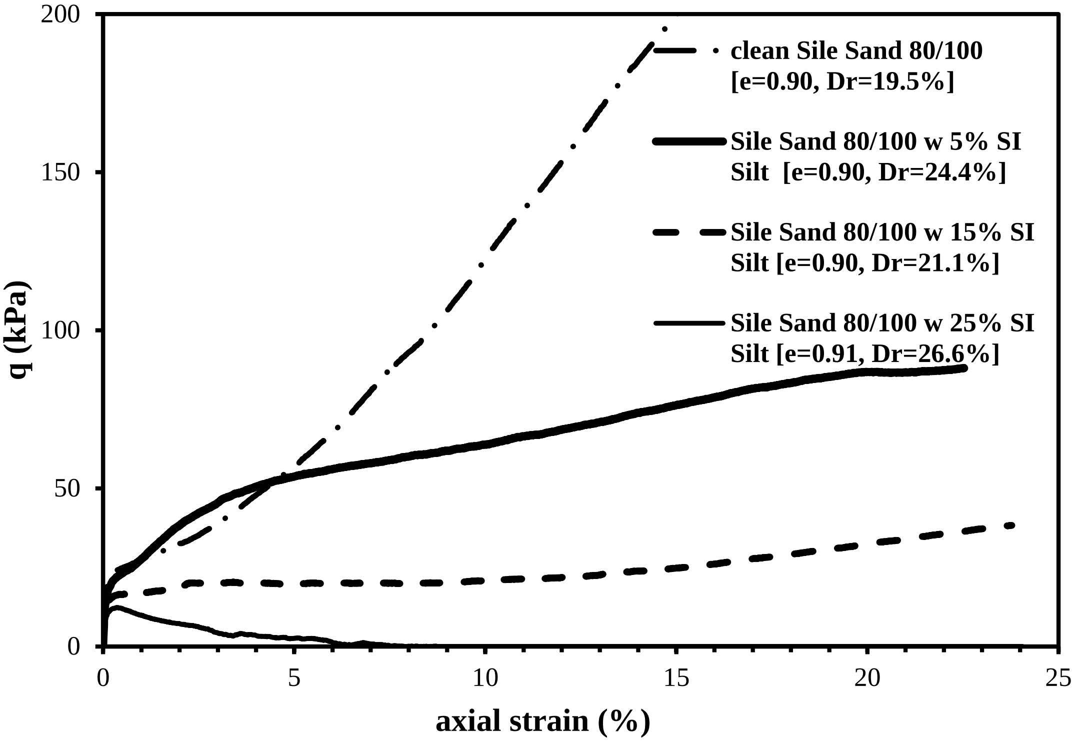

(a)

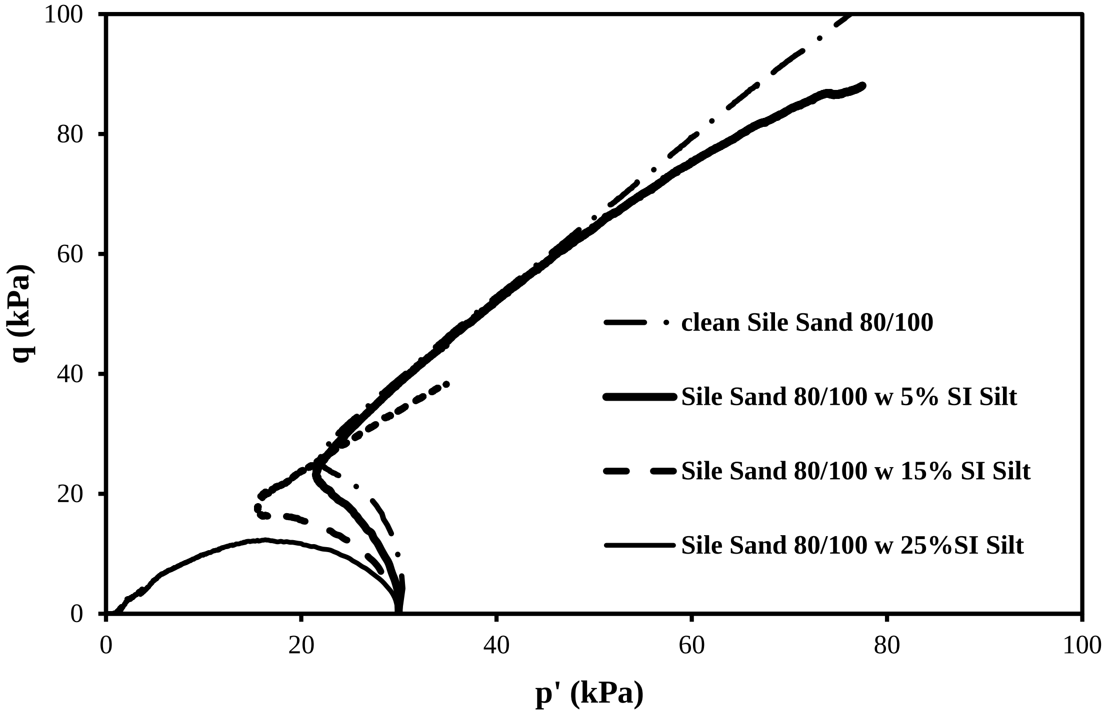

(b)

Figure 4.2 : (a) Deviator stress versus axial strain response; (b) Corresponding effective stress paths for Sile Sand 80/100 with different amounts of SI silt.

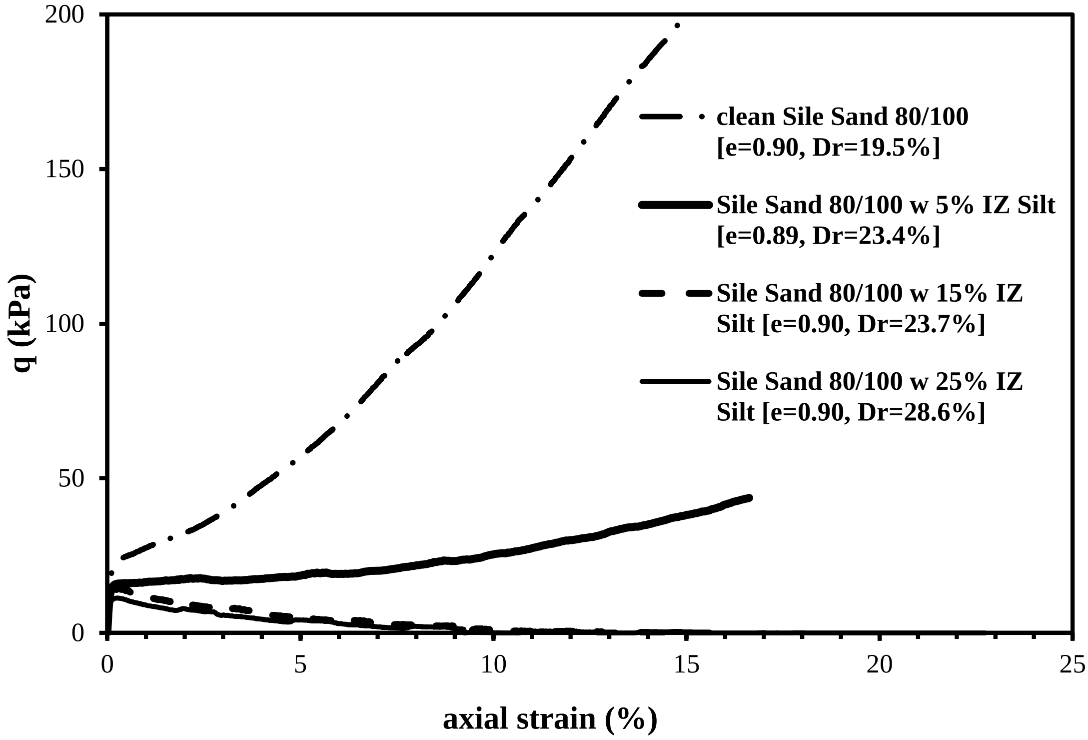

(a)

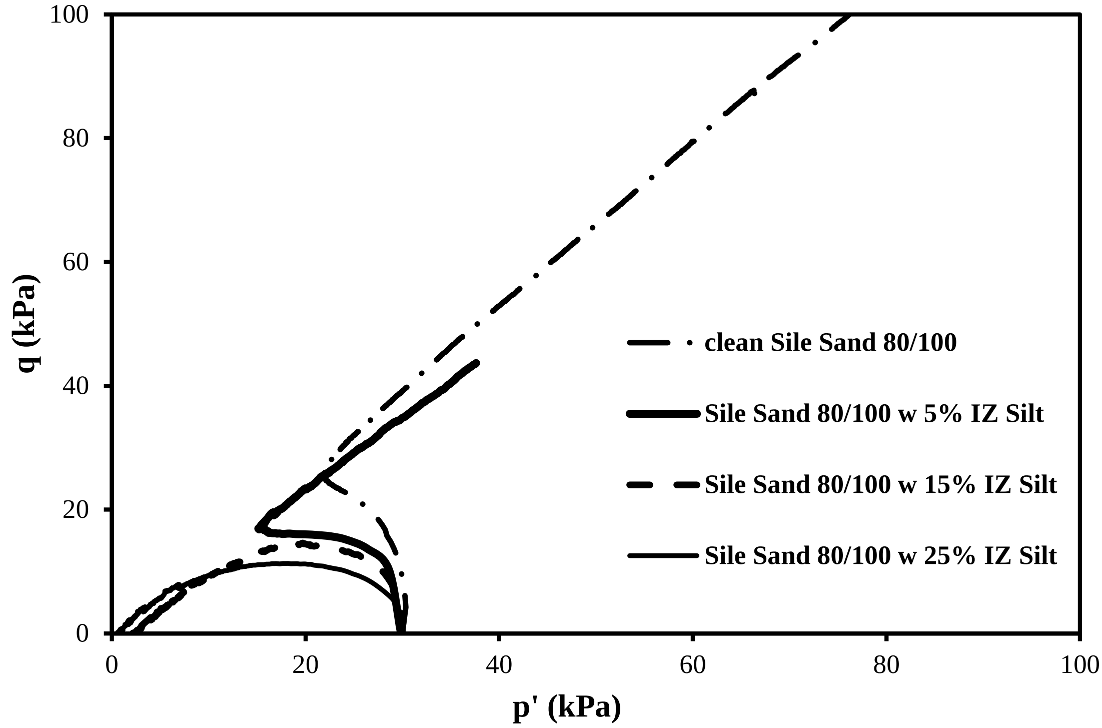

(b)

Figure 4.3 : (a) Deviator stress versus axial strain response; (b) Corresponding effective stress paths for Sile Sand 80/100 with different amounts of IZ silt.

with lower FC were stable (i.e. the deviator stress did not show any noticeable drop and continued to increase throughout shearing).

When IZ silt was added to the Sile Sand 80/100, the resulting stress strain response and the stress paths are shown in Figure 4.3. Similar to other silt types, liquefaction potential of Sile Sand 80/100 had consistently increased with increasing FC. As seen in Figure 4.3(b), Sile Sand 80/100 with 5% IZ silt was barely stable, where stress path became horizontal before the deviator stress further increased after phase transformation. Therefore, this specimen can be assumed to be at the boundary between stable behavior (no decrease in deviator stress) and temporary liquefaction (temporary drop in deviator stress during undrained shearing).

Specimens involving 15% and 25% IZ silt have both shown static liquefaction. The conclusion of increasing liquefaction potential with increasing fines content is valid either the loosest possible density after deposition or same relative density or similar void ratio are used as comparison bases. One can compare the results at a relative density value of 28.6%, at which curves for clean sand, sand with 5% and 15% IZ silt would shift upwards in Figure 4.3. Alternatively, one can compare the results considering similar void ratio of 0.895 ± 0.006 for the specimens in Figure 4.3. Consequently, increasing fines content of three different non-plastic silts have systematically increased the liquefaction potential of Sile Sand 80/100.

4.1.2 Undrained triaxial compression tests on sile sand 50/55

Figure 4.4(a) shows the change of deviator stress with axial strain when TT silt was added to the Sile Sand 50/55. Corresponding stress paths are given in Figure 4.4(b). Accordingly, liquefaction potential consistently increased with increasing fines content (FC) for the studied range (FC≤ 25%). Specimens involving 15% and 25% TT silt have both shown static liquefaction. The conclusion of increasing liquefaction potential with increasing fines content is valid either the “loosest possible density after deposition” or same relative density is used as a comparison basis. One can compare the results considering Dr=26.3%, at which the difference between curves shown in Figure 4.4 would further increase. The void ratios of the tested specimens shown in Figure 4.4 increased with increasing FC, meaning that the base sand matrix became looser with the addition of TT silt.

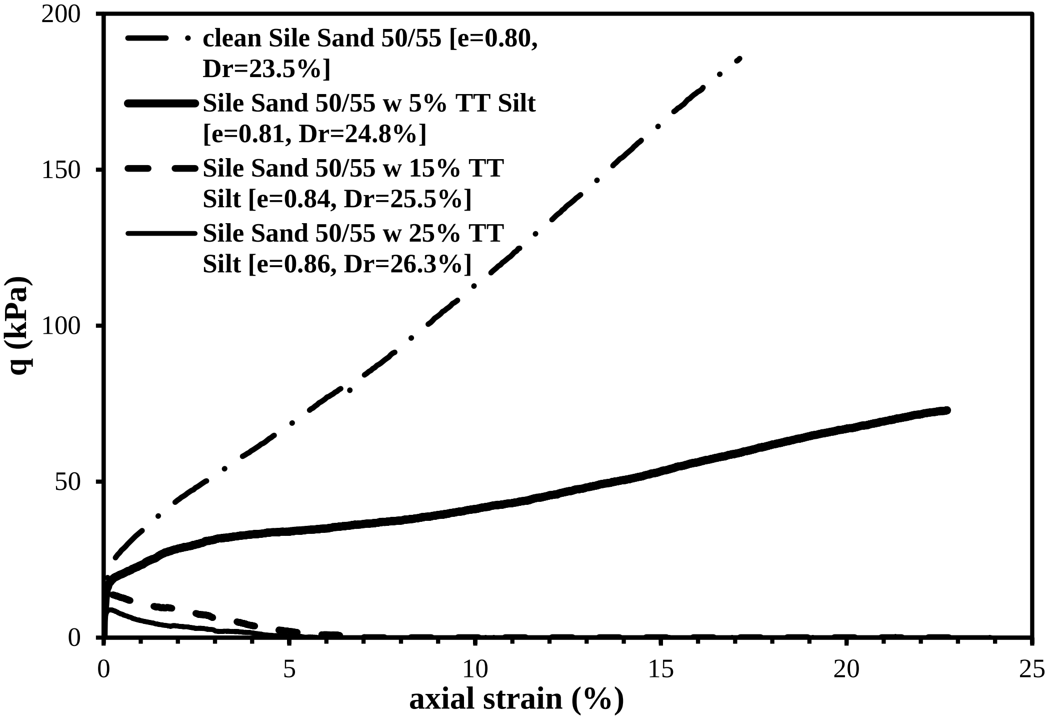

(a)

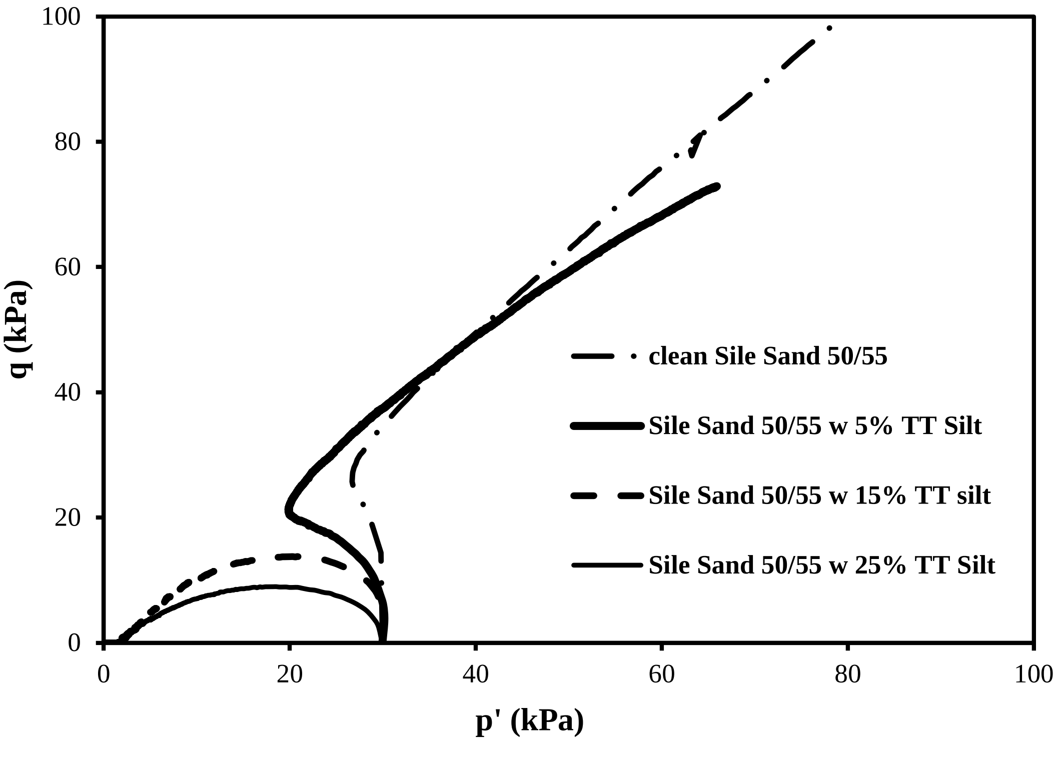

(b)

Figure 4.4 : (a) Deviator stress versus axial strain response; (b) Corresponding effective stress paths for Sile Sand 50/55 with different amounts of TT silt.

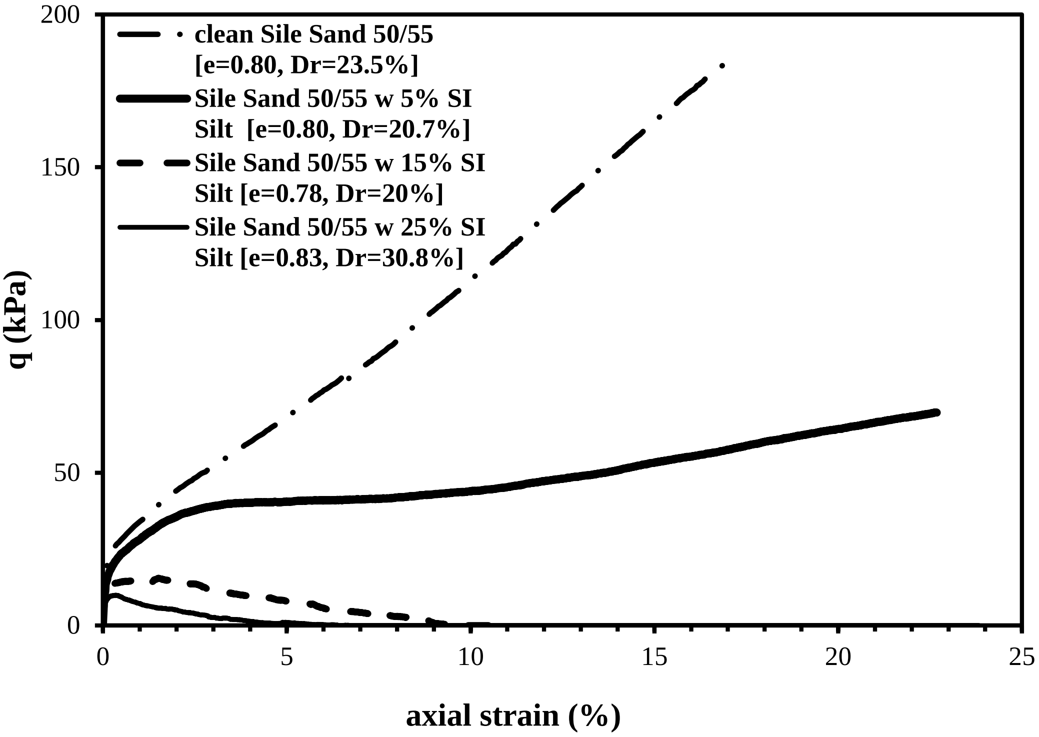

(a)

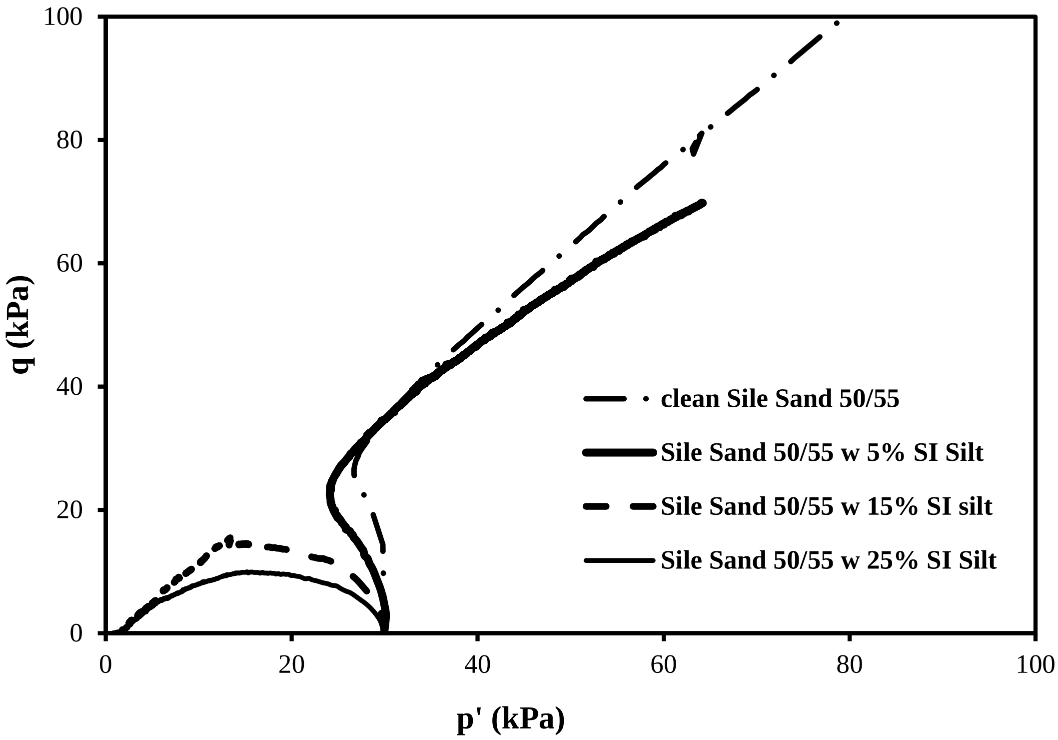

(b)

Figure 4.5 : (a) Deviator stress versus axial strain response; (b) Corresponding effective stress paths for Sile Sand 50/55 with different amounts of SI silt.

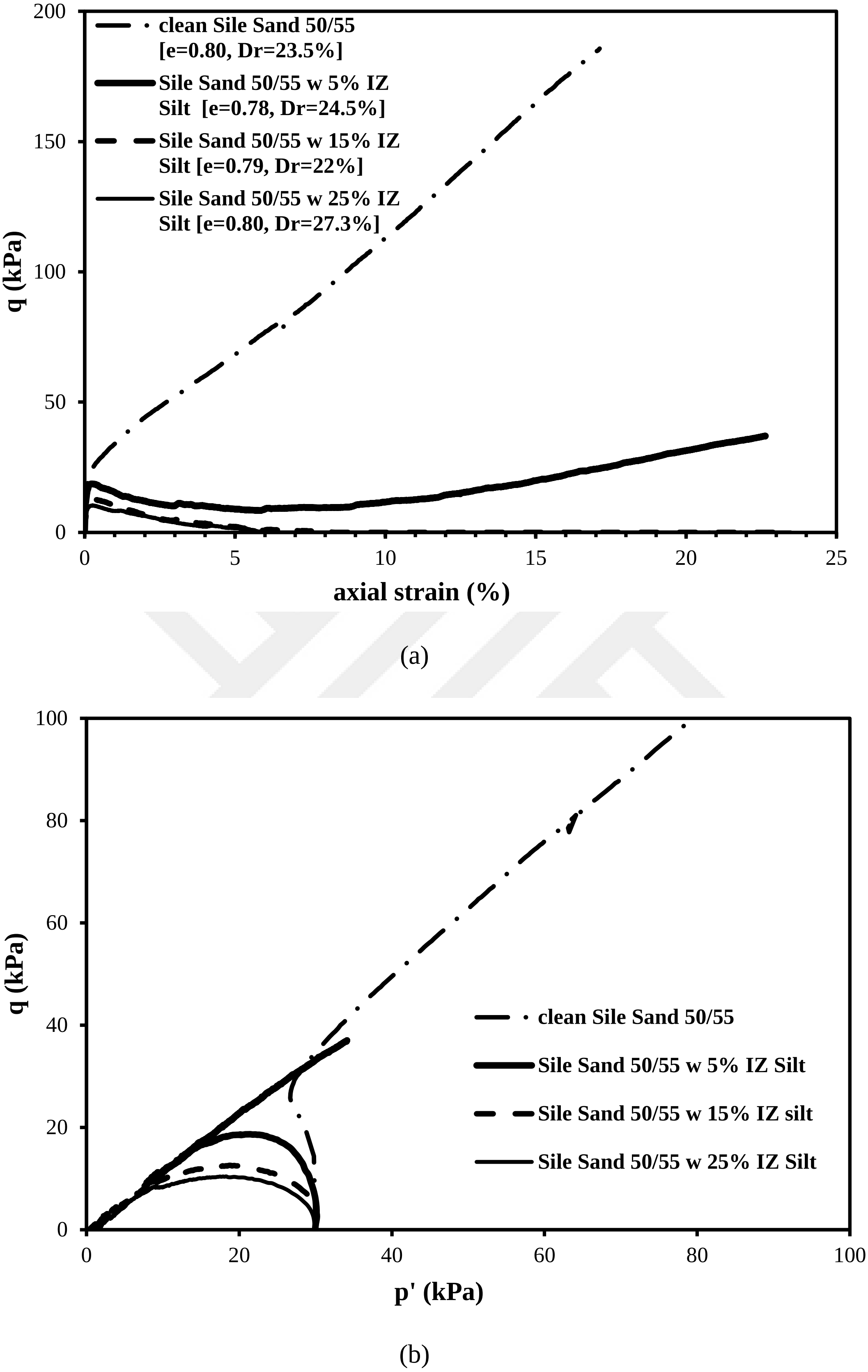

Figure 4.6 : (a) Deviator stress versus axial strain response; (b) Corresponding effective stress paths for Sile Sand 50/55 with different amounts of IZ silt.

When SI silt was added to the Sile Sand 50/55, the resulting stress strain response and the stress paths are shown in Figure 4.5. Similar to TT silt, adding SI silt to Sile Sand 50/55 consistently decreased the liquefaction resistance of resulting silty sands. Specimens with 15% and 25% SI silt have both shown static liquefaction (Figure 4.5b). When stress paths for 15% and 25% SI silt in Figure 4.5(b) are inspected, for both specimens stress paths hit corresponding effective stress failure line at a certain deviator stress level, and then followed the effective stress failure line until the stress origin. The trend of increasing liquefaction potential of soils in Figure 4.5 with fines content is valid either the same relative density (Dr=30.8%), or “loosest possible density after deposition” is used as a comparison basis.

When IZ silt was added to the Sile Sand 50/55, the resulting stress strain response and the stress paths are shown in Figure 4.6, where liquefaction potential of specimens consistently increased with increasing FC. Sile Sand 50/55 with 5% IZ silt showed temporary liquefaction. Temporary liquefaction is the condition at which the deviator stress shows a noticeable drop after an initial peak, but then started to increase again (Yamamuro and Lade, 1997). As seen in Figure 4.6(b), specimens involving 15% and 25% IZ silt have both shown static liquefaction. The conclusion of increasing liquefaction potential with increasing fines content is valid either the loosest possible density after deposition or similar relative density (Dr=23.3% ± 1.3%) are used as comparison bases. Consequently, increasing fines content of three different non-plastic silts have increased the liquefaction potential of Sile Sand 50/55.

4.1.3 Undrained triaxial compression tests on sile sand 20/30

Figure 4.7(a) shows the change of deviator stress with axial strain when TT silt was added to the Sile Sand 20/30. Corresponding stress paths are given in Figure 4.7(b). Accordingly, liquefaction potential consistently increased with increasing fines content (FC) for the studied range (FC≤ 25%). Adding 5% TT silt to Sile Sand 20/30 transformed its behaviour from stable to temporary liquefaction. Specimens involving 15% and 25% TT silt have both shown static liquefaction with similar stress-strain and stress path responses. The conclusion of increasing liquefaction potential with increasing fines content is valid for the “loosest possible density after deposition” as comparison basis. It should be noted that the void ratio of the specimen with 15% TT silt was considerably lower than the other specimens.

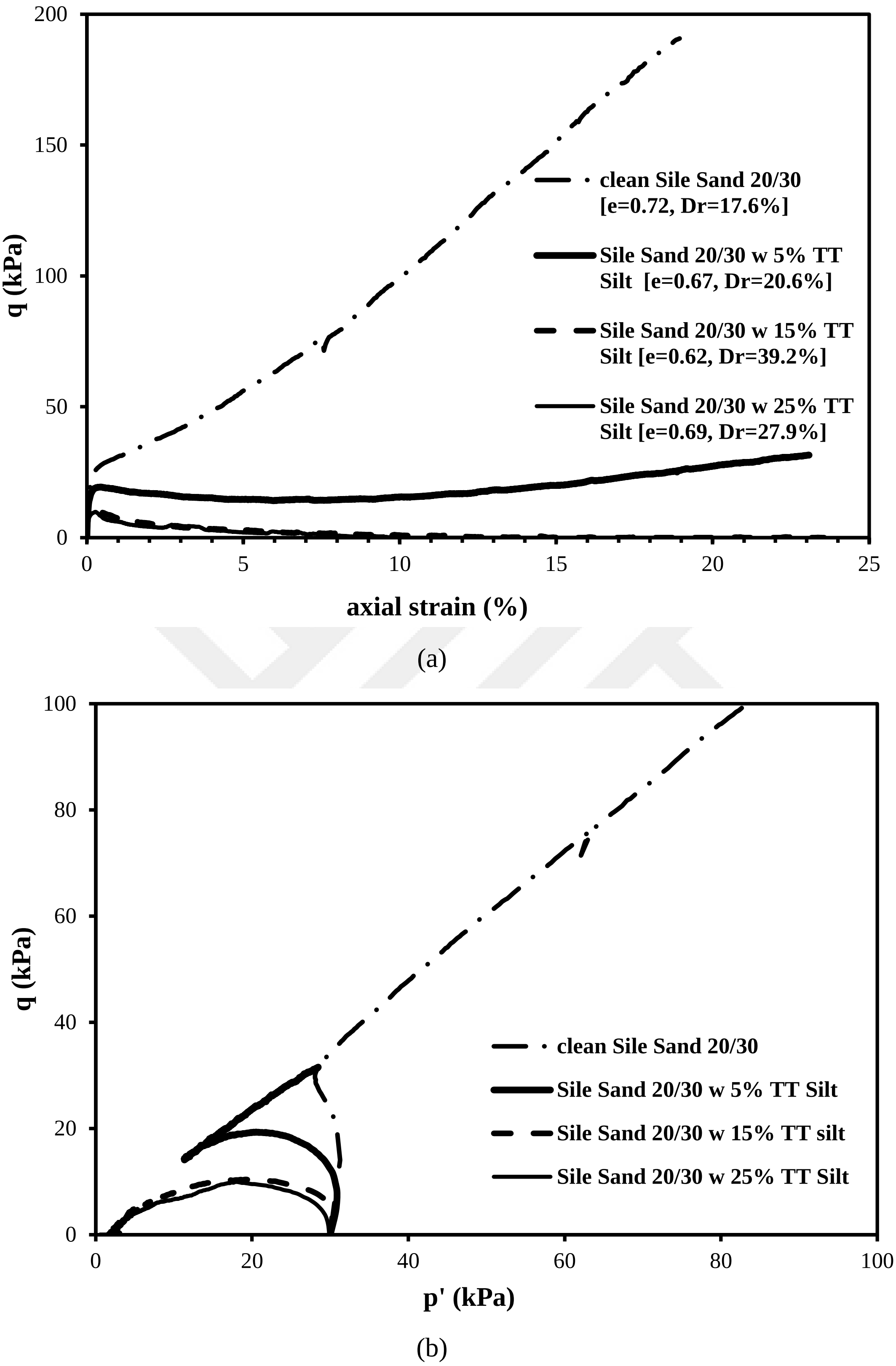

(a)

(b)

Figure 4.7 : (a) Deviator stress versus axial strain response; (b) Corresponding effective stress paths for Sile Sand 20/30 with different amounts of TT silt.

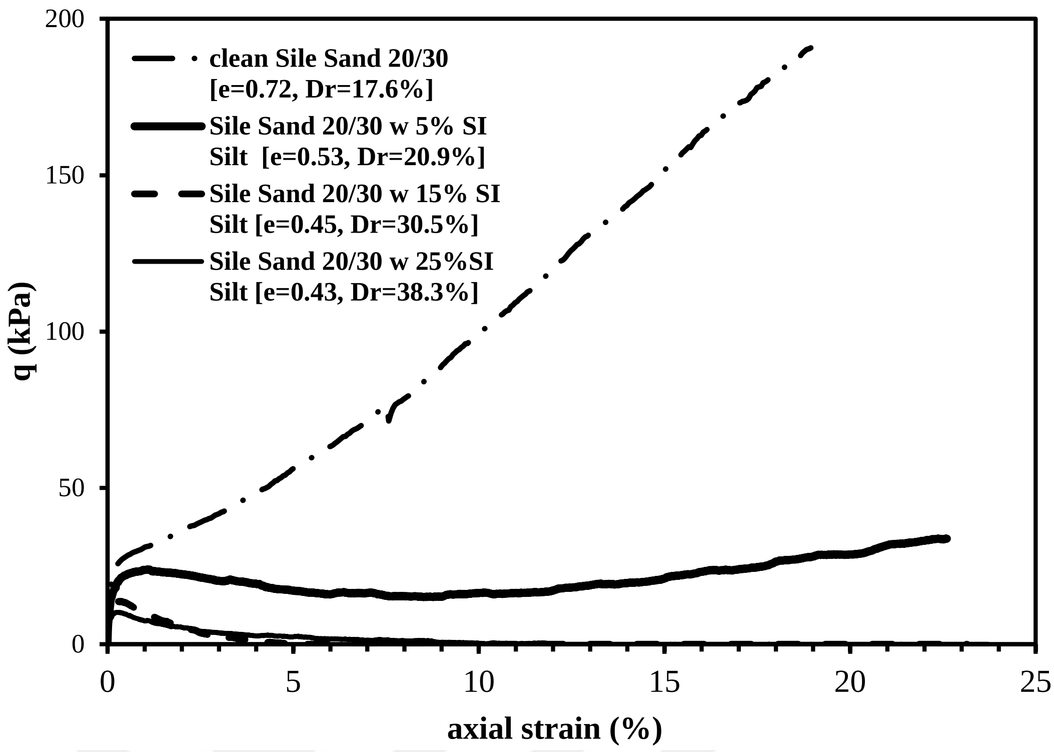

(a)

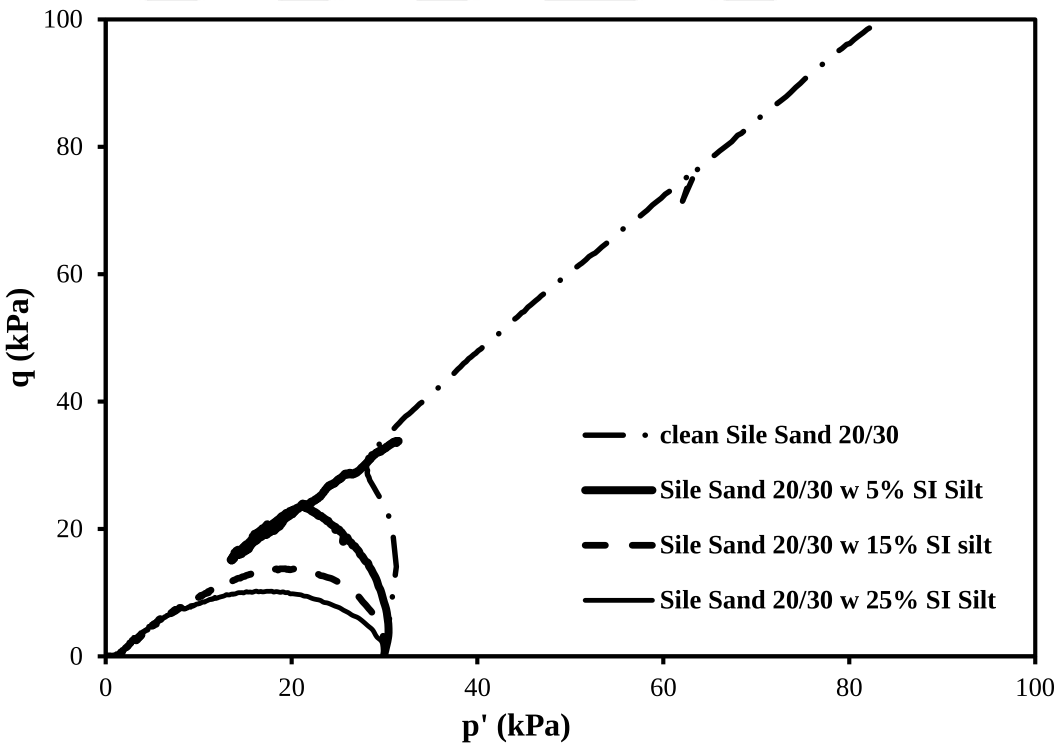

(b)

Figure 4.8 : (a) Deviator stress versus axial strain response; (b) Corresponding effective stress paths for Sile Sand 20/30 with different amounts of SI silt.

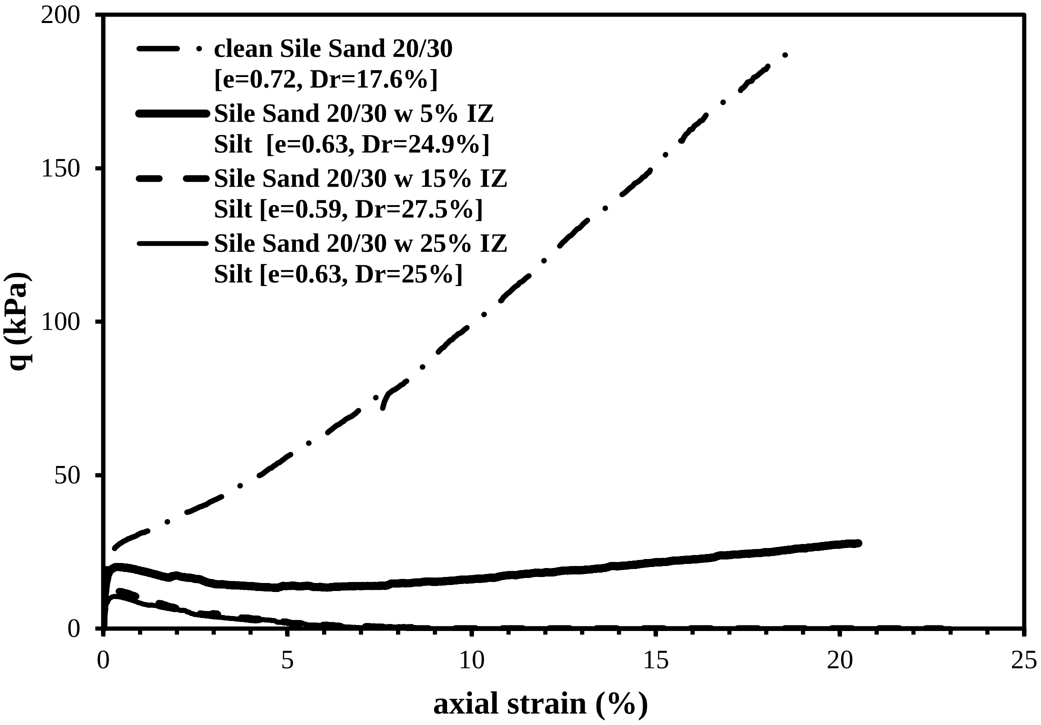

(a)

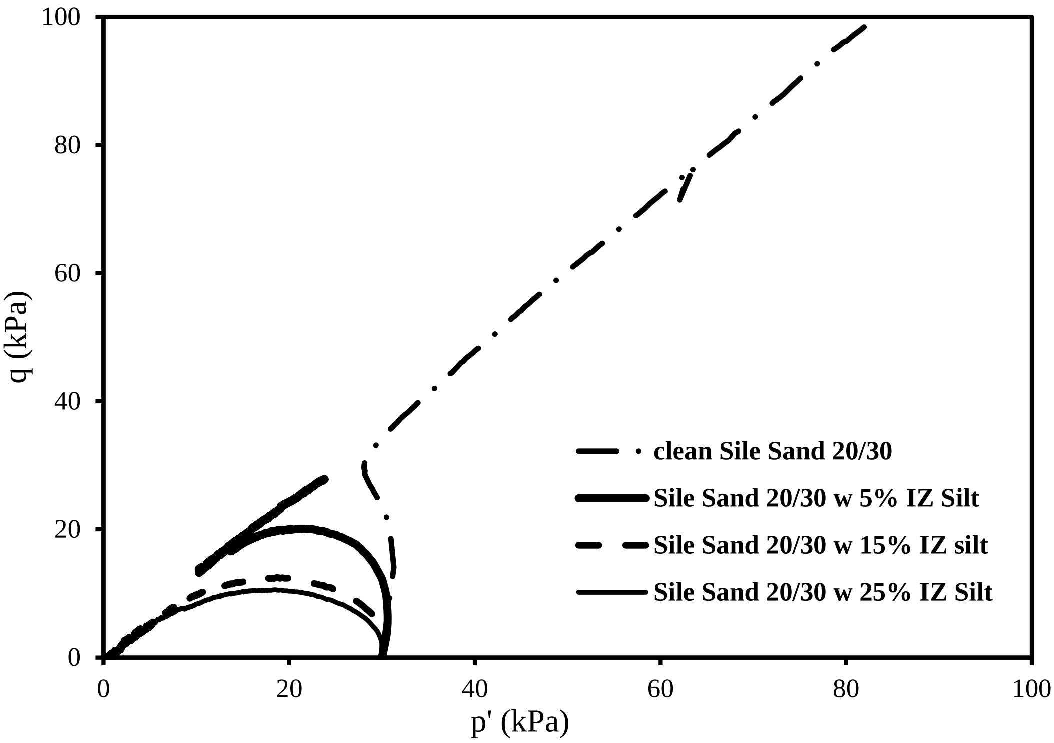

(b)

Figure 4.9 : (a) Deviator stress versus axial strain response; (b) Corresponding effective stress paths for Sile Sand 20/30 with different amounts of IZ silt.

When SI silt was added to the Sile Sand 20/30, the resulting stress strain response and the stress paths are shown in Figure 4.8. Once again, liquefaction potential consistently increased with increasing FC. This conclusion is valid either the loosest possible density after deposition or same relative density or same void ratio are used as comparison bases. One can compare the projection of test results considering Dr=38.3%, as well as considering e=0.43 for the specimens in Figure 4.8, where at e=0.43 or at Dr=38.3% stress-strain curves for clean Sile Sand 20/30, sand with 5% and 15% SI silt would shift further upwards. Adding 5% SI silt to Sile Sand 20/30 transformed its behaviour from stable to temporary liquefaction. For that case, stress path of 5% SI silt hit the corresponding effective stress failure line, and then the deviator stress had decreased along that line until a local minimum value, where it started to increase again along the effective stress failure line. With further addition of 15% and 25% SI silt, the liquefaction potential continued to increase with fines content and both specimens have shown static liquefaction (Figure 4.8b).

When IZ silt was added to the Sile Sand 20/30, the resulting stress strain response and the stress paths are shown in Figure 4.9. Liquefaction potential consistently increased with increasing FC. Sile Sand 20/30 with 5% IZ silt showed temporary liquefaction. Whereas, specimens involving 15% and 25% IZ silt have both shown static liquefaction. The conclusion of increasing liquefaction potential with increasing fines content is valid either the loosest possible density after deposition or similar relative density (Dr=26.2% ± 1.3%) are used as comparison bases. Consequently, increasing fines content of three different non-plastic silts have increased the liquefaction potential of Sile Sand 20/30.

4.1.4 Different comparison bases in literature and fines content effect

Figures 4.1 to 4.9 clearly demonstrated that the liquefaction potential of Sile Sands have increased with increasing fines content in this study (for FC≤25%). This trend is verified for three base sands mixed with three different non-plastic silts at three different fines contents. In fact, the trend of decreasing monotonic undrained shear strength with increasing fines content (below a threshold value) is in good agreement with several previous studies investigating the fines content effect by various comparison bases including loosest possible density after deposition (Zlatovic and Ishihara, 1995; Lade and Yamamuro, 1997; Monkul and Yamamuro, 2011), similar relative density (Dash and Sitharam, 2011; Belkhatir et al., 2013),and similar void ratio (Huang et al., 2004; Dash and Sitharam, 2011; Yang and Wei, 2012). The observed trend is also in agreement with the studies based on critical state framework where a downward shift of steady state line with increasing fines content was reported (Murthy et al., 2007; Papadopoulou and Tika, 2008; Rahman et al., 2008; Yang and Wei, 2012), implying that for a particular void ratio undrained steady state shear strength would decrease with increasing FC.

Note that establishment of the fines content effect was necessary for the soils employed in this study (i.e. for different base sand gradations, silt gradations and shape effects). This is because the influence of some silt characteristics on the liquefaction behavior is interestingly found to be dependent on the amount of fines content, which would be discussed in the following sections of this study.

It should also be noted that densities of various specimens shown in Figures. 4.1 to Figure 4.9 correspond to "loosest possible density after deposition". Detailed discussion about the concept of "loosest possible density after deposition" can be found in the study of Monkul et al. (2016), but basically this comparison basis assumes that soils with different grain compositions would tend to fall in to a "quasi natural" void ratio provided that the deposition style and energy is kept the same. As an example, change of consolidated "quasi natural" void ratios of Sile Sand 20/30 specimens analysed in figures. 4.7 to 4.9 is plotted in figure 4.10. Accordingly, as fines content is increased, both IZ and TT silts had initially caused a decrease in the void ratio of the Sile Sand 20/30 specimens until about 15% FC and then a relative increase. Meanwhile, increasing contents of SI silt had steadily continued to decrease the void ratio of Sile Sand 20/30 for the studied range (i.e. FC≤25%). Observing a decreasing trend of "quasi natural void ratio" with increasing fines content up to a threshold value is not surprising, which implies that silt grains tend to fall in to the intergranular void space between the sand grains during deposition and consolidation stages, causing a decrease in void ratio. However, what is surprising in Figure 4.10 is that specimens involving TT silt had greater quasi-natural void ratios compared to specimens involving other silt types regardless of the value of FC. This is an interesting observation, considering that TT silt is the finest of three non-plastic silts used in this study (Figure 3.3, Table 3.1), and expected to fit and occupy the void space between the sand skeleton easier compared to both IZ and SI silts. Figure 4.10 clearly demonstrates that differences in characteristics of the silt matrix within sand influence the quasi natural void ratio and therefore the initial fabric of the sand specimens.

4.2 Effect of Silt Characteristics on Liquefaction Potential of Sile Sands

In order to investigate how different silt characteristics, influence the static liquefaction potential of Sile Sands, stress-strain graphs of each base sand with different silt types at specific fines contents were re-plotted in Figures 4.11 to Figure 4.13.

Figure 4.11(a) shows the change of deviator stress with axial strain for Sile Sand 80/100 involving 5% fines content of different non-plastic silt gradations. It can be seen that 5% FC have decreased the liquefaction resistance of Sile Sand 80/100 compared to clean sand at different levels, even though all specimens showed stable behavior. Considering that the deposition technique, initial stress conditions, base sand gradation and fines content were kept the same, the variations in liquefaction resistance of Sile Sand 80/100 in Figure 4.11(a) were due to changes in silt characteristics including grain size distribution, grain shape effects and perhaps mineralogy. The stress-strain response of Sile Sand 80/100 with 15% of different silts are shown in

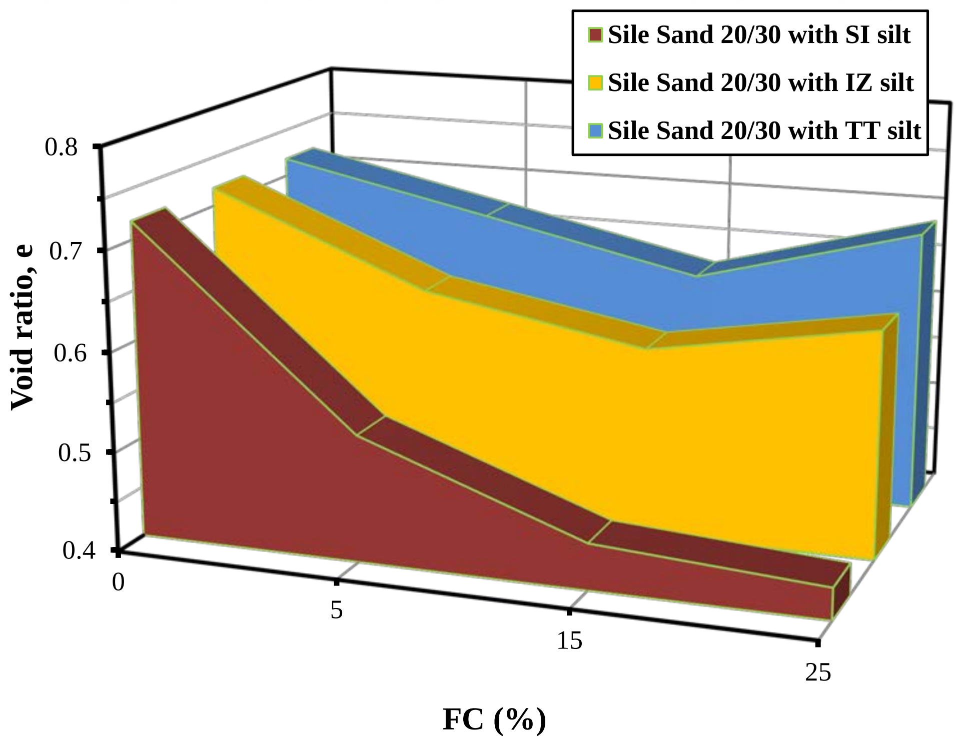

Figure 4.10 : Change of consolidated void ratios of Sile Sand 20/30 specimens with fines content and different silts.

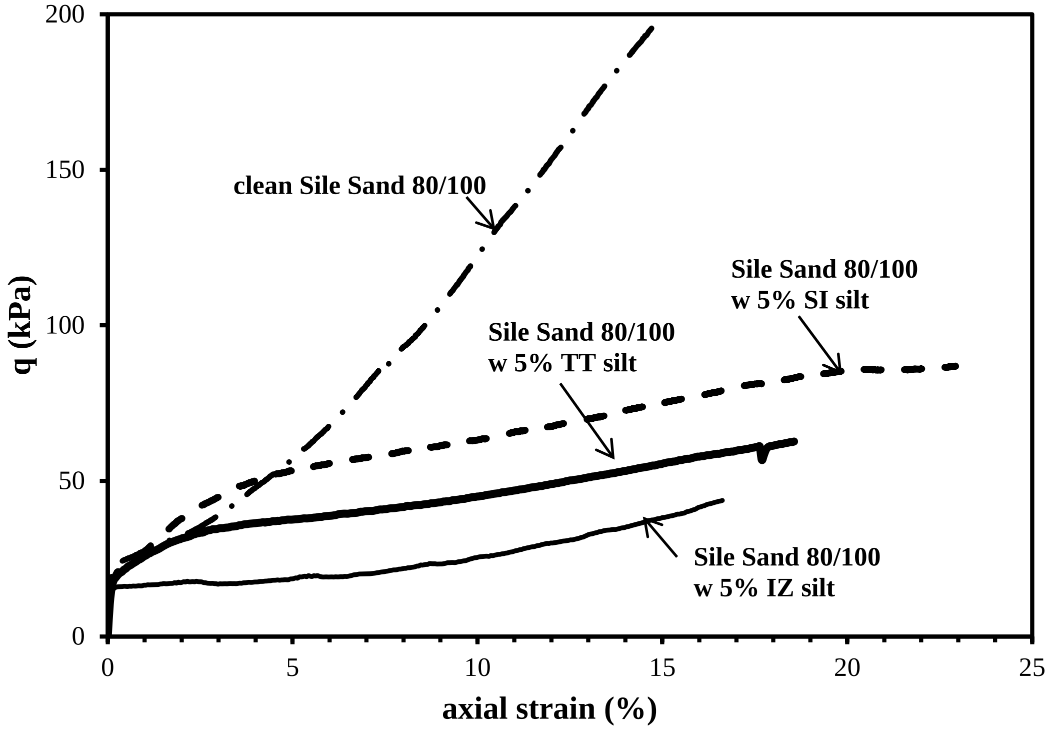

200
150
100
50
0
q (kPa)
0
5
10
15
20
25
axial strain (%)
clean Sile Sand 80/100
Sile Sand 80/100
w 5% SI silt
Sile Sand 80/100
w 5% TT silt
Sile Sand 80/100
w 5% IZ silt

(a)

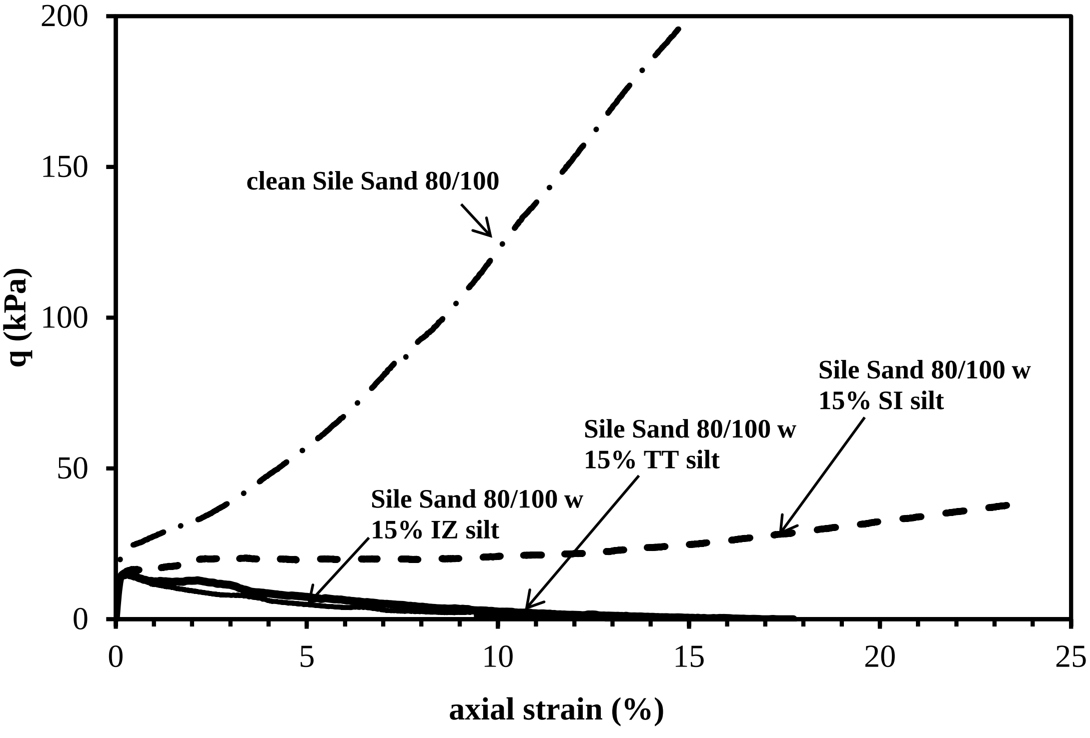

200
150
100
50
0
q (kPa)
0
5
10
15
20
25
axial strain (%)
clean Sile Sand 80/100
Sile Sand 80/100 w
15% SI silt
Sile Sand 80/100 w
15% TT silt
Sile Sand 80/100 w
15% IZ silt

(b)

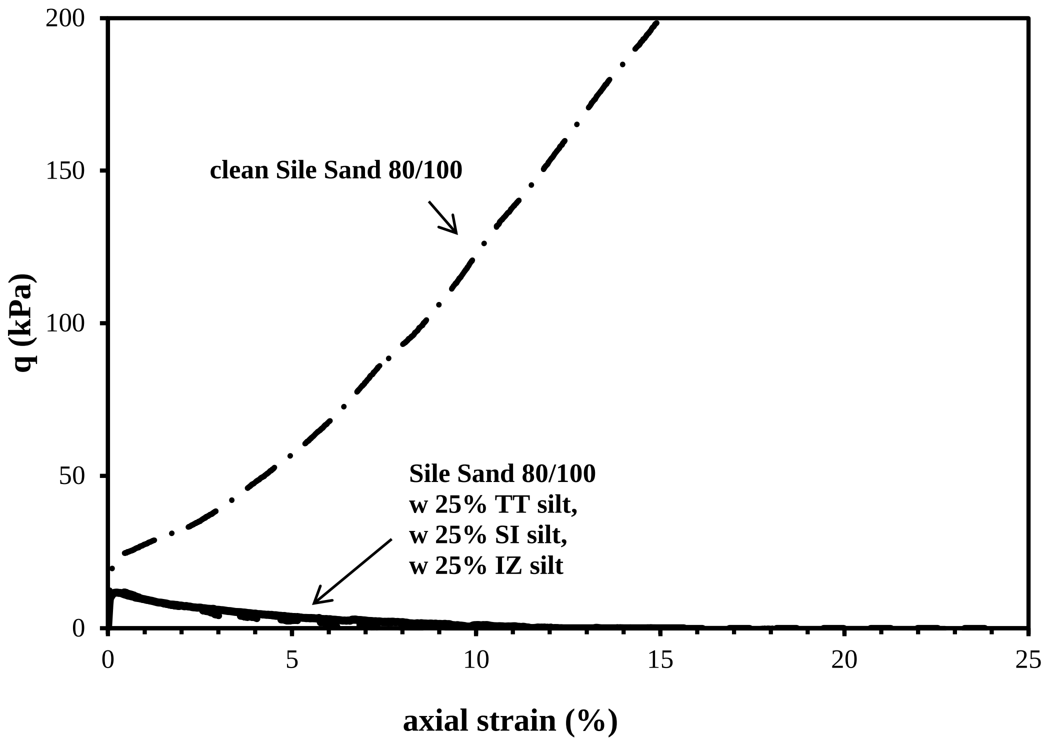

(c)

Figure 4.11 : Deviator stress versus axial strain response of Sile Sand 80/100 (a) with 5% fines content, (b) with 15% fines content, (c) with 25% fines content of different non-plastic silts.

figure 4.11 (b), where specimens with 15% TT and IZ silts have both shown static liquefaction, and stress-strain curve of specimen with TT silt was only very slightly above the specimen with IZ silt. Whereas, specimen with 15% SI silt has shown stable response. As fines content was increased to 25%, all specimens had liquefied and the stress-strain responses of Sile Sand 80/100 specimens became almost identical independent of the silt characteristics (figure 4.11(c)).

When 5% fines are added to Sile Sand 50/55, the resulting stress-strain response of sand specimens with different non-plastic silts is given in Figure 4.12(a). Adding 5% silt to Sile Sand 50/55 has decreased its liquefaction resistance compared to clean sand. Specimens involving 5% of SI and TT silts have both shown stable behavior, with the stress-strain curve of 5% SI silt being slightly above the one of 5% TT silt. Whereas, adding 5% IZ silt caused Sile Sand 50/55 to show temporary liquefaction (Figure 4.12(a)). When 15% silt was added to Sile Sand 50/55, there was a significant increase in liquefaction potential compared to sand with 5% FC. All silty sand specimens with

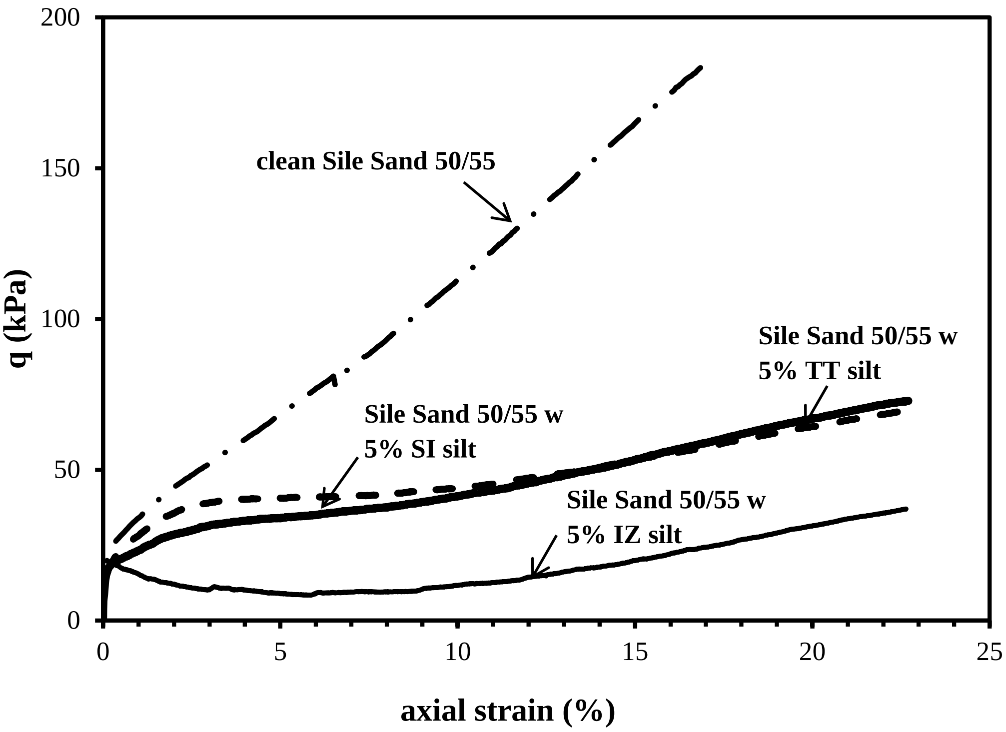
200
150
100
50
0
0
5
10
15
20
25
q (kPa)
axial strain (%)
clean Sile Sand 50/55
Sile Sand 50/55 w
5% TT silt
Sile Sand 50/55 w
5% SI silt
Sile Sand 50/55 w
5% IZ silt

(a)

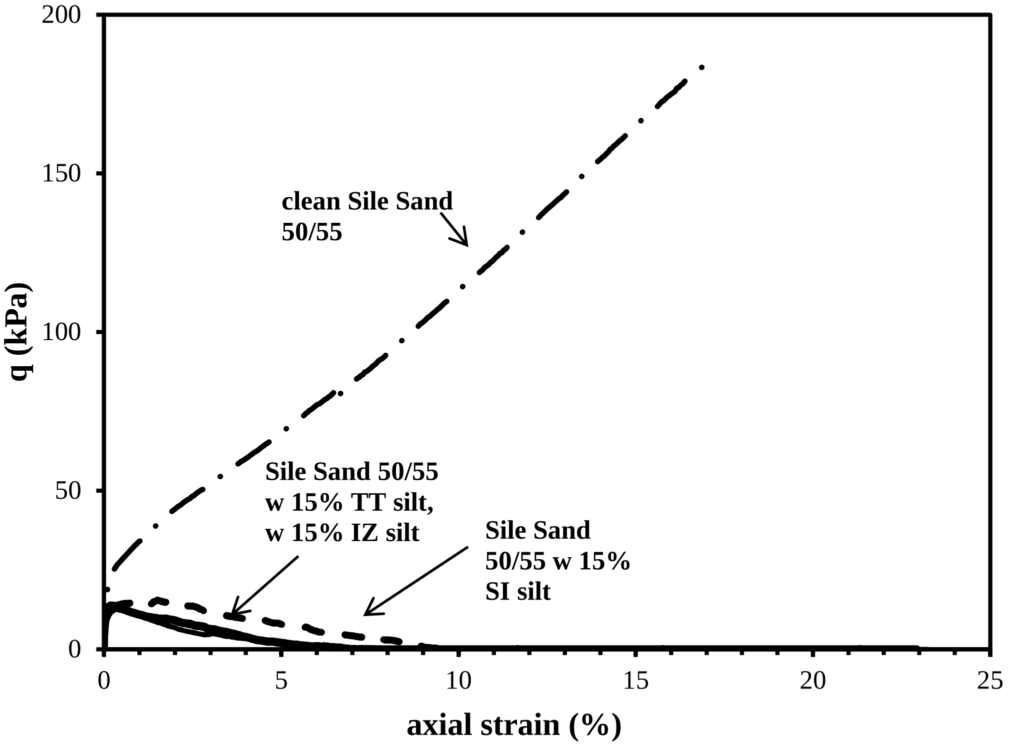
200
150
100
50
0
0
5
10
15
20
25
q (kPa)
axial strain (%)
clean Sile Sand
50/55
Sile Sand 50/55
w 15% TT silt,
w 15% IZ silt
Sile Sand
50/55 w 15%
SI silt

(b)

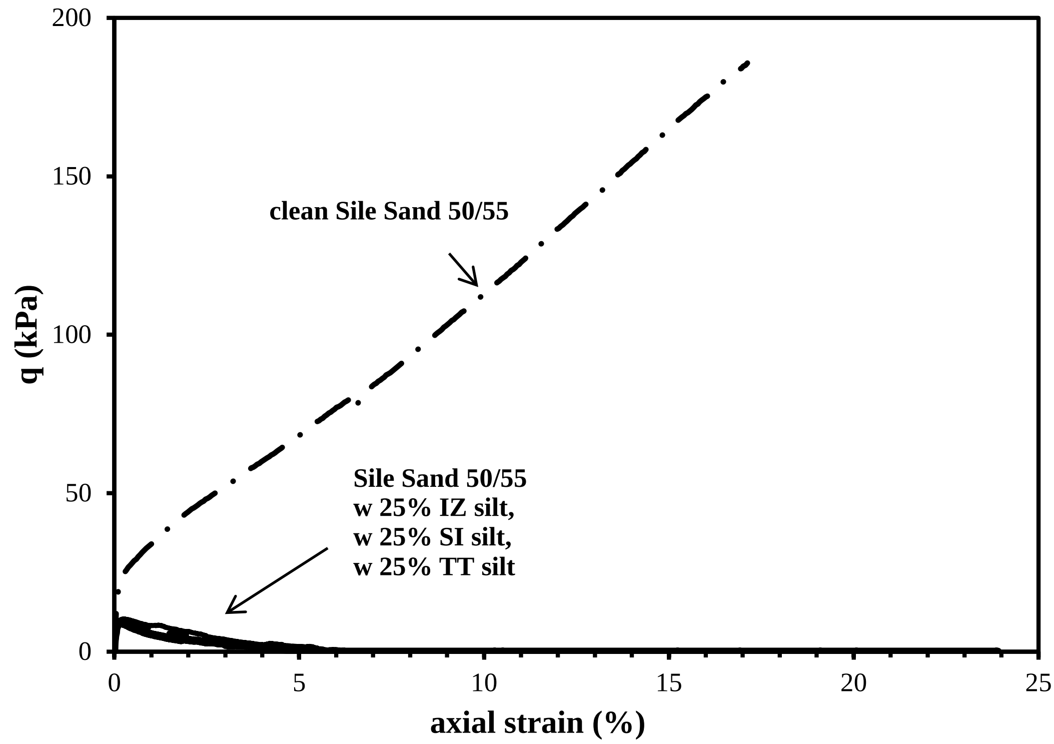

(c)

Figure 4.12 : Deviator stress versus axial strain response of Sile Sand 50/55 (a) with 5% fines content, (b) with 15% fines content, (c) with 25% fines content of different non-plastic silts.

15% FC showed static liquefaction as shown in Figure 4.12(b), in which stress-strain curve for specimen with 15% SI silt was located slightly above the other two specimens. With further increase of fines content to 25%, once again the responses became almost identical independent of the silt characteristics and all specimens continued to liquefy (Figure 4.12(c)).

Stress-strain response of Sile Sand 20/30 involving 5% fines content of different non-plastic silts is given in Figure 4.13(a), in which all specimens had shown temporary liquefaction. Stress-strain curve for the specimen with 5% SI silt was slightly above the curves of other specimens with TT and IZ silts (Figure 4.13(a)). Figure 4.13(b) shows that when 15% silt was added to Sile Sand 20/30, undrained behaviors were transformed from temporary liquefaction to complete static liquefaction for all silt types. Moreover, there was no practical difference between the stress-strain responses of specimens involving different silt types in figure 4.13(b). With further increase of

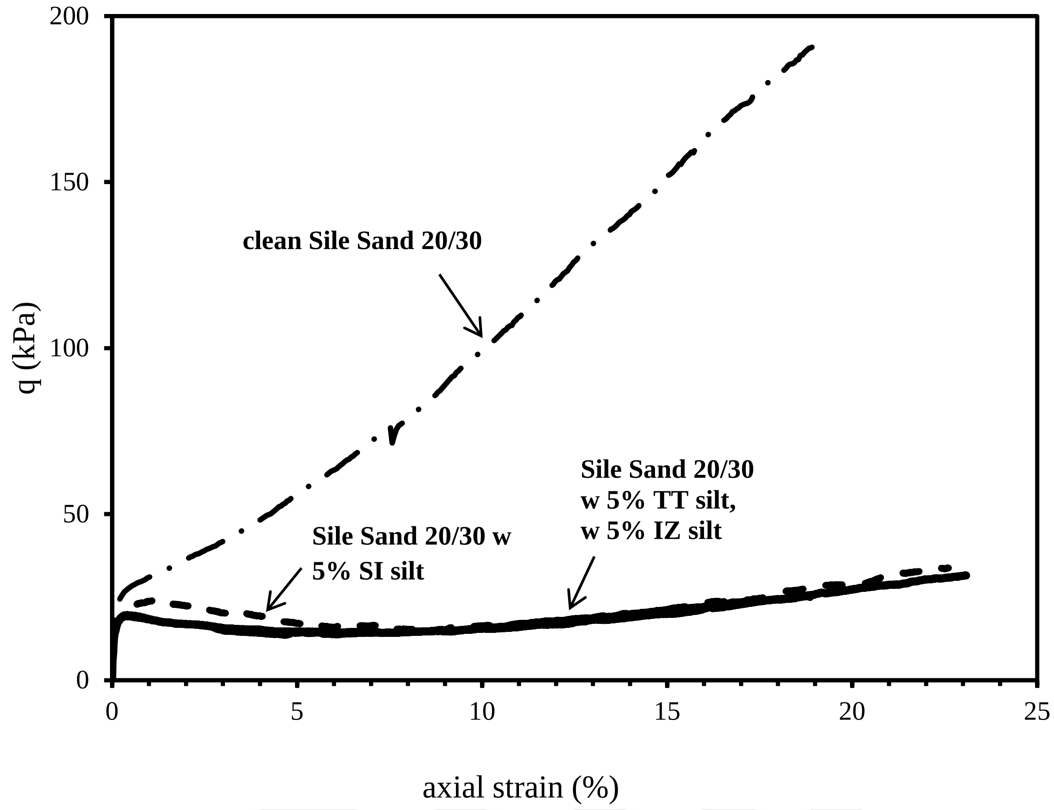

clean Sile Sand 20/30
Sile Sand 20/30
w 5% TT silt,
w 5% IZ silt
Sile Sand 20/30 w
5% SI silt
q (kPa)
axial strain (%)

(a)

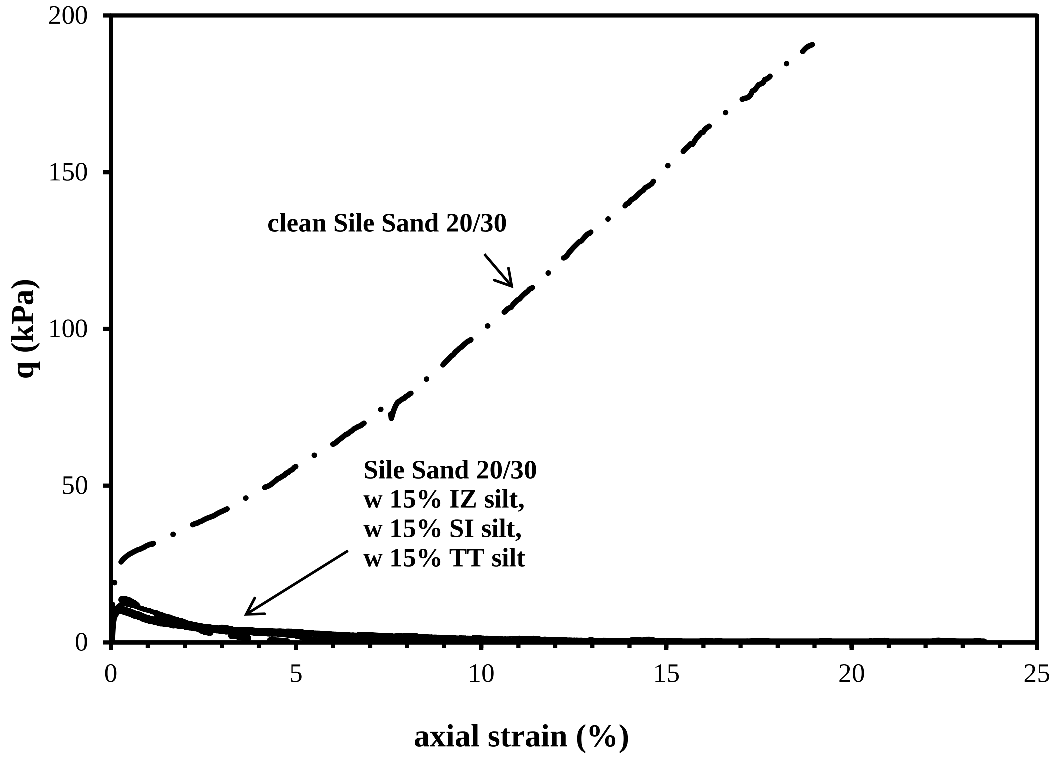

clean Sile Sand 20/30
Sile Sand 20/30
w 15% IZ silt,
w 15% SI silt,
w 15% TT silt
q (kPa)
axial strain (%)

(b)

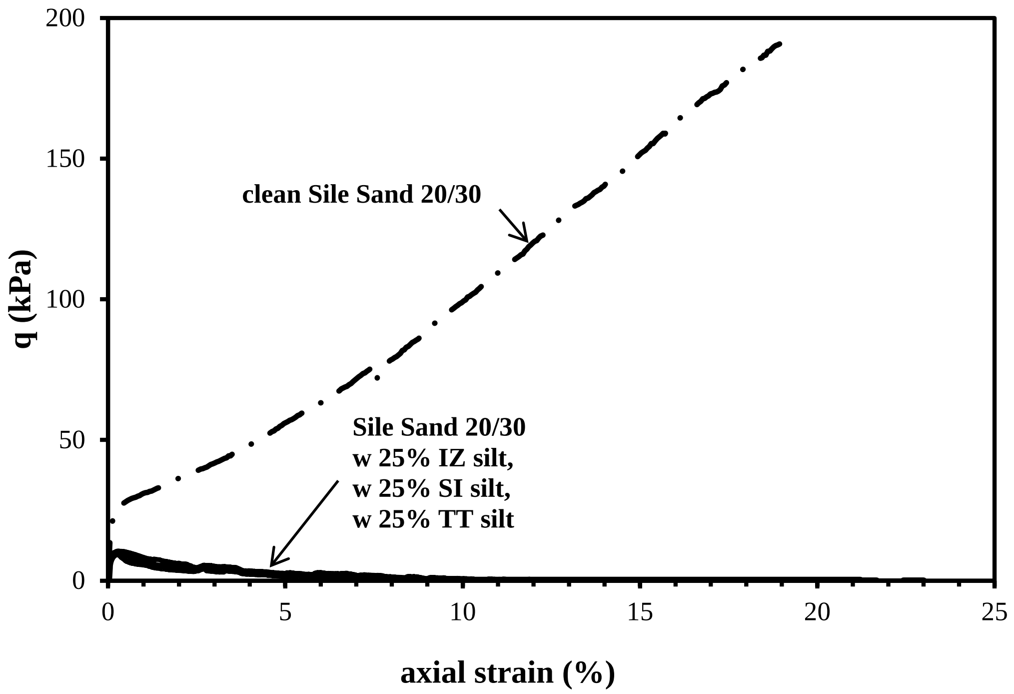

(c)

Figure 4.13 : Deviator stress versus axial strain response of Sile Sand 20/30 (a) with 5% fines content, (b) with 15% fines content, (c) with 25% fines content of different non-plastic silts.

fines content to 25%, the specimens continued to liquefy with identical stress-strain responses independent of the silt characteristics (Figure 4.13(c)).

4.2.1 Influence of mean grain size and grain size distribution of silt grains

Several trends regarding the impact of silt gradation on liquefaction potential can be observed in Figures 4.11 to 4.13. The first one is that, at low fines contents such as 5% and 15%, sands involving SI silt generally had the lowest liquefaction potential (or the greatest liquefaction resistance) compared to sands with TT and IZ silts. Meanwhile, at the same fines contents (i.e. FC=5% and 15%), sands involving IZ silt generally had the greatest liquefaction potential (or the lowest liquefaction resistance). Hence, for the same initial stress conditions, fines content, base sand gradation and mineralogy, the liquefaction potential of the sands in this study increased with SI, TT and IZ silts respectively at low fines contents (i.e. $0<FC\leq15\%$). One might think that for some base sands, such as Sile Sands 50/55 and 20/30, consolidated void ratios (e) at the same FC were considerably different (see Table 4.1) depending on the silt type, which could influence the above mentioned order of liquefaction potential. However, such a

difference in e is the inherent output of the “loosest possible density after deposition” concept explained before. Furthermore, it is clearly visible in Figures 12 to Figure 14 that an increase in consolidated void ratio of particular base sand with different silts does not necessarily imply an increase in liquefaction potential. As an example, consolidated void ratios of specimens involving IZ silt were systematically smaller than the ones involving TT silt for Sile Sands 50/55 and 20/30 (Table 4.1), which can also be visually observed in Figure 4.10 for Sile Sand 20/30 specimens. Yet, the liquefaction potential of specimens involving IZ silt was consistently greater, if not identical, than the ones with TT silt at the same FC (see Figures. 4.11 to Figure 4.13). This is due to the altered soil fabric caused by the differences in silt gradation even though the base sand, fines content and initial stress conditions were the same.

Table 4.1 : Consolidated void ratios of the specimens in figures 4.11 to 4.13.

	Sile Sand 20/30	Sile Sand 50/55	Sile Sand 80/100
clean	0.72	0.80	0.90
with 5% TT silt	0.67	0.81	0.90
with 15% TT silt	0.62	0.84	0.91
with 25% TT silt	0.69	0.86	0.92
with 5% SI silt	0.53	0.80	0.90
with 15% SI silt	0.45	0.78	0.90
with 25% SI silt	0.43	0.83	0.91
with 5% IZ silt	0.63	0.78	0.89
with 15% IZ silt	0.59	0.79	0.90
with 25% IZ silt	0.63	0.80	0.90

One might also think that considerable differences in relative density could be another factor that can influence the above mentioned order of liquefaction potential. However, Dr values given in Figures 4.1 to Figure 4.9 shows that twenty eight out of thirty specimens correspond to loose state in soil mechanics (with Dr≤31%), while remaining two can be classified as loose to medium dense (with Dr values of 38% and 39%). This observation shows that regardless of the gradations of the sand, silt and the amount of fines content (FC≤25%), all the specimens were intrinsically tend to be deposited in a loose state within a narrow range of relative density and also supports the appropriateness of the concept of loosest possible density after deposition as one of the alternative comparison basis for liquefaction behaviors of different sands and silty sands, provided that the deposition technique is kept the same.

Monkul and Yamamuro (2011) had performed an experimental study, in which the static liquefaction behavior of a single base sand (Nevada Sand-B) mixed with three different non-plastic silts (Loch Raven, SilCoSil 125 and Potsdam silts) were investigated. In that study, it was reported that for the same Dr, FC and initial stress conditions, as the D50-sand/d50-silt ratio decreased the sand became more liquefiable. When gradation of three silts are investigated in figure 1, the mean grain size (d50) of the silt grains increased with TT, SI and IZ silts respectively. The largest silt used in the present study is IZ silt, therefore for the same base sand, specimens with IZ silt had the smallest mean grain diameter ratio ($D_{50\text{-sand}}/d_{50\text{-silt}}$) (see table 3.1). In parallel, specimens with IZ silt had the greatest liquefaction potential as expressed before, which fit well with the trend mentioned by Monkul and Yamamuro (2011). However, the liquefaction resistances of the specimens with SI silt were greater than the specimens with TT silt (Figure 4.11a, Figure 4.11b, Figure 4.12a, Figure 4.12b, Figure 4.13a) even though average size of TT silt is smaller than that of SI silt. In other words, for the same base sand, D50-sand/d50-silt ratio was largest for specimens with TT silt among the three silt types (Table 3.1) but the liquefaction resistance of the specimens with TT silt was not the greatest (i.e. the liquefaction trends of specimens with TT and SI silts did not fit to Monkul and Yamamuro (2011)'s mean grain diameter ratio criterion). Therefore, a particular characteristic of the TT silt should have influenced the resulting specimens in such a way that the mean grain diameter ratio effect had been over-ruled for specimens involving TT and SI silts at 5% and 15% FC (i.e. a characteristic that makes specimens with TT silt more liquefiable compared to specimens with SI silt).

Coefficient of uniformities (C_{Usilt}) of TT, SI and IZ silts are 10.6, 18.5, and 7.9 respectively (Table 3.1). Accordingly, the greater and more uniform IZ silt made Sile Sands more liquefiable compared to other silts at low FC. Meanwhile, specimens with SI silt were the least liquefiable among the three silt types. When coefficient of uniformities of the silt matrices are compared; SI silt had a considerably greater C_{Usilt} value and therefore relatively well graded with respect to other silts. This difference in the gradation of silts might have contributed to the drop in liquefaction potential due to the potential of more efficient packing tendency for SI silt grains in between the sand grains. However, when figure 4.10 is investigated, it could be seen that the difference in gradation of silts is not the sole reason for observed variations in liquefaction behavior of the same base sand. As mentioned before in Table 4.1 and figure 4.10; TT silt made Sile Sand 50/55 and 20/30 specimens achieve systematically greater void ratios compared to IZ silt, even though TT silt is smaller and relatively well graded compared to IZ silt. More explicitly, having smaller $d_{50\text{-}silt}$ and greater C_{Usilt}, specimens with TT silt were expected to have smaller quasi-natural void ratios compared to specimens with IZ silt. Yet, it was the opposite as seen in figure 4.10. Hence, a silt characteristic other than mean grain diameter ($d_{50\text{-}silt}$) and coefficient of uniformity (C_{Usilt}) could also have influenced the initial fabric achieved before undrained shearing and therefore affected the liquefaction potential of silty sands, especially for the specimens with TT silt.

4.2.2 Influence of angularity and grain shape effects of silt grains

Another possible silt characteristic that plays role in this case could be the differences in grain shape characteristics of three silts used in this study. For this purpose, an investigation regarding the grain shape characterization of the three different silts used in this study is planned, which involved utilization of Optical Microscope (OM) and Scanning Electron Microscopes (SEM) at Nanobiotechnology Center of Yeditepe University. Figure 4.14 shows the representative SEM images of the TT, SI and IZ Silts. During this investigation a total number of 360 individual silt grains were analyzed in 2-D based on “Krumbein Scale” (Krumbein and Sloss, 1963) given in figure 4.15, and corresponding sphericity and roundness values of the silt grains were determined. Even though more sophisticated 3-D particle morphology measurements (e.g. via X-ray micro-tomography (Fonseca et al., 2012)) or other 2-D measurements

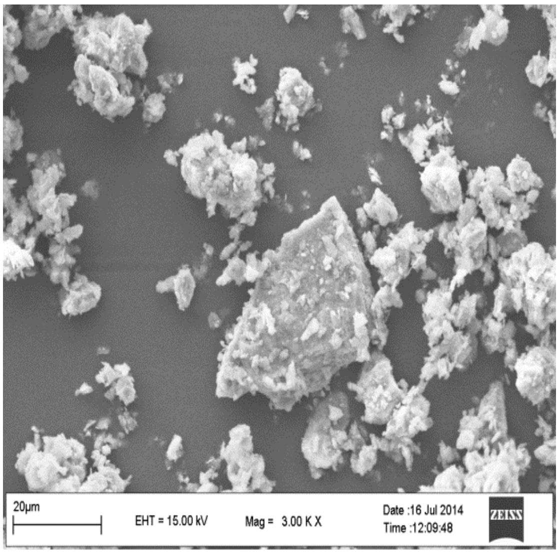

(a)

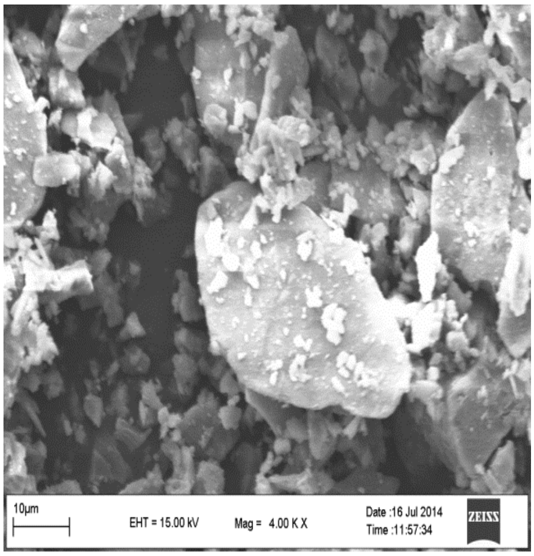

(b)

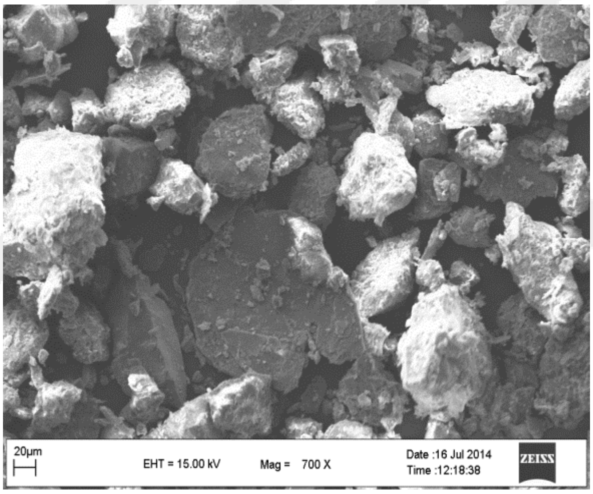

(c)

Figure 4.14 : Scanning Electron Microscope (SEM) images of the three silts employed in this study: (a)TT silt, (b) SI silt, (c) IZ silt.

based on Fourier analysis or Fractal analysis (Vallejo, 1995; Cox and Budhu, 2008) are available, classical chart methods such as Krumbein Scale are also still employed (Cho et al., 2006) in order to investigate the effects of grain shape on geotechnical behavior of sands.

Sphericity (S) is a parameter that represents the similarity between the width, height and length of a grain. In quantitative terms, it is the ratio of the radius of the largest inscribed circle ($r_{max\text{-}inscribed}$) to the radius of the smallest circumscribed circle ($r_{min\text{-}circumscribed}$) as expressed in Equation 4.1 (Cho et al., 2006; Guo and Su, 2007). As shown in Figure 4.15, as the shape of a grain approaches to a perfect circle, its sphericity value approaches to 1.

$$S = \frac{r_{[max-inscribed]}}{r_{[min-circumscribed]}} \tag{4.1}$$

Roundness (R) is another shape characteristic that represents the angularity of the corners and edges of a grain. In quantitative terms, it is the ratio of the average radius

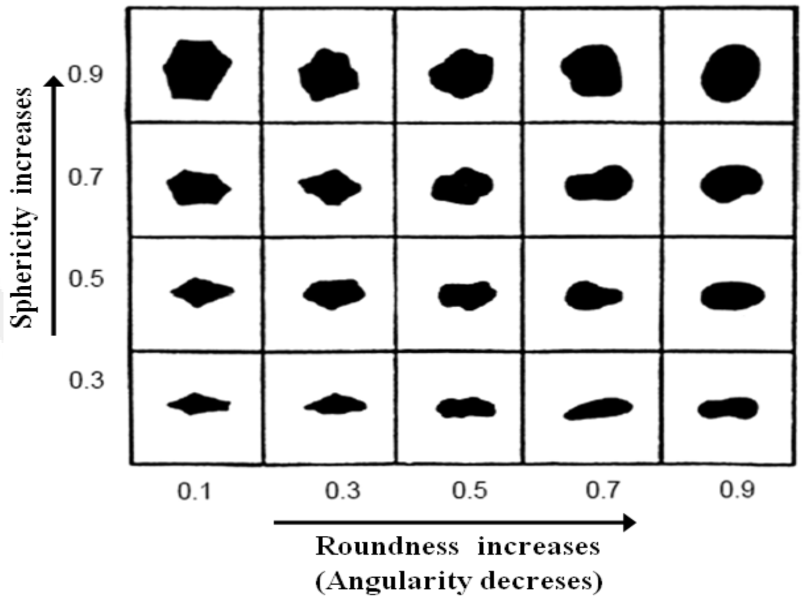

Figure 4.15 : Change of grain shape with sphericity(S) and roundness(R) (modified after Krumbein and Sloss, 1963).

of the inscribed circles located at the curved surface features ($\sum r_{inscribed}$ /N) to the radius of the largest inscribed circle ($r_{max-inscribed}$) in a particular grain as expressed in Equation 4.2, where N is the number of curved surface features (Cho et al., 2006; Guo and Su, 2007; Rouse et al., 2008). Figure 4.15 shows that, as the angularity of the corners of a grain diminishes, the value of averaged rinscribed approaches to the rmax-inscribed, and consequently roundness of a grain approaches to 1.

$$R = \frac{\sum_{i=1}^{N}(r_{i[inscribed]})/N}{r_{[max-inscribed]}} \tag{4.2}$$

Sphericity and Roundness values of the three different silts employed in this study are given in Table 4.2. As seen in Table 4.2, mostly OM images were preferred for IZ and SI silts, because OM is more economical and practical compared to SEM. However, because TT silt is the smallest and in certain aspects the outlier among the three silt types as discussed before, it was decided to take considerable amount of SEM images for the TT silt. Based on the results in Table 4.2, the sphericity values for all of the silts are relatively high (i.e. >0.6), but the sphericity values of TT and SI silts were practically similar and numerically greater than that of the IZ silt. Thus, both TT and SI silts are more spherical compared to IZ silt. When roundness values in Table 4.2 are considered based on Powers's Scale (1953), TT silt is close to the boundary (R=0.25) between sub-angular to angular, while R values for SI and IZ silts are quite close to each other and both located in the lower range of sub-rounded (i.e. R>0.35). In other words, TT silt is definitely more angular relative to both SI and IZ silts, while the latter two had similar roundness (Table 4.2). Note that R and S are independent parameters (Wadell, 1932; Cho et al., 2006; Cox and Budhu, 2008).

Table 4.2 : Quantification of grain shape characteristics of silt matrix.

	Analyzed grains (OM)	Analyzed grains (SEM)	Sphericity (S)	Roundness (R)	$d_{50\text{-silt}}$ (mm)
TT silt	45	148	0.69	0.26	0.011
SI silt	86	3	0.68	0.38	0.017
IZ silt	75	3	0.63	0.37	0.037

As mentioned by Monkul (2012), silt grains have two main positional tendencies during the deposition process: 1) they could locate in to the intergranular void space between adjacent sand grains, 2) they could locate between contact points of sand grains by pushing them apart. Both of those tendencies usually exist simultaneously during the reconstitution process of silty sand specimens as shown in Figure 4.16. The proportion and balance between these two main tendencies is quite influential on liquefaction behavior of silty sands. At low fines content, when silt grains are located between the sand grains they form relatively weaker grain contacts which are called "metastable" contacts, whereas sand to sand grain contacts are called "stable" contacts. In undrained shearing of loose silty sands, static liquefaction behavior is considerably influenced by the destruction of available metastable contacts, during which silt grains are pushed into the intergranular voids between the sand grains, meanwhile sand skeleton is reconfigured with more stable contacts (Wood et. al., 2008; Monkul, 2012).

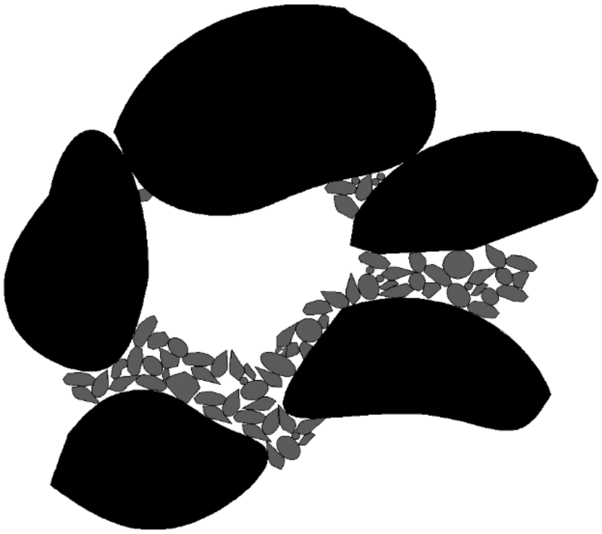

(a)

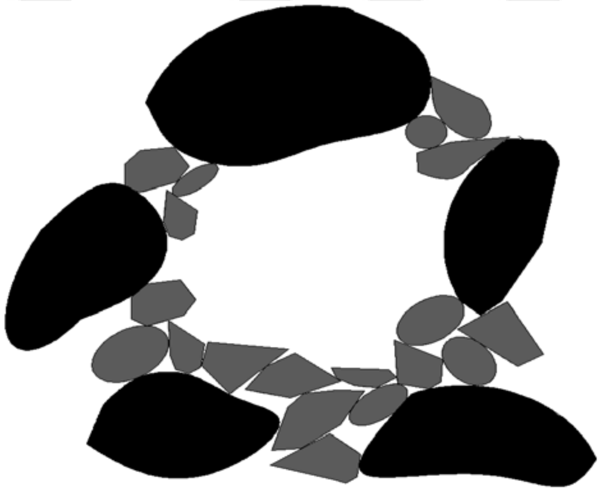

(b)

Figure 4.16 : Change Positional tendencies of silt grains during deposition process: (a) base sand having silt with larger mean grain diameter ratio, (b) base sand having silt with smaller mean grain diameter ratio.

Such a mechanism would contribute to the excess pore pressure generation capacity and therefore the liquefaction potential of specimens. In fact, Yamamuro et al. (2008) had performed a detailed study to quantify different types of grain contacts in a silty sand with the help of epoxy impregnation and SEM. They showed for dry funnel deposited specimens (the same deposition method used in this study) that the ratio of stable to metastable grain contacts before undrained shearing decreased with increasing fines content (FC≤40%). They have also compared the ratio of grain contacts before and after shearing via drained triaxial compression test on a contractive silty sand specimen at 20% FC, and showed that during shearing the ratio of stable to metastable grain contacts have increased. Such a finding of Yamamuro et al. (2008) confirmed that during undrained shearing the disturbance tendency of the metastable contacts would contribute to the pore pressure generation as explained before.

When three silt types used in this study are considered, specimens with TT silt had the largest void ratio after consolidation (Figure 4.10), especially within coarser and relatively well graded base sands such as Sile Sands 50/55 and 20/30 (Table 4.1). Despite the fact that TT silt has the lowest mean grain diameter ($d_{50\text{-silt}}$) among the three silts, the relatively spherical but angular nature of TT silt seems to cause the sand specimens involving it to be deposited at greater “quasi natural” void ratios than the specimens involving other silts (Figure 4.10). This implies that the initial fabrics achieved before shearing, and therefore the liquefaction potentials, were not only influenced by the mean size and gradation of the silts involved in this study, but also influenced by the shape characteristics of those silt grain matrix.

This can also be inferred that at the same fines content, base sand, depositional energy and consolidation stress, TT silt potentially caused more metastable contacts within the specimens because of the relatively higher sphericity and/or angularity of TT silt grains. In fact, this could be the reason why mean grain diameter ratio effect had been over-ruled for specimens involving TT and SI silts at 5% and 15% FC, as mentioned before. Even though the mean grain diameter ratio is larger for specimens with TT silt (e.g. $D_{50\text{-[Sile Sand 50/55]}}$ /$d_{50\text{-[TT silt]}}$= 23.6) than the ratio for specimens with SI silt (e.g. $D_{50\text{-[Sile Sand 50/55]}}$ /$d_{50\text{-[SI silt]}}$= 15.3), because the relatively angular TT silt matrix potentially caused more metastable contacts between the sand grains, specimens involving TT silt were more liquefiable (or had less liquefaction resistance) compared to specimens with SI silt at low fines contents (Figure 4.11(a), Figure 4.11(b), Figure 4.12(a), Figure 4.12(b), Figure 4.13(a)). It seems that such shape effects were not strong enough to over-rule the size effect during the comparison between TT and IZ silts, perhaps because the difference between the mean grain diameter ratios of them were much larger ($D_{50\text{-[Sile Sand 50/55]}}$ /$d_{50\text{-[TT silt]}}$= 23.6 vs. $D_{50\text{-[Sile Sand 50/55]}}$ /$d_{50\text{-[IZ silt]}}$=7). The impact of mean grain diameter ratio on initial soil fabric was conceptually presented in Figure 4.16, where larger silt grains (smaller $D_{50\text{-sand}}/d_{50\text{-silt}}$) in Figure

4.16(b) caused more metastable grain contacts compared to smaller silt grains (greater $D_{50\text{-sand}}/d_{50\text{-silt}}$) in figure 4.16(a).

$$e_s = \frac{V_v + V_f}{V_s} \tag{4.3a}$$

where V_v, V_f, V_s are the volume of voids, fines and sand, respectively. Hence, the V_v+V_f term in the numerator corresponds to the volume of intergranular void space of the sand matrix. Equation 4.3(a) can be rearranged in terms of G, G_f, e and FC as follows in Equation 4.3(b), where e is the overall void ratio, G is the specific gravity of the overall soil (weighted average of sand and silt constituents are used in this study), G_f is the specific gravity of fines in the soil and FC is the fines content.

$$e_s = \frac{e + \left(G/G_f\right).\left(FC/100\right)}{1 - \left(G/G_f\right).\left(FC/100\right)} \tag{4.3b}$$

Intergranular void ratio and its modified versions were used by many researchers regarding the discussions on shear strength and compression of sandy soils (Pitman et al., 1994; Lade and Yamamuro,1997; Thevanayagam, 1998; Ni et al., 2004; Georgiannou, 2006; Monkul and Ozden, 2007; Carraro et al., 2009; Monkul and Yamamuro, 2011; Rahman and Lo, 2012; Monkul et al., 2015). Intergranular void ratios (e_s) of the tested specimens calculated by Equation 4.3(b) are plotted in Figure 4.17. This figure shows that es had generally increased with increasing FC. For specimens involving Sile Sand 80/100 as base sand, it is seen that the magnitudes of the e_s were similar at the same FC, meaning that es for that particular sand was insensitive to the silt gradation and grain shape characteristics of different silts. However, when intergranular void ratio values for Sile Sands 50/55 and 20/30 in figure 4.17 are investigated, it could be easily observed that specimens involving TT silt had greater es than other silt types, despite the fact that TT silt was the smallest of the three silt types. As shown in figure 4.16, one normally expects that the smaller silt such as TT would fit into the intergranular void space between the sand grains easier and this would result in smaller e_s values compared to a larger silt such as IZ. Moreover, one would also expect that together with its smaller size and greater $C_{U\text{-silt}}$, TT silt would pack more effectively within the intergranular void space compared to the larger IZ silt and this would result in smaller es values for TT silt, but figure 18 shows the opposite for Sile Sands 20/30 and 50/55 in a systematic manner. Therefore, the impact of silt grain shape effects on initial fabric, especially for specimens involving TT silt, can also be confirmed via intergranular void ratio values shown in Figure 4.17.

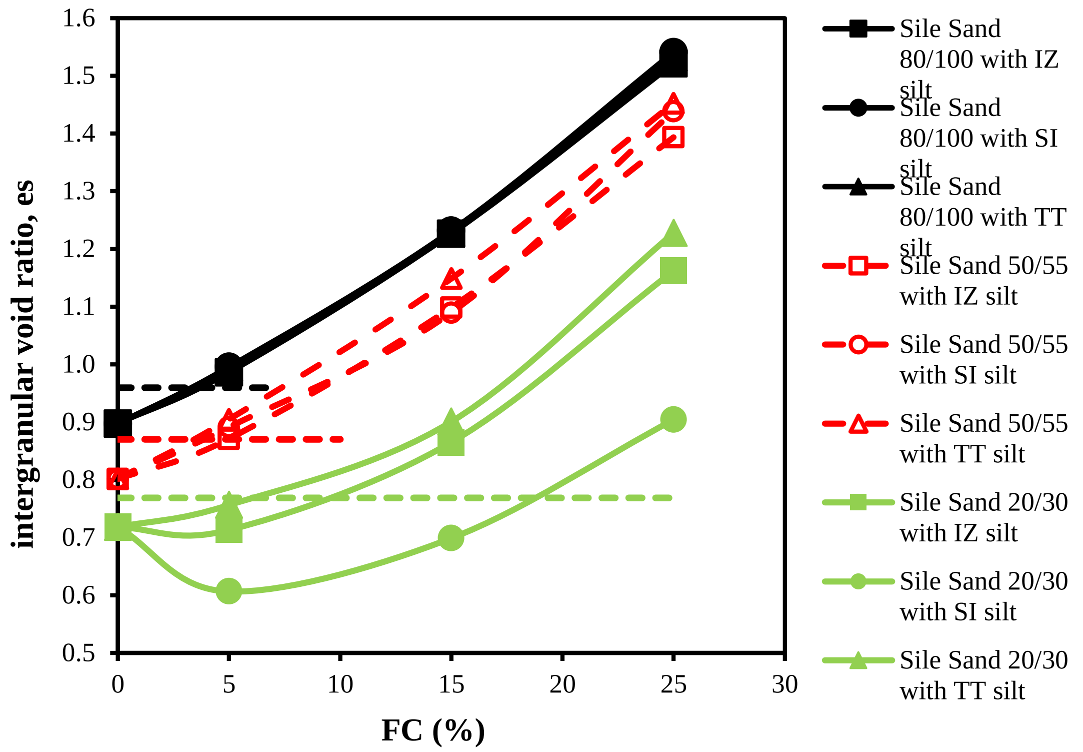

Figure 4.17 : Change of consolidated intergranular void ratios of tested specimens with fines content and different base sand and silt types.

It should be noted that intergranular void ratio by itself cannot be an indicator for comparing the liquefaction potential of a particular base sand involving different non-plastic silts, even though FC and initial stress conditions were the same (i.e., an increase in es does not necessarily imply an increase in liquefaction potential of the soil). For example, at 5% FC, specimen of Sile Sand 50/55 involving TT silt had greater es than specimens involving IZ silt (Figure 18). However, specimens with TT silt had more liquefaction resistance than the specimens with IZ silt (Figure 4.12(a)). As another example, at 5% FC, specimen of Sile Sand 20/30 involving TT silt had also greater es than specimens involving IZ silt (Figure 4.17). However, both specimens had almost identical liquefaction potentials as seen in Figure 4.13(a).

In fact, the inability of intergranular void ratio to capture the liquefaction behavior of silty sands had also been observed in previous studies, and some researchers (Ni et al., 2004; Rahman et al., 2008) have suggested using its modified version "equivalent granular void ratio", which was introduced by Thevanayagam et al. (2002). Even though equivalent granular void ratio (es-eq) concept is beyond the scope of this study, an aspect related to it is worth to note. There is an empirical parameter "b" in the definition of $e_{s\text{-}eq}$, which represents the ratio of fine grains that are active in the force transfer chain of soil grains as mentioned in the introduction section. In the early studies regarding the equivalent granular void ratio, an appropriate value for parameter "b" was assumed based on the convergence of the steady state lines (Thevanayagam et al., 2002; Ni et al., 2004) or normalized initial peak deviator stress curves (Yang et al., 2006) of a sand with different fines contents. But recently, Rahman et al. (2008) suggested a semi-empirical equation for the prediction of parameter "b", where b is a function of several factors including void ratio, fines content and $d_{50\text{-silt}}/D_{10\text{-sand}}$. Utilizing the ratio of $d_{50\text{-silt}}/D_{10\text{-sand}}$ imply that gradation of soil and mean size of the silt grains are important for the contribution of silt grains on the overall force transfer mechanism. This implication is parallel with the finding that liquefaction behavior of a particular base sand is influenced by grain size distribution of silt matrix, which was discussed in the previous section. Moreover, it is possible that the parameter "b" can also be influenced by the grain shape characteristics of the silt grain matrix based on the findings in this study. However, the level of influence is difficult to speculate and requires a specific research.

Consequently, the trend observed by Monkul and Yamamuro (2011), which states that at the same Dr, FC, initial stress conditions, base sand gradation and mineralogy, the liquefaction potential of a silty sand increases as the mean grain diameter ratio ($D_{50\text{-sand}}/d_{50\text{-silt}}$) decreases, is generally verified also for the silty sands in this study (e.g. IZ silt vs. SI silt and IZ silt vs. TT silt in three different base sands). However, there was an exception for the specimens involving TT silt versus SI silt. It was hypothesized that the angular nature of TT silt grains caused them to form more metastable contacts compared to the sub-rounded SI silt grains and resulted in more liquefiable specimens, over-ruling the mean grain diameter ratio effect for specimens involving those two silt types.

4.2.3 Influence of angularity and grain shape effects of silt grains

Another finding observed in Figures 4.11 to Figure 4.13 is that the impact of silt gradation and shape characteristics on liquefaction potential of sand specimens is dependent on the value of their fines content. As discussed previously, silt type and gradation were shown to influence the liquefaction potential of sands in this study at lower fines contents such as 5% and 15%. However, as the fines content is further increased to 25%, virtually all specimens had liquefied with identical stress-strain responses and the influence of silt gradation and shape characteristics on static liquefaction potential became negligible (Figure. 4.11(c), Figures 4.12(c) and Figures 4.13(c)). The primary reason for such an observation could be related with the variations in initial fabric of specimens with increasing fines content.

At low fines content, sand grain matrix generally dominates the undrained shearing response, even though some of the silt grains could also be quite influential on the pore pressure generation via metastable contacts explained before. However, as the fines content increases, sand grain matrix starts to gradually loose the domination over the undrained shearing response. And when FC increases beyond a certain value, which is called transition fines content (FC_t), sand grains start to float within the silt grain matrix. Transition fines content can be expected to depend on many factors including but not limited to the gradation and initial density conditions of the soil. Based on the findings in previous literature, such a transition can be expected to occur somewhere between 20% and 30% fines content. For example, Pitman et al. (1994) reported for Ottawa sand mixed with angular crushed silica fines that below 20% FC, a sand dominated behavior was observed during undrained triaxial compression tests. Zlatovic and Ishihara (1995) conducted undrained triaxial compression tests on Toyoura sand with silt, and stated that specimens had weakened until 30% fines content, and started to gain resistance again with further increase in FC. Vallejo and Mawby (2000) reported based on direct shear tests on Ottawa sand mixed with kaolinite clay that the shear strength of the mixtures was controlled by the sand matrix when FC was smaller than 25%. Polito and Martin (2001) run cyclic triaxial tests on Monterey and Yatesville sands mixed with Yatesville silt, and reported FCt values of 25% for the Monterey sand, and 36% for Yatesville sand. Monkul and Ozden (2007) investigated the 1-D compression behavior of a clayey sand, and observed that a transition between a sand like compression behavior and a clay like compression behavior occurred between a fines content range of 20% to 34%, depending on the stress and initial density conditions.

Recently, some researchers have also proposed various equations to predict the value of transition fines content. Thevanayagam et al. (2002) proposed equation 4.4, where FC_t is a function of intergranular void ratio and maximum void ratio of the silt grain matrix. Later Yang et al. (2006) proposed a similar version of equation 4.4, where the specific gravities of the sand (G_{sand}) and silt (G_{silt}) matrices are also considered as shown in Equation 4.5. Based on several previous studies in literature Rahman and Lo (2012) suggested to use equation 4.6 in order to predict the transition fines content. Accordingly, FC_t is a function of various factors including void ratio and gradation parameters of sand and silt grain matrices in a soil. Recently, Zuo and Baudet (2015) compiled the different methodologies in literature for estimating the transition fines content and also come up with Equation 4.7, in which FC_t is a function of minimum void ratios and specific gravities of the sand and silt grain matrices constituting the soil.

$$FC_t(\%) \leq \frac{100\,.\,e_s}{1+e_s+e_{max-silt}} \tag{4.4}$$

$$FC_t(\%) \leq \frac{100\,.\,e_s\,.\,G_{silt}}{G_{silt}\,.\,\,e_s + G_{sand}.(1+e_{max-silt})} \tag{4.5}$$

$$FC_t(\%) \leq 40.\left[\frac{1}{1+e^{\left(0.5-0.13\left[D_{10-sand}/d_{50-silt}\right]\right)}} + \frac{D_{10-sand}}{d_{50-silt}}\right] \tag{4.6}$$

$$FC_t(\%) \leq \frac{100\,.\,e_{min-sand}\,.\,G_{silt}}{G_{silt}\,.\,\,e_{min-sand} + G_{sand}.(1+e_{min-silt})} \tag{4.7}$$

Because FC_t is expected to occur between 20% to 30% fines content based on the experimental findings in the aforementioned literature, FC_t values of specimens having 25% fines content in this study were also calculated based on the proposed equations (Equations 4.4, 4.5, 4.6, 4.7). The predicted transition fines content values are shown in Table 4. In general, Equations 4 and 5 gave greater FC_t values compared to the Equations 6 and 7. But it should be reminded that it is a very difficult task, if not impossible, to precisely predict transition fines content from equations only, hence Equations could only provide an approximation of estimated FCt values. Therefore, averages of the values obtained by four equations were also calculated at the last column in table 4.3. It is interesting to note that regardless of the base sand type, the smallest average transition fines content values (FC_{t-avg}) were predicted for the specimens involving SI silt among the three silt types. Similarly, the specimens involving IZ silt had the greatest FC_{t-avg}, while the specimens involving TT silt had intermediate FCt-avg values consistently in Table 4. Nevertheless, FCt-avg values in table 4.3 are between 22% and 34%, which is consistent with the range reported in literature.

It seems from table 4.3 that most of the specimens at FC=25%, had not reached their transition fines content yet, however some of them were relatively close. Furthermore, some of the specimens such as Sile Sand 20/30 had started to liquefy with almost identical stress-strain responses (i.e. liquefaction behavior became independent of silt characteristics) even at 15% fines content (e.g. see Figure 4.13b), which was definitely smaller than the predicted FC_t. Considering these points, the dependency of relationship between silt characteristics (mean size, grain size distribution, shape effects) and liquefaction behavior, on the value of fines content cannot be firmly explained with the transition fines content concept. In other words, the fines content values of the tested specimens imply that they are expected to have a sand dominated behavior, because of having $FC<FC_t$. But even so, the influence of silt characteristics (i.e. gradation and shape) gradually diminished with increasing fines content smaller than FCt. But what is more interesting is that the influence of silt characteristics (i.e. gradation and shape) on liquefaction of sands increases with decreasing fines content values below FC_t, where a domination of the sand grain matrix on the engineering behavior is most expected based on the previous literature. It seems that at low fines contents such as 5%, silt characteristics definitely influence the liquefaction behavior of sands (figures 4.11(a), 4.12(a), 4.13(a)). As fines content increases, such an influence seems to decay, and somewhere between 15% to 25% FC it disappears, during which the liquefaction response of a sand became identical for different non-plastic silts at the same FC, independent of silt characteristics. More explicitly, there is a coupled influence between the different silt characteristics (mean size, grain size distribution, shape effects) and the amount of fines content on the static liquefaction behavior of sands.

It should also be reminded that fines content influence and discussions above is based on the responses of loose silty sand specimens tested in this study. For the liquefied specimens, once the deviator stress started to decline after the peak point, it is reduced to zero with progressing axial strain, without any chance to show dilative tendency afterwards. In other words, high excess pore pressure generation and resulting static liquefaction could have suppressed the influence of different silt characteristics on undrained shearing and could be another reason why silt characteristics became negligible at higher fines contents for the specimens in this study. However, had those specimens been tested at denser states such that static liquefaction would not occur, it is possible that different silt characteristics could still influence the undrained response of sands even at relatively higher fines content (e.g. FC=25%).

Table 4.3 : Approximate values of transition fines contents predicted by various equations.

Soil Type	Transition Fines Content (FC_t) (%)				
	Equation 4.4	Equation 4.5	Equation 4.6	Equation 4.7	Average
Sile Sand 80/100 w. 25% TT silt	35.9	36.8	23.8	30.6	31.8
Sile Sand 80/100 w. 25% SI silt	34.5	34.8	25.6	20.3	28.8
Sile Sand 80/100 w. 25% IZ silt	39.1	39.7	31.8	26.4	34.3
Sile Sand 50/55 w. 25% TT silt	34.7	35.5	23.7	28.1	30.5
Sile Sand 50/55 w. 25% SI silt	32.9	33.2	25.4	18.4	27.5
Sile Sand 50/55 w. 25% IZ silt	37.1	37.5	30.8	24.2	32.4
Sile Sand 20/30 w. 25% TT silt	31.0	31.8	23.3	24.8	27.7
Sile Sand 20/30 w. 25% SI silt	23.6	23.8	26.3	16.0	22.4
Sile Sand 20/30 w. 25% IZ silt	32.9	33.4	27.0	21.2	28.6

5. INFLUENCE OF COEFFICIENT OF UNIFORMITY, BASE SAND GRADATION AND VOLUMETRIC COMPRESSIBILITY

5.1 Influence of Sand Gradation on Density Index Parameters

5.1.1 Different comparison bases and loosest possible density after deposition

Several different density index parameters such as void ratio (e), relative density (Dr), intergranular void ratio (void ratio of the sand matrix, e_s) were used in literature in order to compare the drained/undrained behaviors of clean and silty sands at various fines contents. More explicitly, some researchers compared the stress-strain behaviors at similar void ratio (Troncoso and Verdugo, 1985; Pitman et al., 1994; Erten and Maher, 1995; Papadopoulou and Tika, 2008; Maleki et al., 2011; Dash and Sitharam, 2011; Monkul et al., 2015), some compared the behaviors at similar relative density (Koerner, 1970; Shapiro and Yamamuro, 2003; Polito and Martin, 2003; Kokusho et al., 2004; Igwe et al., 2007; Carraro et al., 2009; Dash and Sitharam, 2011; Belkhatir et al., 2011). While some others compared the behaviors at similar intergranular void ratios (Shen et al., 1977; Kuerbis et. al., 1988; Thevanayagam and Mohan, 2000; Dash and Sitharam, 2011; Maleki et al., 2011).

Another comparison basis is the loosest possible density after deposition. Accordingly, soils would tend to fall into “quasi-natural” void ratios, provided that the specimen preparation technique was exactly the same for each specimen (Lade and Yamamuro, 1997). Here, the term “loosest possible density after deposition” should not be mixed with the minimum void ratio (e_{min}). The loosest possible density after deposition refers to the smallest density that a specimen can be reconstituted when a specific deposition technique is applied (e.g. dry funnel deposition, slurry deposition, air pluviation etc.). Whereas, minimum void ratio (e_{min}) represents the smallest packing density for a particular soil determined by the relevant standards or methods. For a particular soil, the value of loosest possible density after deposition changes depending on the applied deposition technique, however the value of emin remains the same. The term “quasi-natural void ratio” represents the void ratio values achieved by the loosest possible density after deposition for different soils, when the same amount of deposition energy was applied with the same specimen preparation technique. The value of quasi-natural void ratios can be influenced by the combined effects of several factors

including grain size distribution, grain shape characteristics, amount of fines, deposition method etc., but the corresponding values are always greater than e_{min}.

The loosest possible density after deposition is also a commonly used comparison basis in literature for assessing the influence of fines content on liquefaction resistance of sands (Kuerbis et al., 1988; Vaid, 1994; Zlatovic and Ishihara, 1995; Lade and Yamamuro, 1997; Georgiannou, 2006; Murthy et al., 2007; Bahadori et al., 2008; Monkul and Yamamuro, 2011; Monkul et al., 2014). Specimens in this study are also prepared with the same deposition method and energy, and hence loosest possible density after deposition is employed regardless of the gradation of different clean and silty sands. Consequently, no special effort or manipulation was made during the deposition stage to prepare the specimens of different silty sands used in this study at exactly the same density index parameter (i.e. e, Dr, e_s). It should also be noted that all of the mentioned studies are valuable and all of the mentioned comparison bases are legitimate; hence the goal of this study is not to argue about the appropriateness or superiority of a specific comparison basis.

5.1.2 Influence of base sand gradation on density index parameters

Consolidated void ratios of the tested specimens involving different base sands and silts are shown in figure 5.1, which inherently are influenced by the gradation of silts, base sands, particle shape and the amount of fines content. Several trends can be observed in figure 5.1. The first one is that, as the base sand gradation became finer (or $D_{50\text{-}sand}$ became smaller) (see Figure 3.1 or Table 3.1), the consolidated void ratios of the resulting specimens of clean sands had increased. Meaning, clean Sile Sand 80/100 had the greatest quasi natural void ratio, while clean Sile Sand 20/30 had the smallest. This trend is also consistent with the change of their e_{max} and e_{min} values given in table 3.1, where clean Sile Sand 80/100 had the greatest extreme void ratio values, while clean Sile Sand 20/30 had the smallest (i.e. among the three clean sands

Sile Sand 80/100 had the greatest emax and emin, while Sile Sand 20/30 had the smallest e_{max} and e_{min}).

The second trend is that, similar to the clean sands, the consolidated void ratios of the silty sand specimens had increased as the base sand gradation became finer (or $D_{50\text{-}sand}$ became smaller) regardless of the silt type and content. Therefore, the silty sand specimens involving Sile Sand 80/100 had greater void ratios compared to specimens involving Sile Sand 50/55, which also had greater void ratios compared to specimens involving Sile Sand 20/30 (Figure 5.1).

The third trend is that the quasi natural void ratio (loosest possible density) values and their variation with fines content were influenced by the grain size distribution of base sands. It is very interesting to see that the void ratio remained relatively constant for Sile Sand 80/100 with increasing content of three different silts (Figure 5.1). Whereas, the change of void ratio with increasing fines content became clearly visible for specimens involving Sile Sand 50/55 and became most pronounced for specimens involving Sile Sand 20/30 as base sand. Therefore, as $D_{50\text{-}sand}$ of the base sand became larger, the variation of quasi natural void ratio with increasing fines content started to be more pronounced even the same silt type was used (i.e. CU_{silt} and $d_{50\text{-}silt}$ is kept constant). Soils in this study can be considered similar to binary granular mixtures, hence as $D_{50\text{-}sand}$ became larger, the resulting silty sands technically turn out to be more gap graded, which also contributes to the observed trend mentioned above.

One might think that the three trends explained can also be influenced by other characteristics of base sand matrix such as CU_{sand} and shape of sand grains, which is certainly true. But, one can verify the explained trends by comparing Sile Sands 20/30 and 50/55 which had almost the same CU_{sand} but considerably different $D_{50\text{-}sand}$ (Table 3.1). In terms of shape effect, all the three base sands in this study had the same geologic origin (i.e. obtained from the same sand quarry) but with different gradations. Therefore, the effects of grain shape and mineralogy of the sand grain matrix are assumed to be negligible on the resulting trends and engineering behaviors. Consequently, $D_{50\text{-}sand}$ is used because it is a simple, yet reflective parameter to express the influence of base sand gradation on the resulting quasi natural void ratios of the specimens in this study (Figure 5.1) (not because it is the only influencing factor).

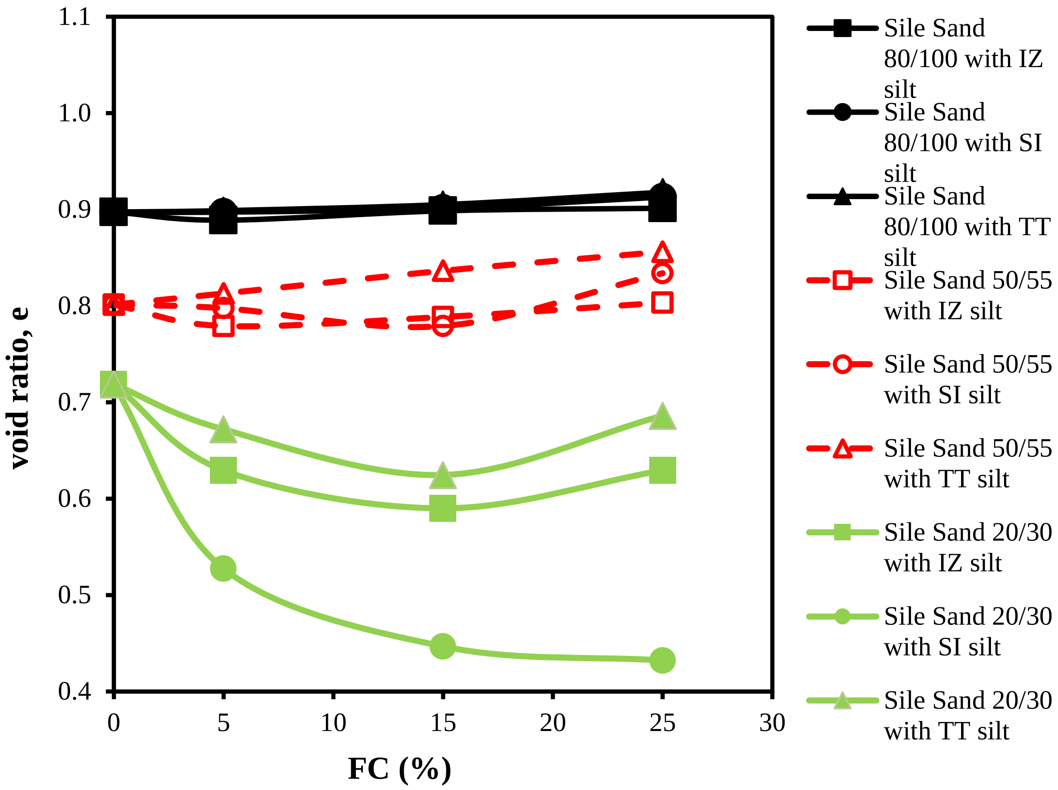

Figure 5.1 : Change of consolidated void ratios of tested specimens with fines content and different gradations.

Relative densities after consolidation stage of the tested specimens involving different base sands and silts are shown in Figure 5.2. It could be observed from Figure 5.2 that the relative densities of the majority of the specimens were located in a quite narrow band between Dr= 18% and Dr= 31% (with two exceptions around 39%), which correspond to loose state in soil mechanics. This observation shows that regardless of the gradations of the sand, silt and the amount of fines content (FC≤25%), all the specimens were intrinsically tend to be deposited in a loose state within a narrow range of relative density. This observation also supports the appropriateness of the concept of loosest possible density after deposition as one of the alternative comparison basis for liquefaction behaviors of different sands and silty sands, provided that the deposition technique is kept the same.

5.2 Effect of Base Sand Gradation

5.2.1 Monotonic undrained response of clean and silty sile sands

Undrained monotonic triaxial compression tests were conducted on the specimens with density index parameters given in Figure 3 and Figure 4. As mentioned before, the effects of grain shape and mineralogy of the sand matrix are assumed to be negligible as they had the same geologic origin. Other factors such as initial stress conditions were also kept the same (σ'_{3c}) in order to investigate the differences in liquefaction behaviours of Sile Sands due to variations in base sand gradations.

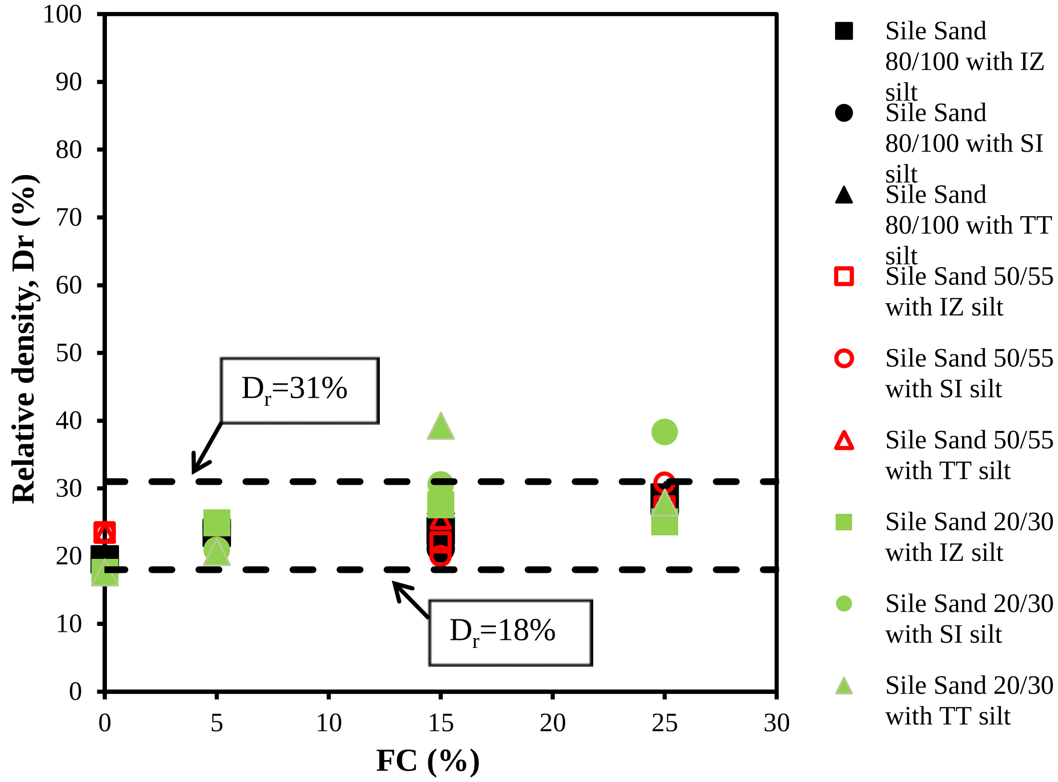

Figure 5.2 : Relative densities (D_r) of tested specimens after consolidation.

Stress paths of the clean Sile Sands were shown in Figure 5.3 on a Cambridge p'-q diagram, where $q=(\sigma_1-\sigma_3)$, $p'=(\sigma'_1+2\sigma'_3)/3$. All the three clean sands showed stable response (i.e. no drop in deviator stress until failure). However, the liquefaction resistance of base sands slightly decreases as the sand becomes finer. Sile Sand 80/100 had the lowest liquefaction resistance, while Sile Sand 20/30 had the highest. Note that this observation is based on the "loosest possible density after deposition" as a comparison basis. Void ratios and relative densities after consolidation were shown in the legend of Figure 5.3. As mentioned before, the consolidated void ratios of the specimens increased as the sands became finer (Figure 5.3). Hence, it is unclear what the trend would be if they had been tested at exactly the same void ratio. However, it can reasonably be assumed that the consolidated relative densities of the tested specimens in Figure 5.3 are similar, i.e. practically in a narrow range of Dr=21 ± 3%. Therefore, the liquefaction resistance of the base sands in this study decreases as they become smaller when similar relative density or loosest possible density after deposition is used as a comparison basis. Consequently, Sile Sand 80/100 was observed to have the least liquefaction resistance among the three clean base sands tested.

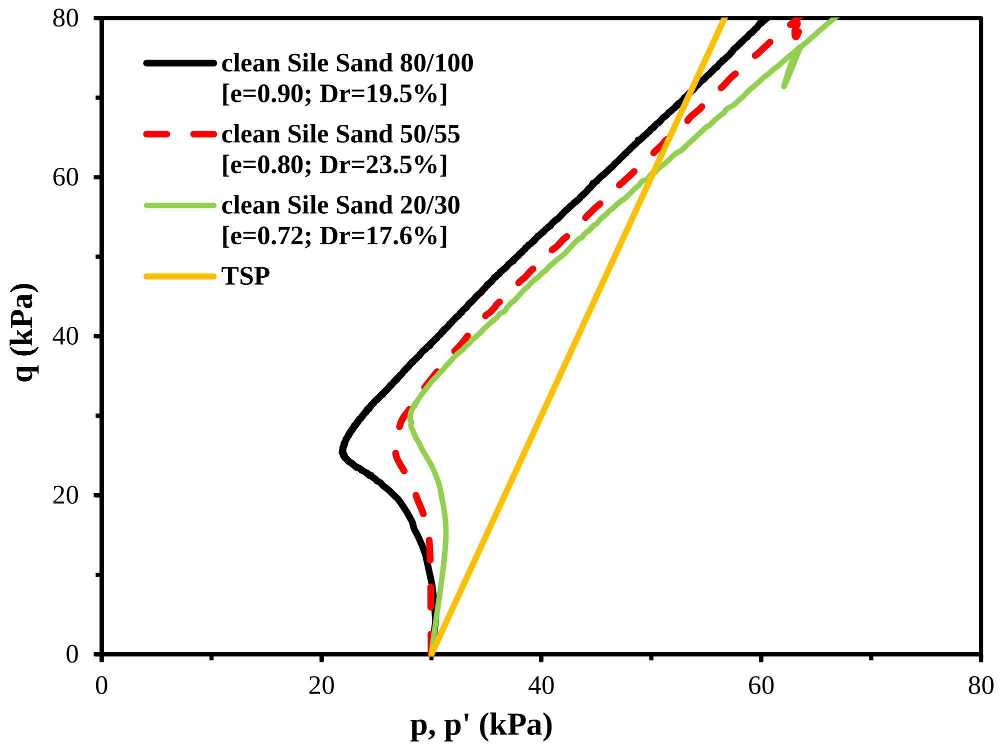

Figure 5.3 : Effective stress paths of the clean Sile Sands in the p'-q diagram.

Figure 5.4 shows the change in undrained response when TT silt was mixed within different base sands. When 5% TT silt is considered in Figure 5.4(a), stress strain curve of specimen with Sile Sand 80/100 was slightly above than that of Sile Sand 50/55, and both specimens showed stable response. Meanwhile, temporary liquefaction was observed for the specimen involving Sile Sand 20/30 as base sand. Temporary liquefaction is exhibited by the deviator stress achieving an initial peak (q_{peak}), which then reduces to a local minimum nonzero value (quasi steady state, q_{qss}), and then increasing again towards the steady state. Stress paths of different base sands with 5% TT silt were shown in Figure 5.4(b). When 15% TT silt is considered in Figure 5.4(c and d), the undrained behavior was transformed to static liquefaction for all base sands. However, the peak deviator stress in Figure 5.4 (c and d) decreases for specimens involving Sile Sand 80/100, 50/55 and 20/30 respectively. Static liquefaction occurs when the deviator stress is reduced to zero and remains at zero with progressive axial strains, while the excess pore-water pressure reaches its maximum value at a plateau,

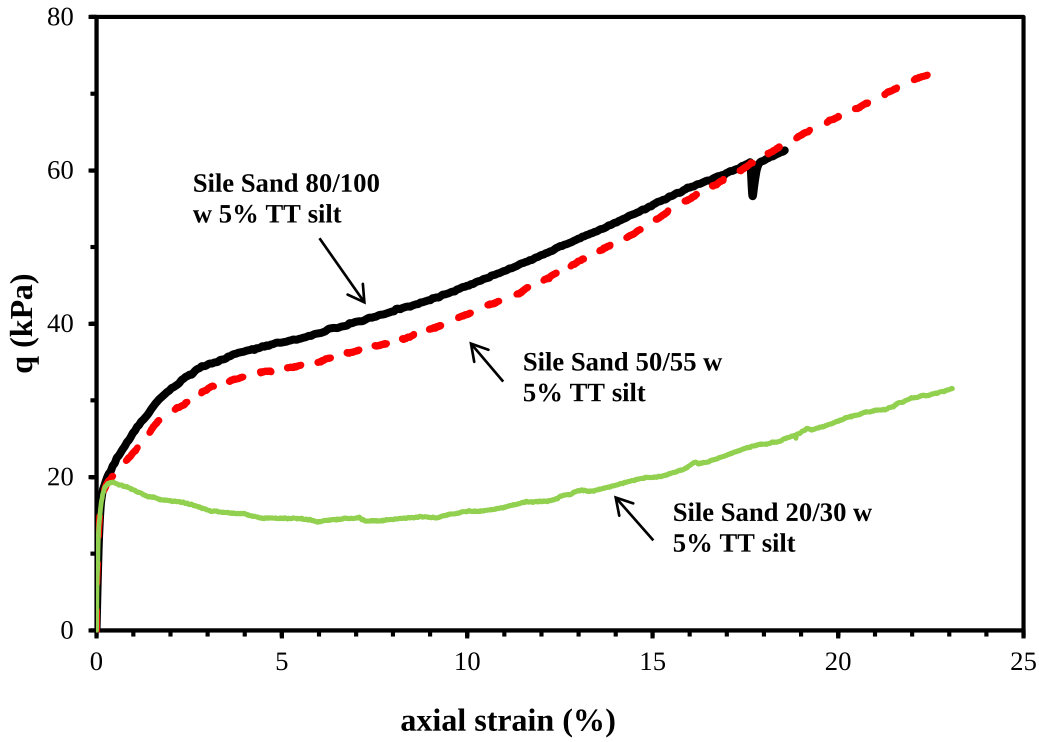

80
60
40
20
0
q (kPa)
Sile Sand 80/100
w 5% TT silt
Sile Sand 50/55 w
5% TT silt
Sile Sand 20/30 w
5% TT silt
0
5
10
15
20
25
axial strain (%)

(a)

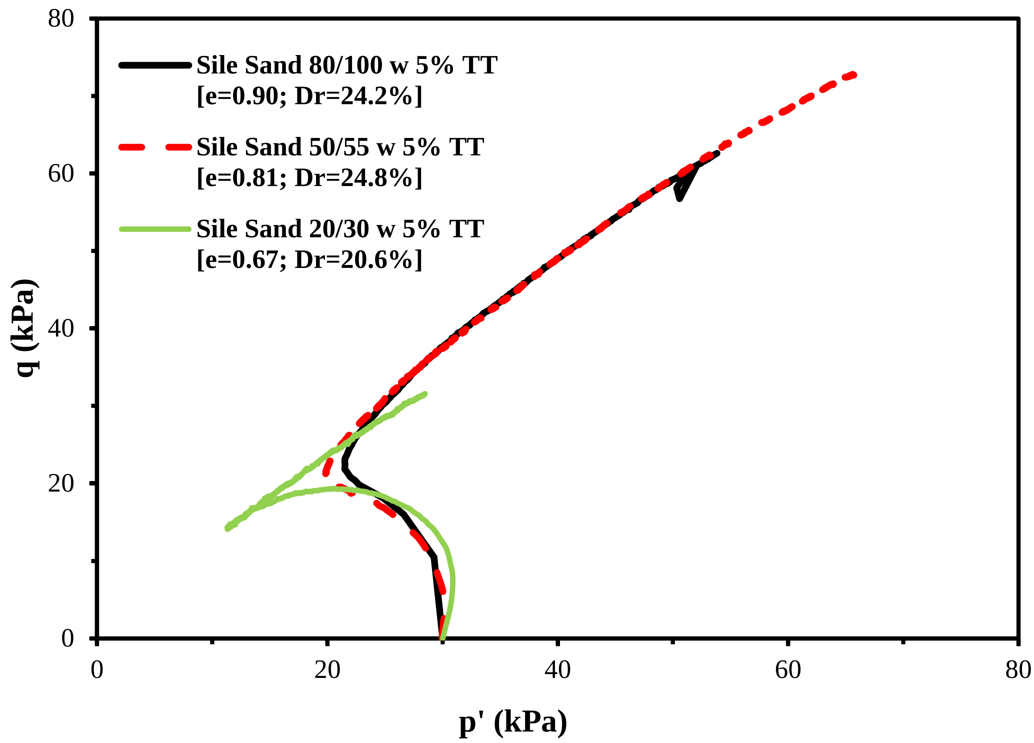

80
60
40
20
0
q (kPa)
Sile Sand 80/100 w 5% TT
[e=0.90; Dr=24.2%]
Sile Sand 50/55 w 5% TT
[e=0.81; Dr=24.8%]
Sile Sand 20/30 w 5% TT
[e=0.67; Dr=20.6%]
0
20
40
60
80
p' (kPa)

(b)

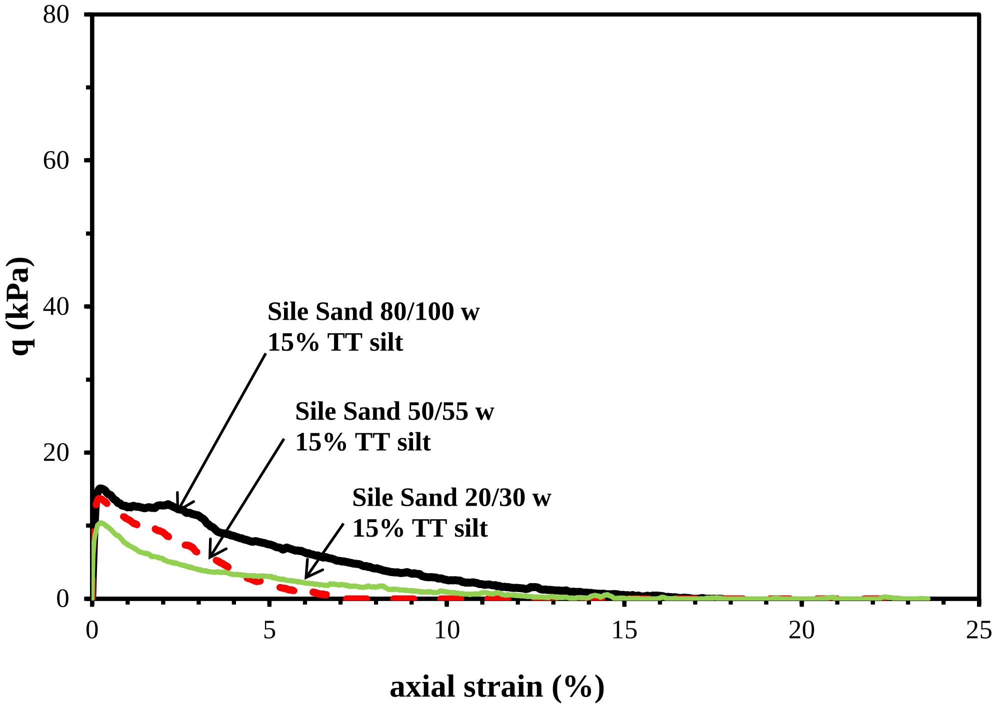

(c)

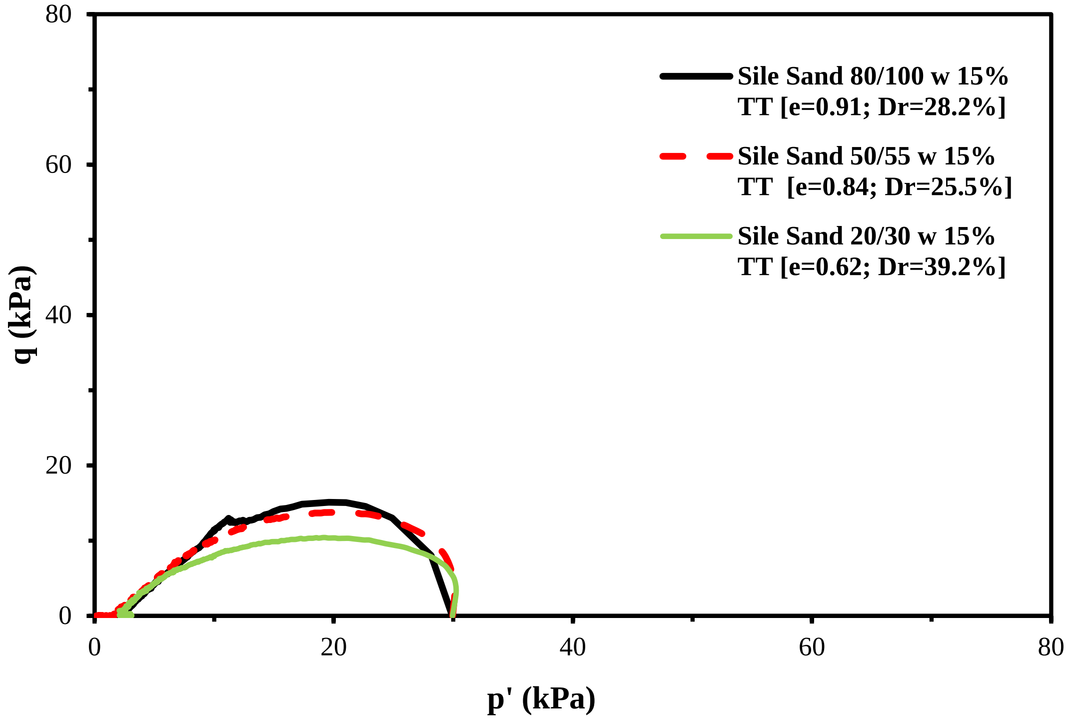

(d)

Figure 5.4 : (a) Deviator stress versus axial strain response, (b) Corresponding effective stress paths for different Sile Sands with 5% TT silt; (c) Deviator stress versus axial strain response, (d) Corresponding effective stress paths for different Sile Sands with 15% TT silt.

meanwhile stress path reaches the stress origin. Formation of large wrinkles in the membranes around the specimens occurred during static liquefaction.

Figure 5.5 shows the change in undrained response when different base sands were mixed with SI silt this time. When 5% SI silt is considered in Figure 5.5(a), stress strain curve of specimen with Sile Sand 80/100 showed the strongest response among the three base sands. Specimen with Sile Sand 50/55 also showed stable response but its stress strain curve was below the specimen with Sile Sand 80/100. Meanwhile, temporary liquefaction was observed for the specimen involving Sile Sand 20/30 as base sand (Figure 5.5(a and b)). Figure 5.5(c and d) shows the change of liquefaction potential different base sands at 15% SI silt. Specimen with Sile Sand 80/100 showed stable response while the specimens with other base sands showed static liquefaction.

Figure 5.6 shows the change in undrained response when different base sands were mixed with IZ silt. When 5% IZ silt is considered in Figure 5.6(a), stress strain curve of specimen with Sile Sand 80/100 showed stable response, while specimens with Sile Sand 50/55 and 20/30 showed temporary liquefaction with corresponding stress paths given in Figure 5.6(b). When 15% IZ silt is considered in Figure 5.6(c), the undrained behavior was transformed to static liquefaction for all base sands, where the stress strain curve for specimen with Sile Sand 80/100 was only slightly above the other two base sand types (i.e. qpeak for Sile Sand 80/100 was only slightly greater than the other two base sands, Figure 5.6(d)).

It should be reminded that the consolidated void ratios of the specimens of different Sile Sands in all the three figures (Figure 5.4, 5.5 and Figure 5.6) had systematically decreased as the base sands became larger (e.g. e for specimens with Sile Sand 20/30 were considerably smaller than e for specimens with Sile Sand 80/100, as also mentioned in figure 5.1). Therefore, had those specimens in Figure 5.4, Figure 5.5 and Figure 5.6 been tested at exactly the same void ratio (i.e. e of the Sile Sand 80/100), the difference between the stress-strain behaviours and resulting stress paths of different base sands would even increase more. Therefore, the difference between the corresponding static liquefaction potentials would further be amplified.

When relative density is considered as a comparison basis, one can observe that D_r of

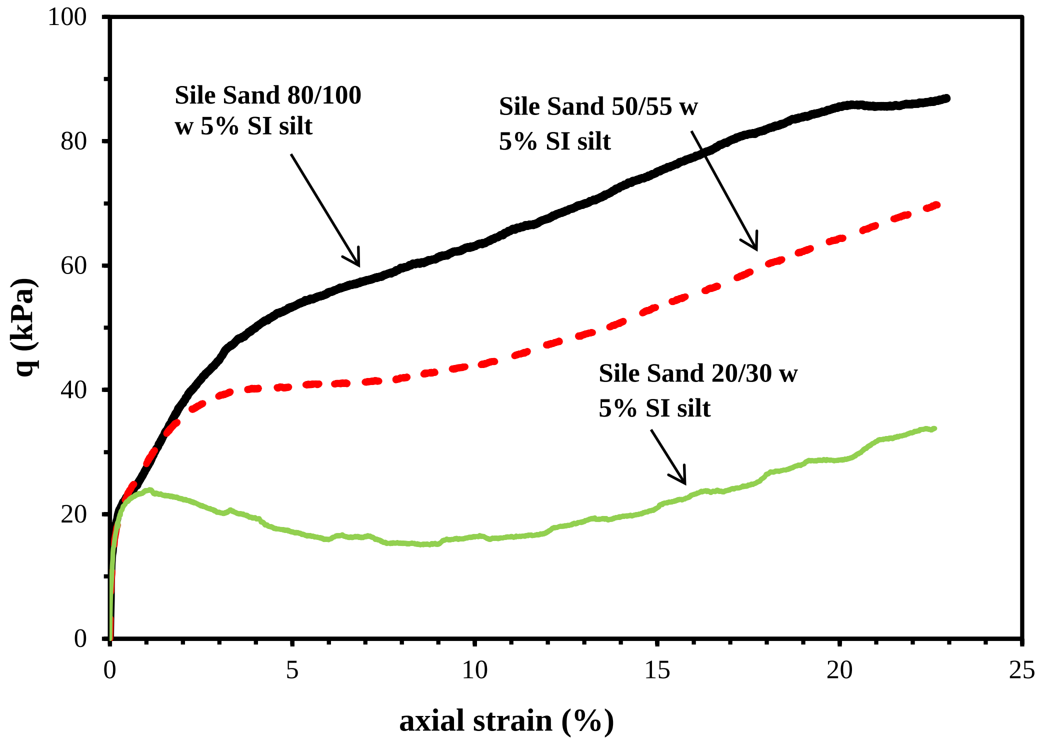

Sile Sand 80/100
w 5% SI silt
Sile Sand 50/55 w
5% SI silt
Sile Sand 20/30 w
5% SI silt
q (kPa)
axial strain (%)
100
80
60
40
20
0
0
5
10
15
20
25

(a)

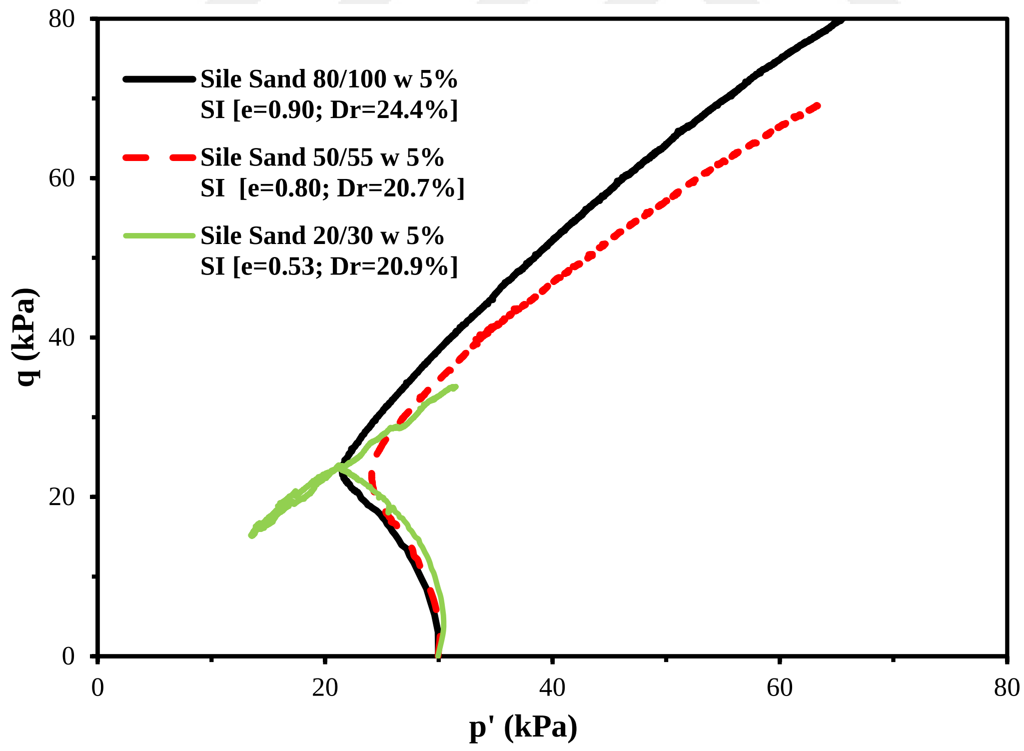

Sile Sand 80/100 w 5%
SI [e=0.90; Dr=24.4%]
Sile Sand 50/55 w 5%
SI [e=0.80; Dr=20.7%]
Sile Sand 20/30 w 5%
SI [e=0.53; Dr=20.9%]
q (kPa)
p' (kPa)
80
60
40
20
0
0
20
40
60
80

(b)

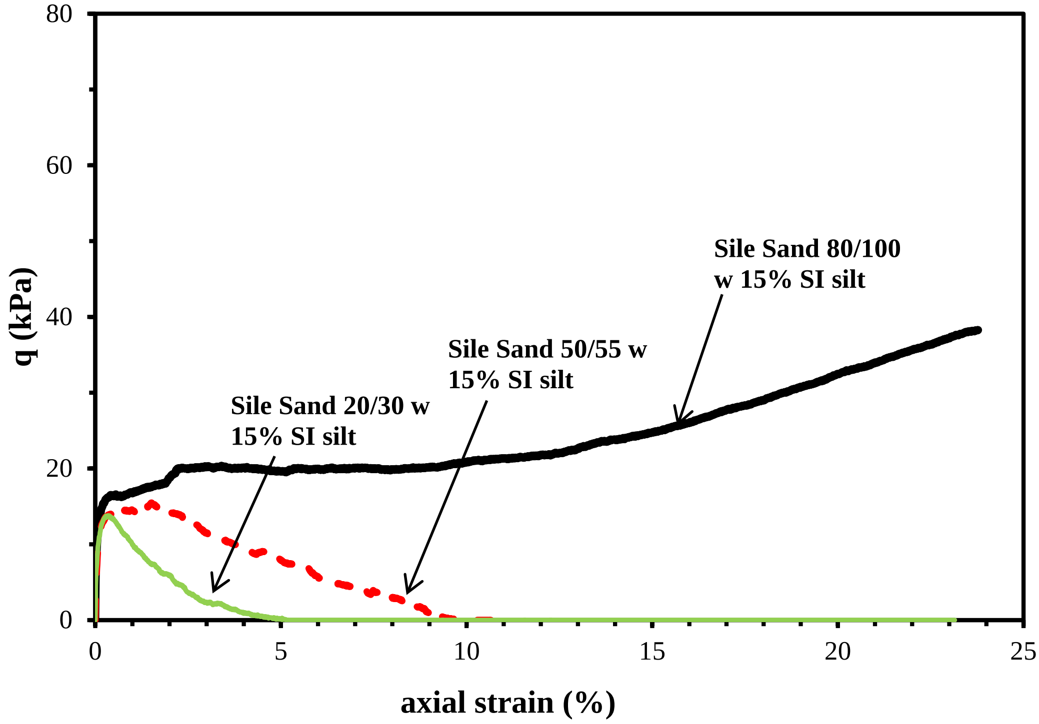

(c)

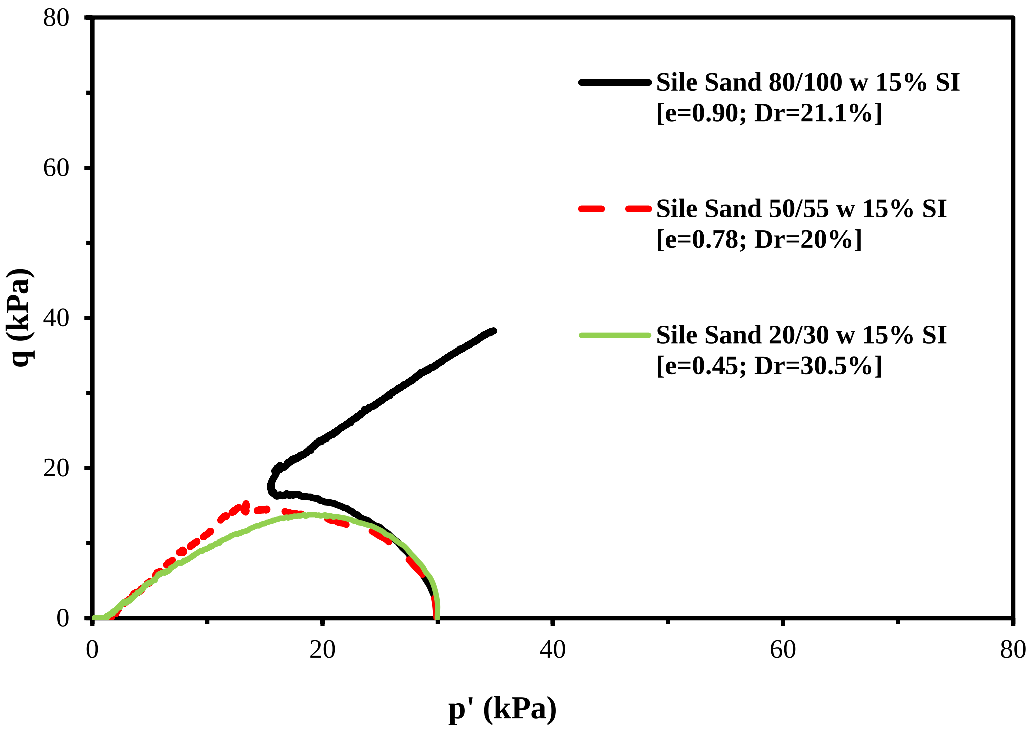

(d)

Figure 5.5 : (a) Deviator stress versus axial strain response, (b) Corresponding effective stress paths for different Sile Sands with 5% SI silt; (c) Deviator stress versus axial strain response, (d) Corresponding effective stress paths for different Sile Sands with 15% SI silt.

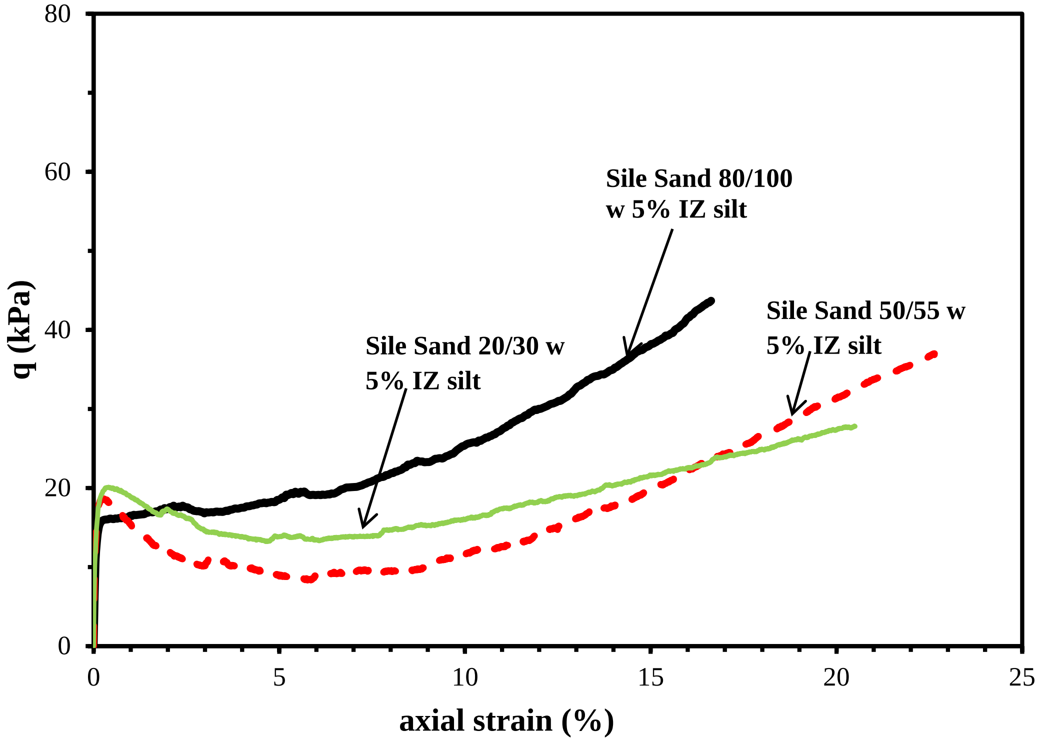

q (kPa)
axial strain (%)
Sile Sand 80/100
w 5% IZ silt
Sile Sand 50/55 w
5% IZ silt
Sile Sand 20/30 w
5% IZ silt

(a)

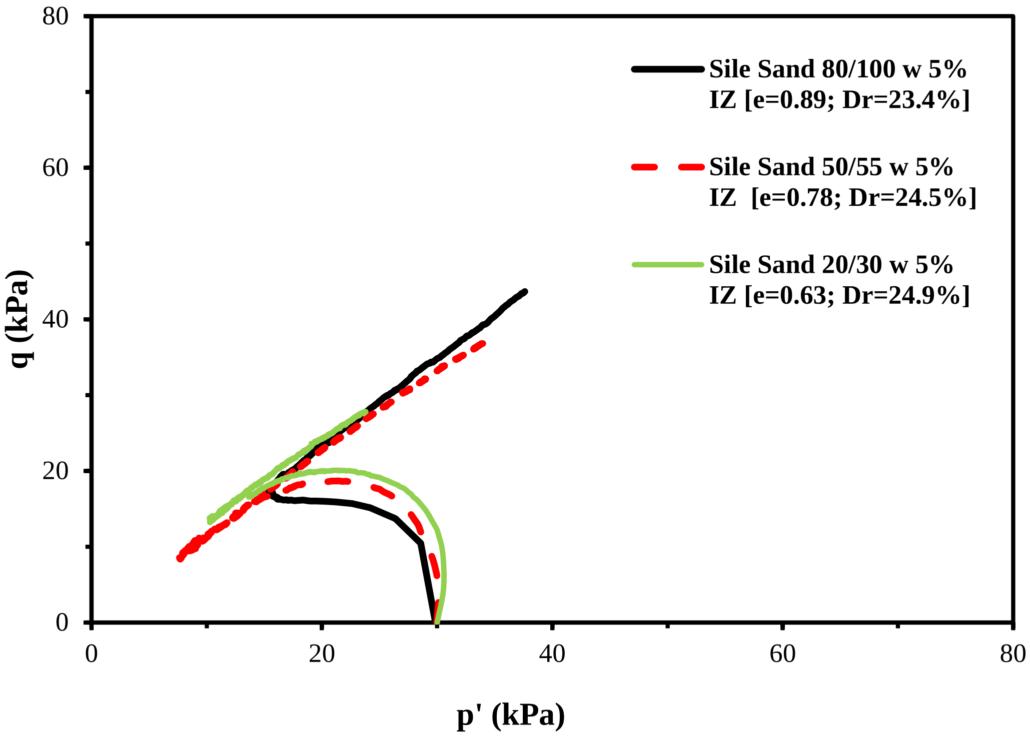

q (kPa)
p' (kPa)
Sile Sand 80/100 w 5%
IZ [e=0.89; Dr=23.4%]
Sile Sand 50/55 w 5%
IZ [e=0.78; Dr=24.5%]
Sile Sand 20/30 w 5%
IZ [e=0.63; Dr=24.9%]

(b)

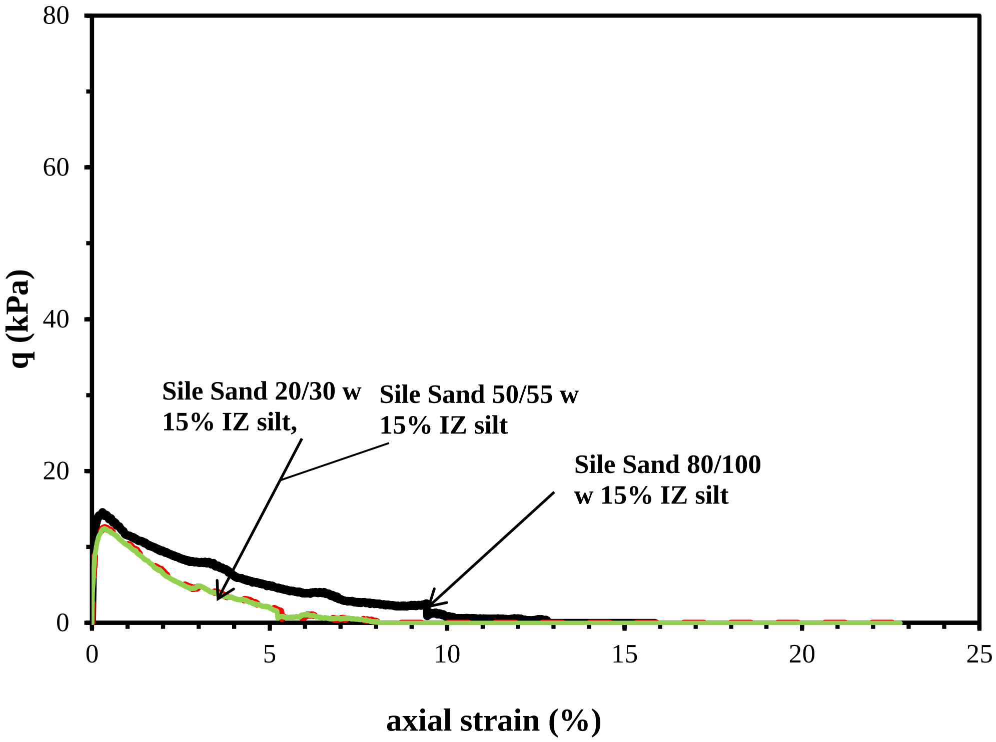

(c)

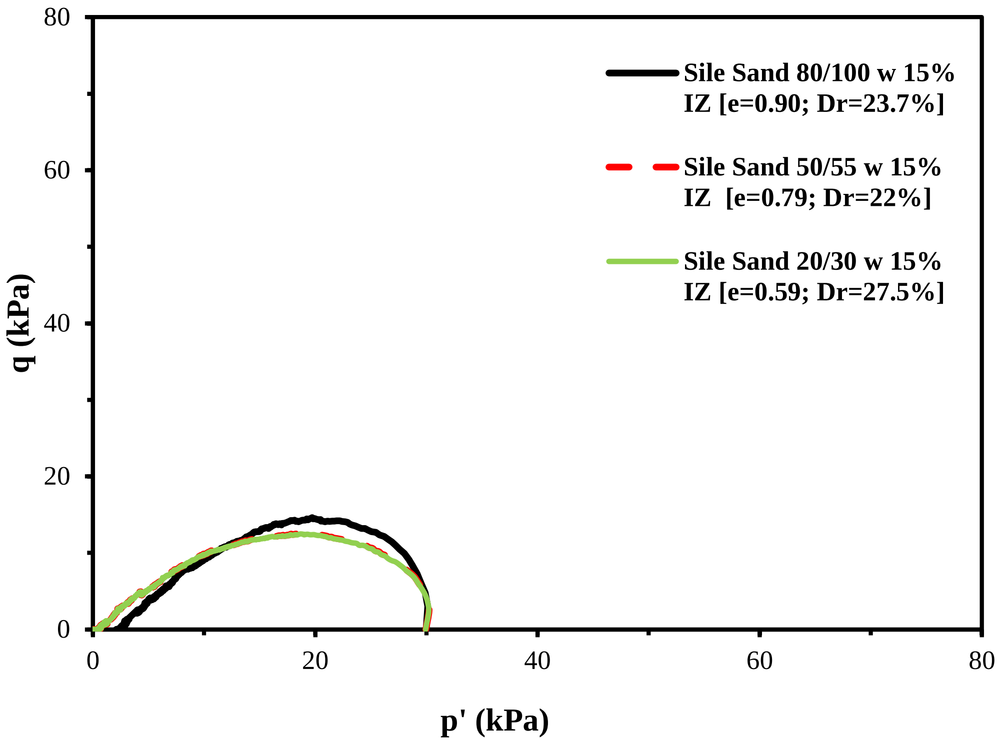

(d)

Figure 5.6 : (a) Deviator stress versus axial strain response, (b) Corresponding effective stress paths for different Sile Sands with 5% IZ silt; (c) Deviator stress versus axial strain response, (d) Corresponding effective stress paths for different Sile Sands with 15% IZ silt.

specimens are in a narrow range for each set of base sands (at a given FC) in Figure 5.4, Figure 5.5 and Figure 5.6 (D_r=22.7±2.1% for Figure 6(a and b); D_r=32.4±6.8% for Figs. 6 (c and d); D_r=22.6±1.9% for figures 5.5(a and b); D_r=25.3±5.2% for Figures 5.5 (c and d); D_r=24.2±0.8% for figures 5.6(a and b); D_r=24.8±2.8% for Figures 5.6 (c and d)). Because the variation of D_r values for specific sets of base sands are generally below ±3% (with two exceptions slightly above ±5%), one can practically conclude that the liquefaction potentials of silty sands in this study had increased as the base sand becomes larger both at a given void ratio or at similar relative density, regardless of the silt type.

5.2.2 The impact of base sand gradation on static liquefaction response

Figures 5.4, Figure 5.5 and Figure 5.6 clearly indicated that the liquefaction potential of silty sand is influenced by the gradation of base sand, when silt type is kept the same. For the soils tested in this study silty sand specimens became more liquefiable in the base sand order of Sile Sand 80/100, Sile Sand 50/55 and Sile Sand 20/30 systematically, and this trend is verified for three different silt types. The observed trends in figures 5.4, 5.5 and 5.6 are also interesting in a way that the order of liquefaction resistance of base sands were reversed when they were mixed with silt (i.e. specimens with Sile Sand 20/30 had the least liquefaction resistance in Figures 5.4, Figure 5.5 and Figure 5.6) as opposed to when they were tested as clean sands (i.e. Sile Sand 80/100 had the least liquefaction resistance in Figure 5.3). When coefficient of uniformities of the base sands in Table 3.1 are investigated, the order is $C_{U20/30} \approx C_{U50/55} > C_{U80/100}$. Hence, when clean sand behavior in figure 5.3 is considered, it could be expressed that the more uniform and smaller Sile Sand 80/100 had the least liquefaction resistance. This observation is consistent with some of the previous findings in literature, which stated that the liquefaction resistance of loose clean sands decrease as they became uniformly graded (Vaid et al., 1990; Kokusho et al., 2004; Igwe et al., 2007).

But why then, the larger and relatively well graded Sile Sand 20/30 suddenly had the least liquefaction resistance when those sands were mixed with different silts? Neither gradation parameters such as mean grain size ($D_{50\text{-sand}}$), coefficient of uniformity (C_{Usand}) of sands, nor density index parameters such as void ratio (e), relative density can be the reason for such an order of liquefaction resistance for silty sand specimens.

More specifically, Sile Sand 20/30 was relatively well graded and/or larger compared to other base sands, and specimens involving it had smaller void ratio and similar relative density compared to specimens with other base sands. Hence, when other influencing factors such as FC, silt type, silt gradation, initial stress conditions, deposition method were kept constant, the mentioned gradation (e.g. $D_{50\text{-}sand}$, C_{Usand}) and density index (e.g. e) parameters were all in favour of greater liquefaction resistance for Sile Sand 20/30.

The reason behind the more liquefiable specimens of Sile Sand 20/30 compared to other base sands may be the different levels of gap gradations in silty sand specimens induced by the base sand gradation. As an example, grain size distribution curves for the specimens of 5% TT silt mixed with Sile Sand 20/30 and Sile Sand 80/100 as base sands were shown in Figure 7(a), and corresponding stress-strain responses were re-plotted in Figure 7b. As expected, specimen involving Sile Sand 20/30 was more gap graded than the specimen involving Sile Sand 80/100. Because silty sands involving Sile Sand 20/30 as base sand were more gap graded compared to silty sands with other base sands in this study, specimens with Sile Sand 20/30 could became more liquefiable than the specimens with other base sands. In other words, gap gradation could be the reason behind the reversed order of liquefaction resistance mentioned before (between clean versus silty Sile Sands). Gap gradation has shown to considerably decrease the undrained shear strength of clean sands (Igwe et al., 2012), but to authors knowledge its influence on static liquefaction behaviour of silty sands is not known.

In order to verify the impact of gap gradation induced by base sand gradation on static liquefaction behaviour of silty sands as hypothesized in this study, authors have produced another base sand by sieving Sile Sand 20/30 through sieve with 0.425mm opening and then mixed the new Sile Sand obtained with 5% TT silt. By doing so even a more gap graded silty sand was obtained with the resulting gradation shown in figure 5.7(a). The resulting new Sile Sand with 5% TT silt had even weaker liquefaction resistance compared to specimens with other base sands and had shown temporary liquefaction as seen in Figure 5.7(b). Note that the "quasi-natural" void ratios of the specimens after consolidation in Figure 5.7(b) had decreased as the base sands became

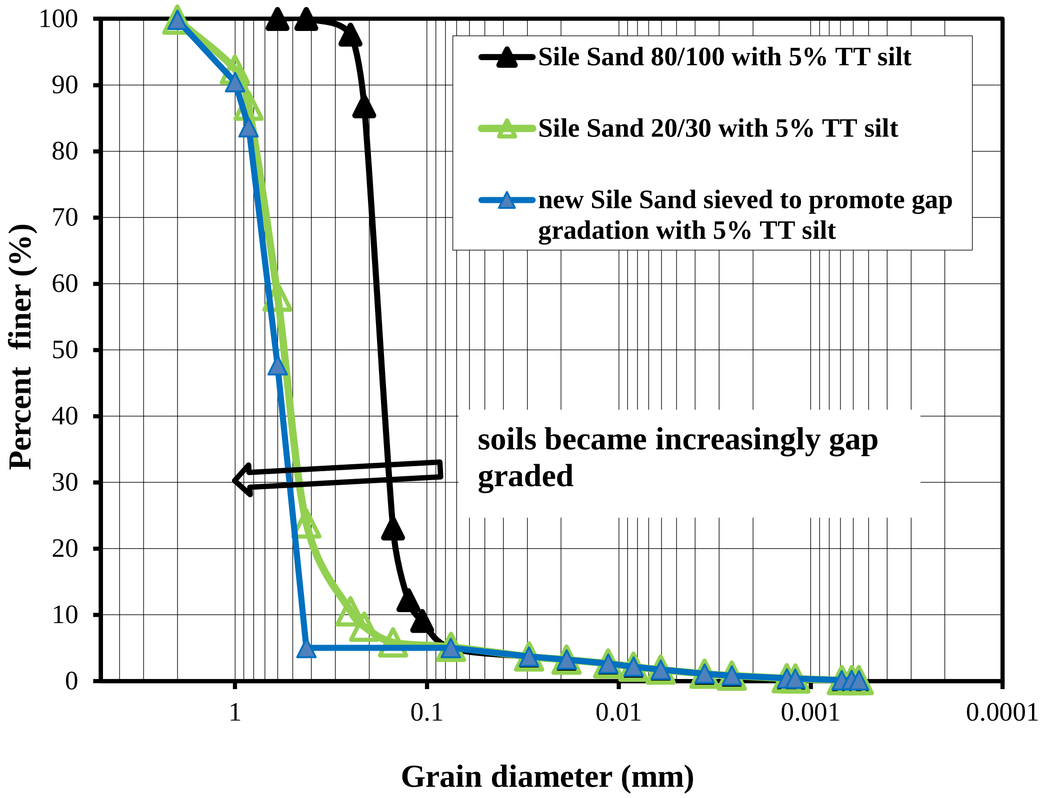

(a)

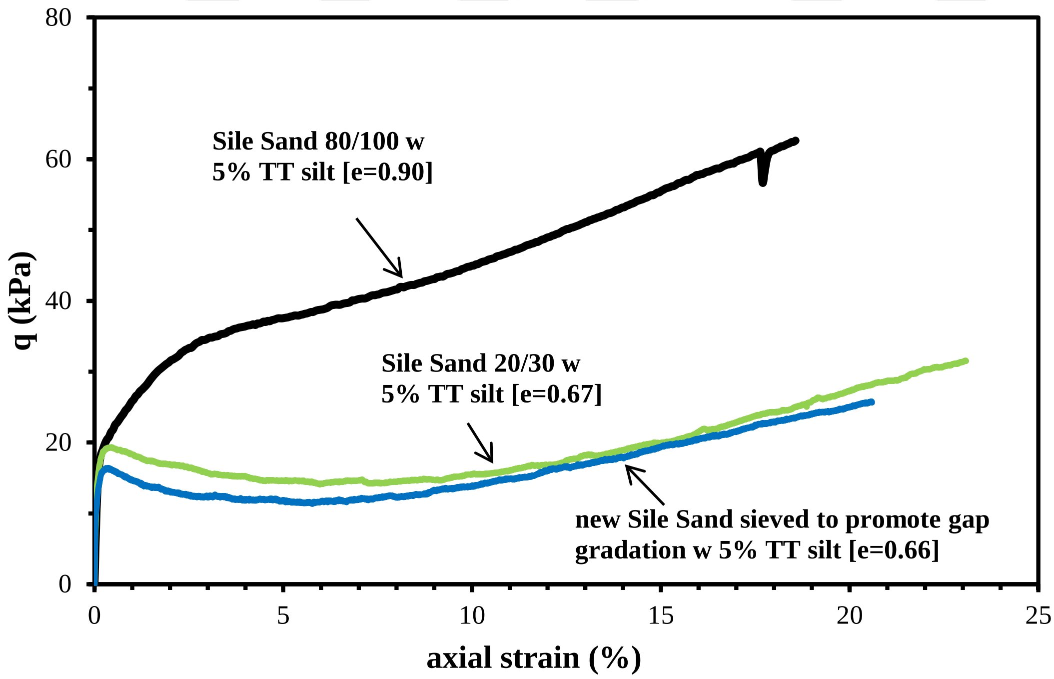

(b)

Figure 5.7 : (a) Grain size distributions and variations in gap gradations for three base sands involving 5% TT silt, (b) Corresponding stress-strain responses.

coarser meanwhile the resulting silty sands with 5% TT silt became more gap graded. Meaning, TT silt could fill into the intergranular void space between the sand grains more effectively as the sand matrix became coarser and more gap graded, yet the static liquefaction potential interestingly continues to increase. Moreover, had the soils in Figure 5.7 been tested at exactly the same void ratio (i.e. e of the new Sile Sand), the difference between their liquefaction potentials would even be more pronounced.

Discussions on figures 5.3 to 5.7 clearly demonstrated that silty sands in this study become more liquefiable as the base sand gradation became coarser, which also resulted in increasingly gap graded silty sands. This conclusion implies that grain size distributions of natural sandy soils had a significant effect from static liquefaction point of view. Cubrinovski and Ishihara (2002) conducted a detailed investigation on the extreme void ratio characteristics of over 300 natural sandy soils and reported that natural sands do not show any appreciable drop in either emax or emin with increasing fines content, implying a gradual transition between the fine and coarse grain matrices in their grain size distribution curves. On the contrary, most laboratory produced silty sands were reported to shown an appreciable drop in both emax and emin curves with increasing fines content up to 30%, due to gap gradation (Cubrinovski and Ishihara, 2002). When Cubrinovski and Ishihara (2002)'s statements are considered together with the influence of base sand gradations observed in this study, it is highly possible that most laboratory studies in literature is on the conservative side (i.e. more liquefiable) in terms of static liquefaction potential. This is because laboratory prepared sand-silt mixtures are generally considerably gap graded compared to natural silty sands.

Another interesting observation in Figures 5.4, Figure 5.5 and Figure 5.6 is that the influence of base sand gradation is most noticeable at FC=5% (Figure 5.4a, Figure 5.5a, Figure 5.6a), and appears to relatively weakened as fines content is increased to 15%, especially for TT and IZ silts (Figure 5.4c and Figure 5.6c) where all specimens had liquefied. Though, it was still considerable for Sile Sands with 15% SI silt (Figure 5.5c). Figure 5.8 gives the effective stress paths of Sile Sands when FC is increased to 25% by different silt types. Even though effective stress path of specimens with Sile Sand 80/100 were only slightly above the specimens of other two base sands, the

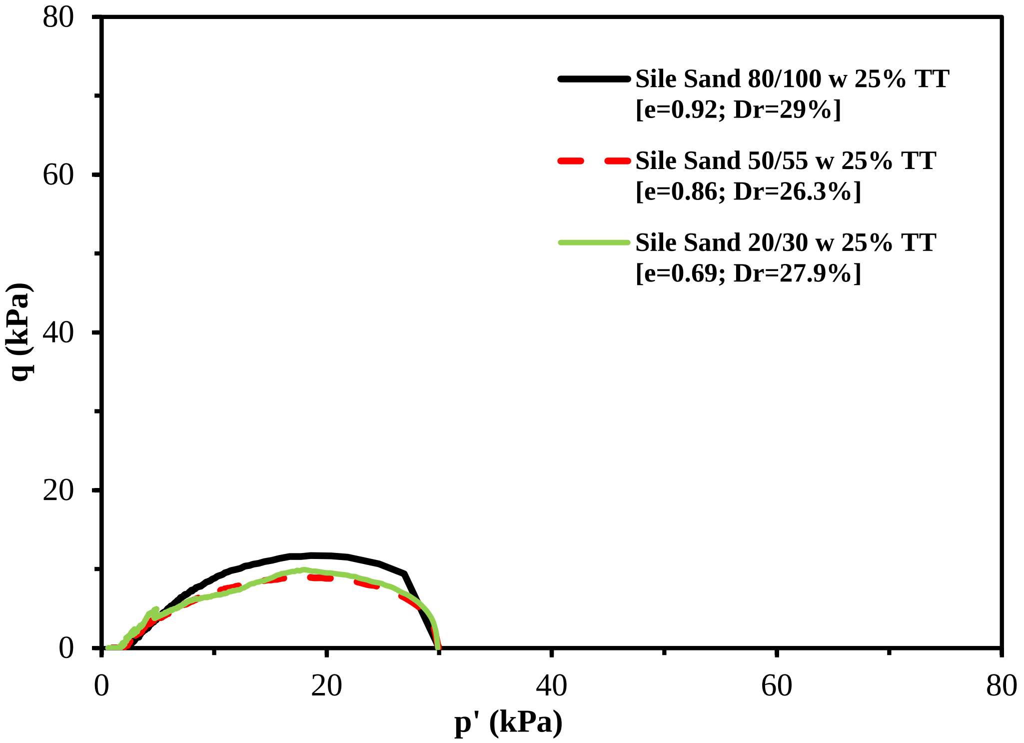

Sile Sand 80/100 w 25% TT
[e=0.92; Dr=29%]
Sile Sand 50/55 w 25% TT
[e=0.86; Dr=26.3%]
Sile Sand 20/30 w 25% TT
[e=0.69; Dr=27.9%]
q (kPa)
p' (kPa)
0
20
40
60
80

(a)

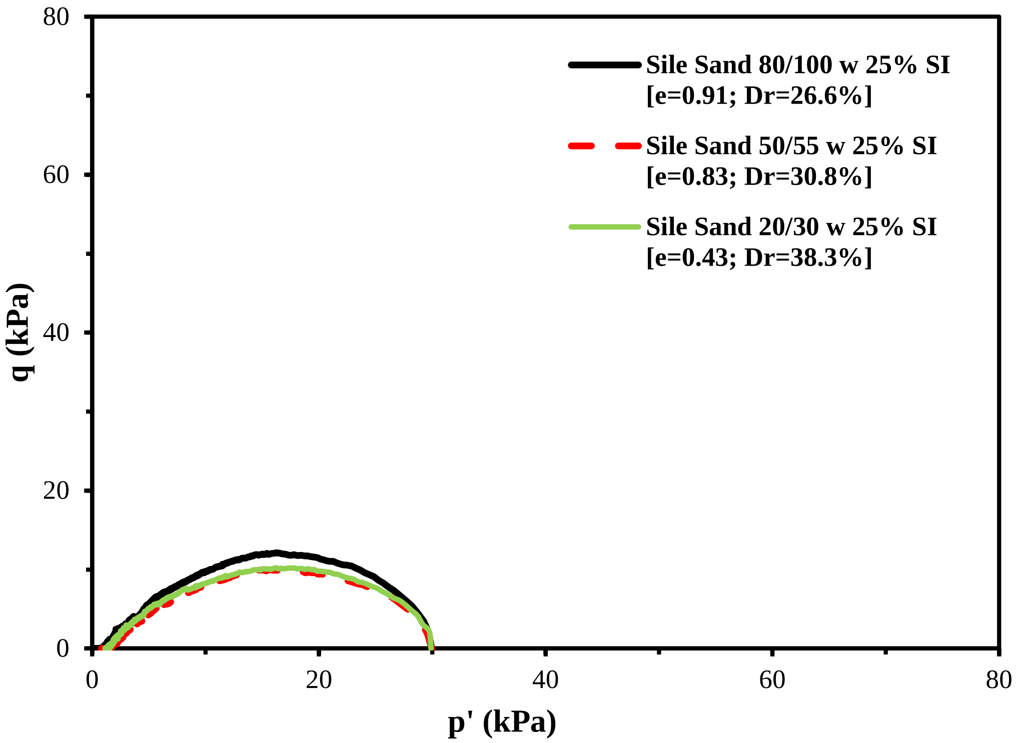

Sile Sand 80/100 w 25% SI
[e=0.91; Dr=26.6%]
Sile Sand 50/55 w 25% SI
[e=0.83; Dr=30.8%]
Sile Sand 20/30 w 25% SI
[e=0.43; Dr=38.3%]
q (kPa)
p' (kPa)
0
20
40
60
80

(b)

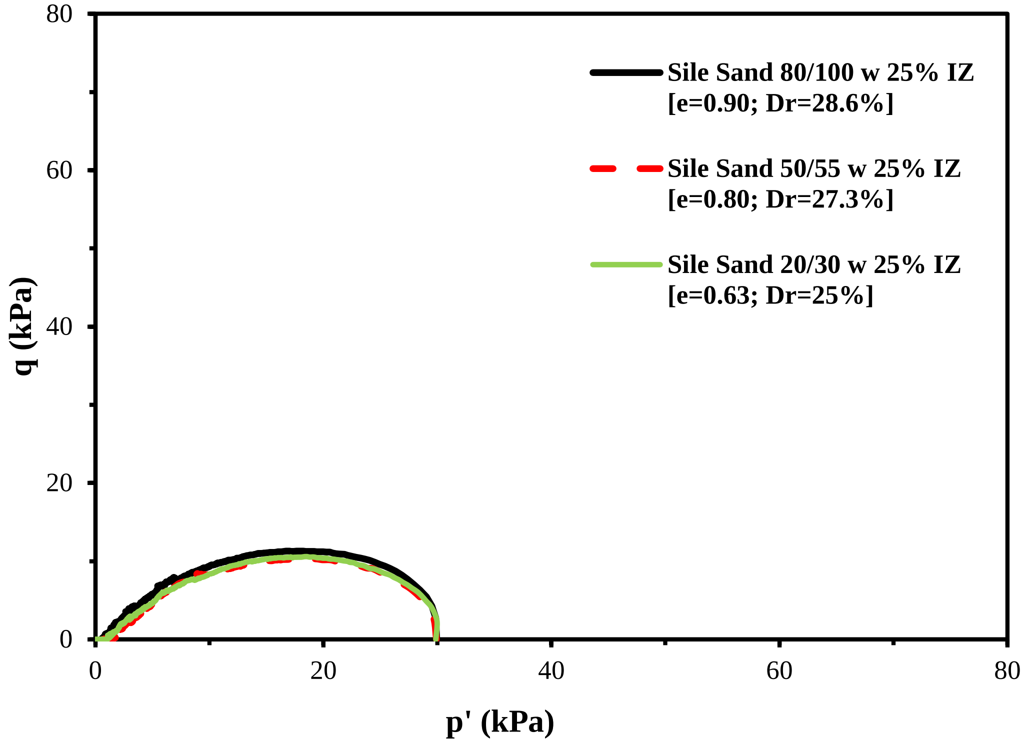

(c)

Figure 5.8 : Effective stress paths for different Sile Sands (a) with 25% TT silt; (b) with 25% SI silt; (c) with 25% IZ silt.

practical difference between the liquefaction behaviours due to change in base sand gradations became negligible at 25% fines content. More explicitly base sand liquefaction tendency could have suppressed the influence of different base sand gradations on undrained shearing for loose specimens at relatively higher fines contents (e.g. 25%). However, had those specimens in figure 5.8 been tested at denser states such that static liquefaction would not occur, it is possible that different base sand gradations could still influence the undrained response even at relatively higher fines contents (e.g. FC=25%).

5.3 Change in the Liquefaction Behavior of Sands with Coefficient of Uniformity

Figure 5.9(a) shows the change in undrained shear strengths of all the tested specimens in this study, which were analyzed through Figure 5.3 to Figure 5.8, with coefficient of uniformity (C_U). For specimens which showed stable response the value of peak deviator stress (q_{peak}) was chosen at the point of effective stress failure where the principle effective stress ratio became maximum (i.e. at $(\sigma'_1/\sigma'_3)_{max}$). For other specimens which showed temporary liquefaction and liquefaction, qpeak values were chosen at the initial peak point of deviator stress. The qpeak values were then normalized by the initial effective confining stress (i.e σ'_{3c}=30kPa).

Figure 5.9(b) shows how the liquefaction behaviors of the specimens in figure 5.9(a) have changed for different coefficient of uniformities. The three distinct responses regarding the liquefaction behavior: stable(S), temporary liquefaction(TL), and liquefaction(L) were shown with different symbols in figure 5.9(b). Unlike loose clean sand behavior reported in literature, in which liquefaction resistance increases with increasing C_U (Vaid et al., 1990; Kokusho et al., 2004; Igwe et al., 2007), liquefaction resistance of silty sands in this study generally decreased with increasing C_U. However, the observed trend is interesting and could be expressed in two stages. For $C_U \leq 2.5$ the decrease in q_{peak}/σ'_{3c} was very sharp with minor increase in C_U, and specimens showing stable and temporary liquefaction responses can be represented with the same trend shown in figure 5.9(b) (with one exception labeled with question mark on figure) and the corresponding relationship is given in Equation 5.1, where “a” and “b” are line fitting coefficients. For Sile Sands mixed with different non-plastic silts in this study, the value of a is 5.84 and the value of b is 2.09. The rapidly decreasing trend of qpeak/σ'3c with C_U (≤2.5) given in figure 5.9 corresponds to low fines content range (FC≤5%), where the magnitude of CU (i.e. D_{60}/D_{10}) was relatively insensitive to silt addition. However, undrained shear strengths of specimens were still considerably varied.

$$\frac{q_{peak}}{\sigma'_{3c}} = a - b.CU \quad \text{(for specimens which were stable or temporarily liquefied)} \quad (5.1)$$

As C_U is further increased beyond 2.5, liquefaction resistance probably decreased gradually and for $C_U \geq 5$ all specimens had shown static liquefaction as shown in figure 5.9. However, unlike the almost vertical trend representing the stable and temporarily liquefied specimens, the trend for liquefied specimens became almost horizontal as shown in Fig. 11b and the corresponding relationship is given in Equation 5.2, where “c” and “d” are curve fitting coefficients. For Sile Sands mixed with different non-plastic silts in this study, the value of c is 1.512 and the value of d is 0.179.

$$\frac{q_{peak}}{\sigma'_{3c}} = \frac{1}{c\,.\,CU^{d}} \qquad \text{(for loose specimens which were liquefied)} \qquad (5.2)$$

Equation 5.2 implies that regardless of the grain size distribution characteristics of sands in this study, the magnitude of q_{peak}/σ'_{3c} and corresponding liquefaction response became much less sensitive to coefficient of uniformity especially for large C_U values (see also Figure 5.9(b)). However, it should be reminded that all the base sands used in this study were poorly graded (SP) (Table 3.1) and coming from the same geologic origin. Note that many factors including gradation, shape effects, fines' type and content could have their own contribution to the resulting undrained response of specimens and therefore to coefficients of the given equations. Also, the Equations. 5.1 and 5.2 were developed based on the response of loose (figure 5.2) clean and silty Sile Sands and includes the combination of all those effects.

The validity of these equations for other loose sands studied in literature is also an important question. Unfortunately, the available data in literature regarding the coefficient of uniformities of specimens that have shown static liquefaction are extremely limited. Monkul and Yamamuro, (2011) had previously investigated the influence of silt size and content on static liquefaction of sands. In that study, loose specimens of Nevada Sand mixed with various percent of Loch Raven silt had shown static liquefaction. The individual grain size distribution curves of the liquefied specimens were plotted based on the gradation data from the archive of the author and corresponding C_U values were calculated. The resulting relationship between the q_{peak}/σ'_{3c} versus C_U for Nevada Sand with Loch Raven fines is shown in Figure 5.10. Accordingly, Equation 5.2 represents the observed trend very well and the back calculated parameters (c and d) together with the other information regarding the soils and testing conditions are summarized in Table 5.1.
Another set of data was taken from the pioneering study of Lade and Yamamuro (1997), in which loose clean and silty Nevada Sand 50/200 specimens had shown static liquefaction. The individual grain size distribution curves of the liquefied specimens were plotted based on the gradation data from Covert (1998) and corresponding C_U values were calculated. The resulting relationship between the q_{peak}/σ'_{3c} versus C_U for Nevada Sand 50/200 is also shown in Figure 5.10. Similar to the specimens of Monkul and Yamamuro (2011), the liquefied specimens of Lade and Yamamuro (1997) are also quite well represented by Equation 5.2 (Figure 5.10). In both studies the range of

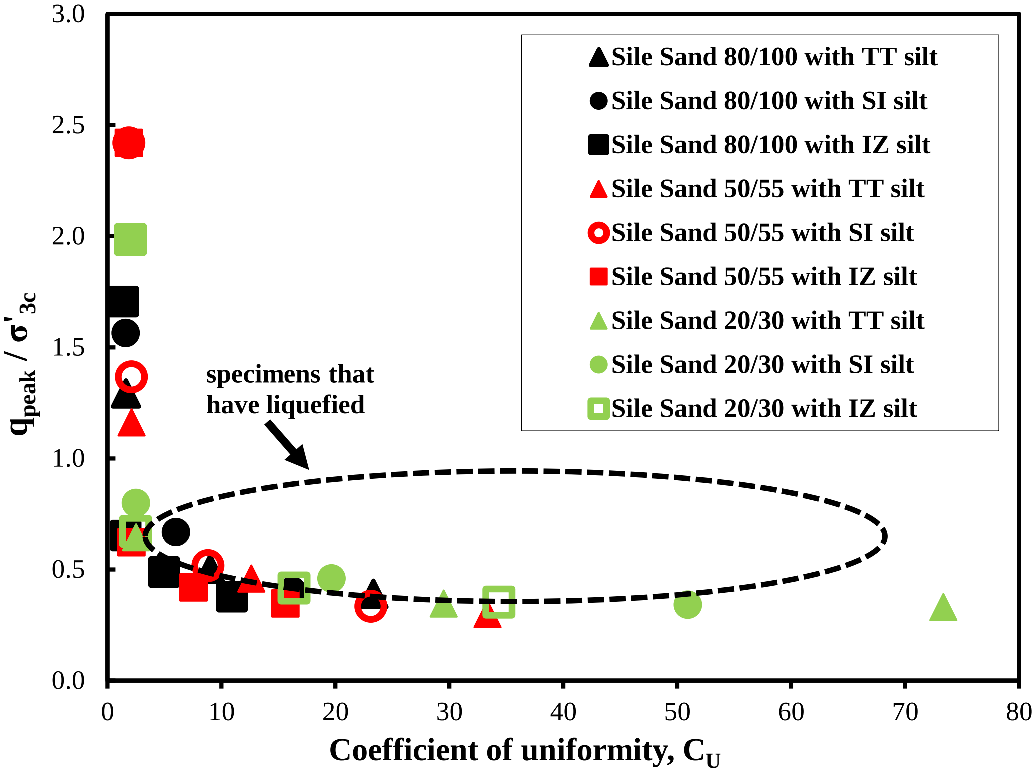

(a)

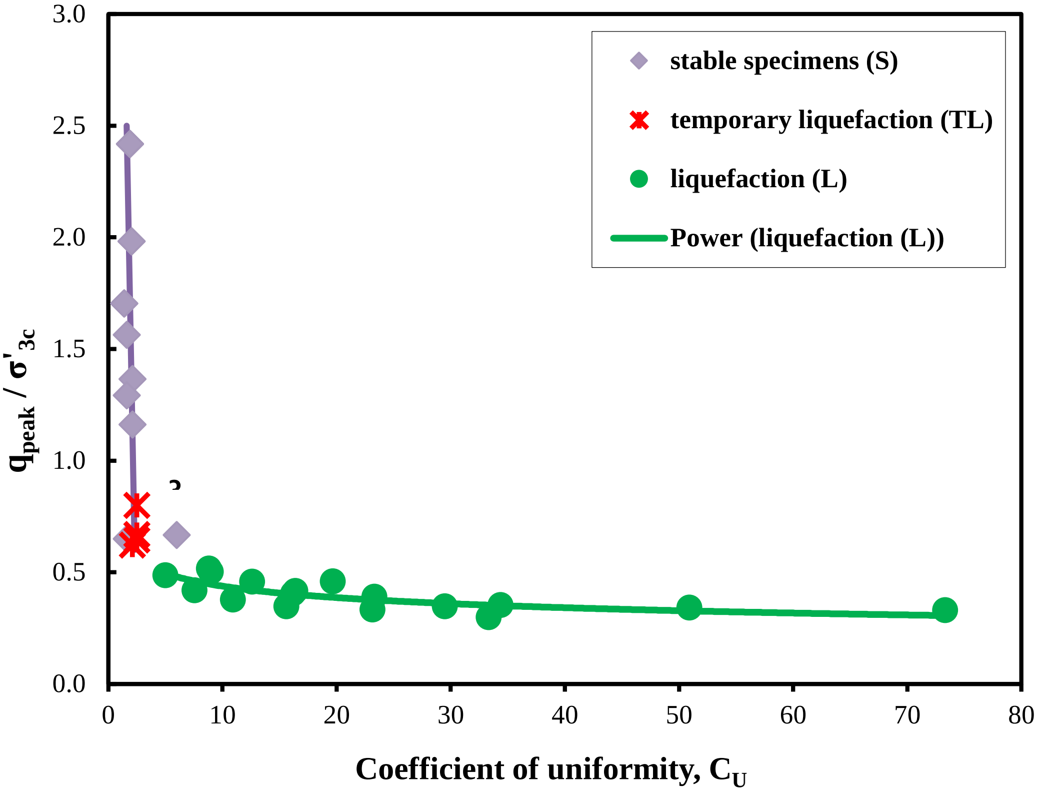

(b)

Figure 5.9 : (a) Change in normalized peak deviator stress with coefficient of uniformity for the tested specimens, (b) Corresponding change in liquefaction behaviors of the tested specimens with C_U.

C_U of the tested soils were narrow (Figure 5.10) compared to the range of C_U of the tested soils in this study (figure 5.10), however the extrapolated curves in Figure 5.10 towards greater C_U values based on Equation 5.2 are harmonic for all studies and implies a decreasing sensitivity of q_{peak}/σ'_{3c} to coefficient of uniformity as C_U increases for the liquefied soils.

Table 5.1 : Testing conditions and back-calculated parameters of Equations 5.1 and 5.2 for different soils in literature.

Reference	Monkul and Yamamuro (2011)	Lade and Yamamuro (1997)	Belkhatir et al. (2011)
Base Sand (USCS)	Nevada (SP)	Nevada 50/200 (SP)	Chlef (SP)
Silt	Loch Raven	Nevada	Chlef
FC range (%)	0-20	0-30	0-50
Specimen prep. method	dry funnel deposition	dry funnel deposition	under-compaction
Dr (%)	29±3	26.5±6.5	20
σ'_{3c} (kPa)	30	25	100
specimen response	all liquefied (L)	all liquefied (L)	all stable (S)
a (in Eq.1)	-	-	1.082
b (in Eq.1)	-	-	0.032
c (in Eq.2)	2.0	2.253	-
d (in Eq.2)	0.287	0.447	-

Regarding the stable response, the set of data was taken from the study of Belkhatir et al. (2011), where loose Chlef Sand specimens were tested at various fines content. The resulting relationship between the q_{peak}/σ'_{3c} versus C_U for Chlef Sand is shown in Fig. 5.10. Even though, the deviator stress at maximum principle effective stress ratio, $(\sigma'_1/\sigma'_3)_{max}$ was considered as q_{peak} for stable specimens during the development of Equation 5.1, q_{peak} values corresponding to the maximum point of the deviator stress-strain curves of Belkhatir et al. (2011) were taken as no information was available regarding the change of principle effective stress ratio. Nevertheless, Equation 5.1 represents the relationship between q_{peak}/σ'_{3c} and C_U of Chlef Sand specimens, which were all stable, surprisingly well as shown in Figure 5.10, and back calculated parameters (a and b) are given in Table 5.1. Note that, similar to the Sile Sands in this study, the base sands of the re-visited studies in Table 5.1 are all poorly graded (SP). This is perhaps somewhat conservative as liquefaction resistance of clean sands typically increases as they become well graded. To extend the validity of the proposed equations to silty sands with well graded (SW) base sand matrix could be a good direction for future research.

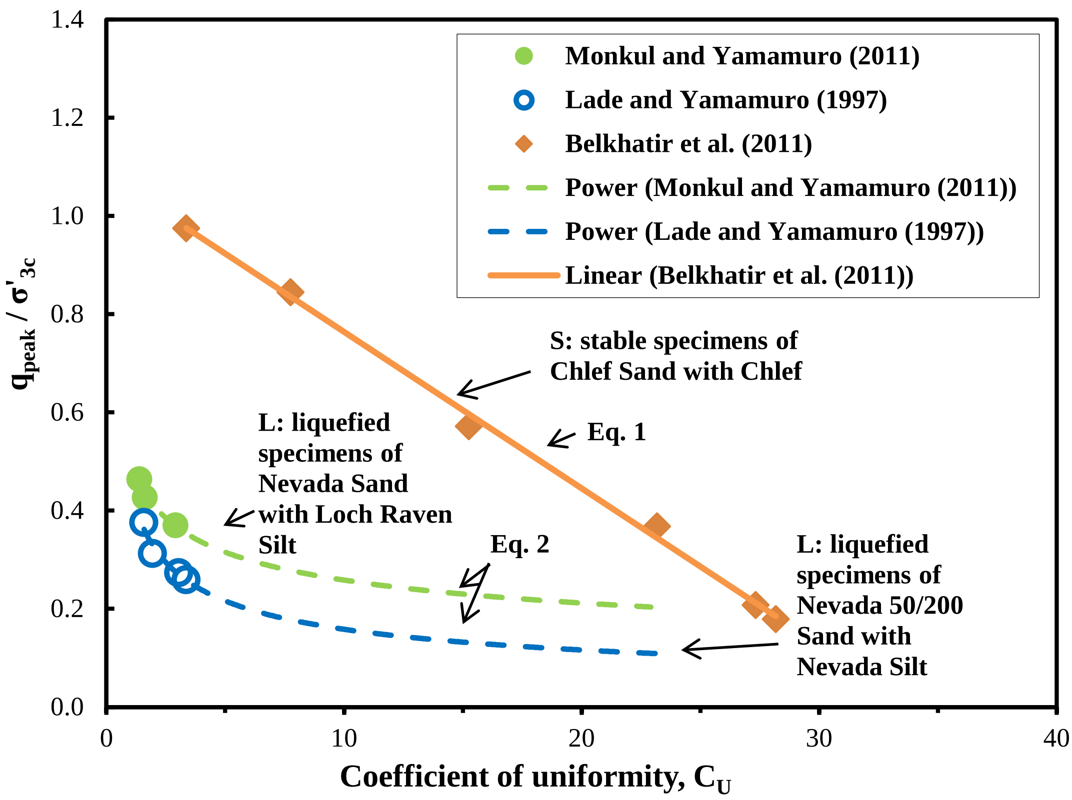

Figure 5.10 : Change in normalized peak deviator stress (q_{peak}/σ'_{3c}) with coefficient of uniformity (C_U) for different types of soils in literature.

5.4 Compressibility as an Indicator of Liquefaction Potential

5.4.1 Isotropic compression tests

The results of the undrained triaxial tests revealed a consistent increase in liquefaction potential of Sile Sand 80/100 with increasing non-plastic fines content. The volumetric strains (ε_v) plotted versus effective confining stresses (σ'_{3c}) during isotropic compression are given in Figures 5.10(a) and (b) for sand with TT and IZ Silts, respectively. Note that those are the same specimens used in the undrained triaxial compression tests.

It may be observed from Figure 5.10 that the volumetric strains increase almost linearly with increasing confining stress, and the amount of volumetric strain at the end of isotropic compression increases with increasing fines content for both silts. Volumetric compressibility, m_v, sometimes called the coefficient of volume change, is a parameter mostly used in analyzing consolidation of soils. Equation 5.3 shows that m_v is the increment of volumetric strain, $\varepsilon_v = \Delta V/V_{sat}$ divided by the increment of effective confining pressure:

$$m_v = \frac{d\varepsilon_v}{d\sigma'_{3c}} = \frac{\Delta\varepsilon_v}{\Delta\sigma'_{3c}} \tag{5.3}$$

The change of volumetric compressibility of Sile Sand 80/100 obtained by equation 5.3 with fines content is plotted in figure 5.11. This figure clearly demonstrates that volumetric compressibility of a sand increases with fines content. This observation is parallel to the trend found in the undrained shearing stage, where liquefaction potential of Sile Sand 80/100 increased with fines content. In other words, volumetric compressibility could be an indicator for liquefaction potential.

Figure 5.11 also shows that the m_v-values for both silt types are close to each other and increasing in an almost parallel fashion until 15% FC, and then started to deviate considerably towards 25% FC. Based on the results shown in Fgure 4.1 and practical difference between the liquefaction behaviours due to change in base sand gradations became negligible at 25% fines content. More explicitly base sand 4.3, approximate boundaries for stable response and static liquefaction are also drawn in figure 5.11, and the region in between is named the transition zone between stable behavior and liquefaction. Accordingly, sandy specimens with volumetric compressibility values smaller than 0.17 (1/MPa) were stable, while all specimens with volumetric compressibility values greater than 0.23 (1/MPa) liquefied. It should be noted that these boundaries are approximate based on the specimens prepared at "quasi-natural void ratios" explained before, and the precise transition zone could be slightly narrower. However, it may be expected that somewhere in the transition zone, shown in Figure 5.11, the behavior of Sile Sand 80/100 would change from stable to temporary liquefaction, and then the behavior would gradually transform towards static liquefaction. Temporary liquefaction occurs when the deviator stress reaches an initial peak (q_{peak}) and then temporarily drops before it increases again until reaching steady state.

Figure 5.11 also shows that the numerical values of m_v do not enable a direct comparison of liquefaction potential of a sand at specific FC but with different silts. For example, at FC=5%, m_v for sand with TT Silt is slightly greater than m_v for sand

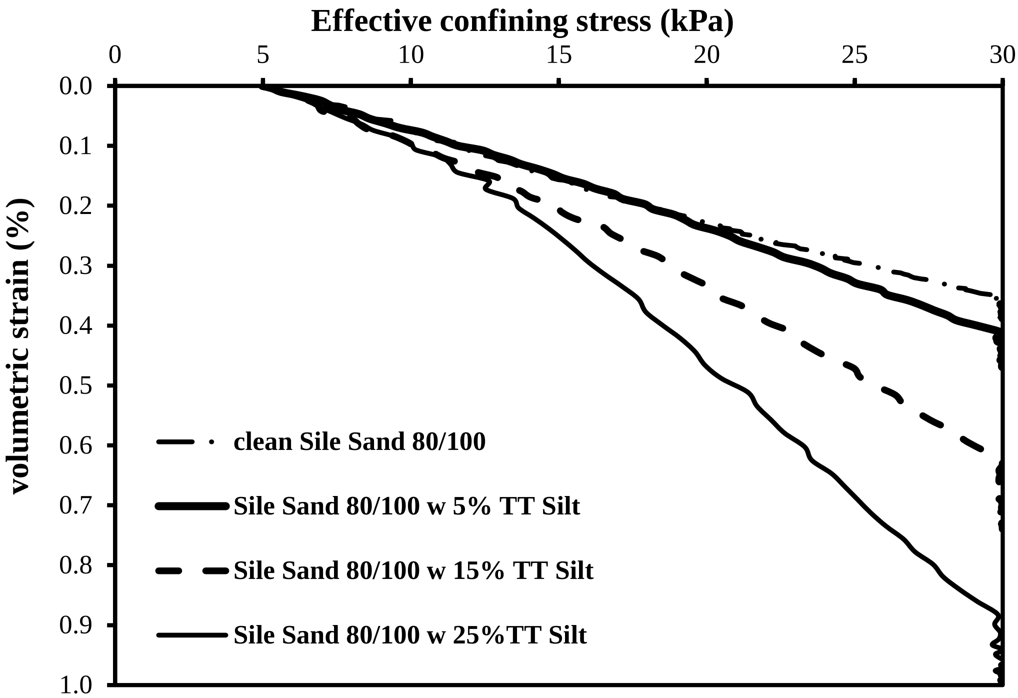

(a)

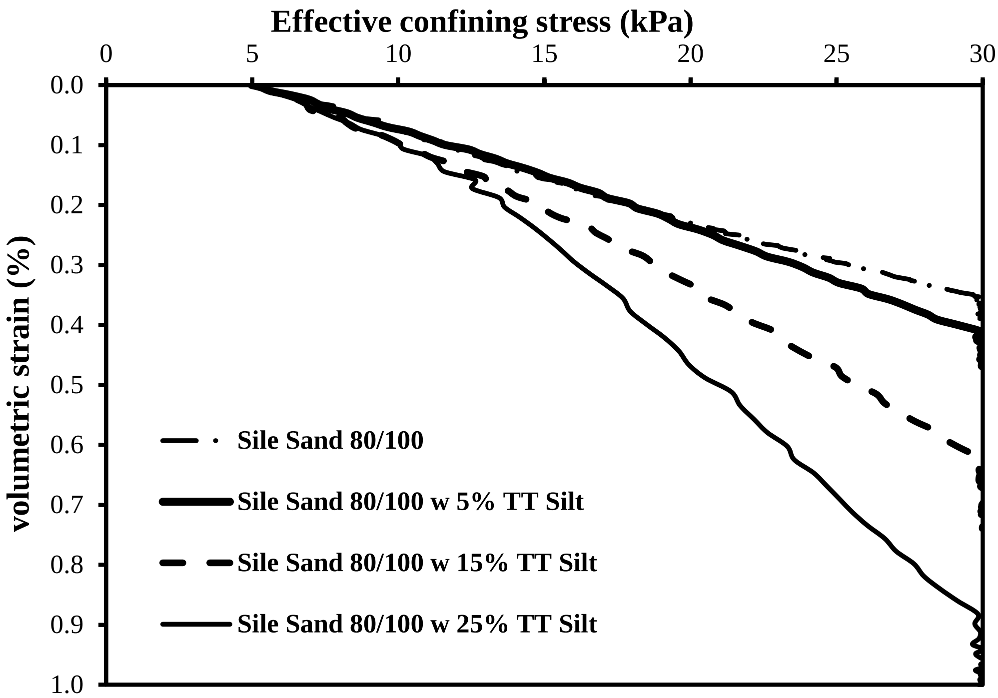

(b)

Figure 5.11 : Volumetric strain variation with effective confining stress for Sile Sand 80/100 with (a) TT Silt and (b) IZ Silt.

with IZ Silt, but sand with IZ Silt was more liquefiable than sand with TT Silt (see Figure 4.1 and Figure 4.3). In fact, these comparisons confirm the complexity of the liquefaction problem. Even though the same base sand is used, adding different silts while keeping plasticity and fines content the same may still change the soil fabric, which is critical for the resulting liquefaction behavior (Monkul and Yamamuro, 2011; Monkul 2012). There could be many factors influencing the fabric of sandy soils including but not limited to fines gradation, size, plasticity, content, angularity, mineralogy etc.

The change of volumetric strain of clean sands with confining stress is given in Figure 5.12. Once again numerical values of mv do not enable a direct comparison of liquefaction potential of different sands even with same geologic origin. As observed in Figure 4.1, the liquefaction resistance of the clean sands in this study have decreased as they become finer and more uniform. Hence, Sile Sand 20/30 was the least liquefiable among the three clean sands, yet its volumetric compressibility was greater than the mv-values of the other two clean sands as shown in Figure 5.12. However, it is important to note that mv-values of clean sands are all in the range of the "stable response" zone discussed in Figure 5.11, which correlates well with the observed undrained behavior.

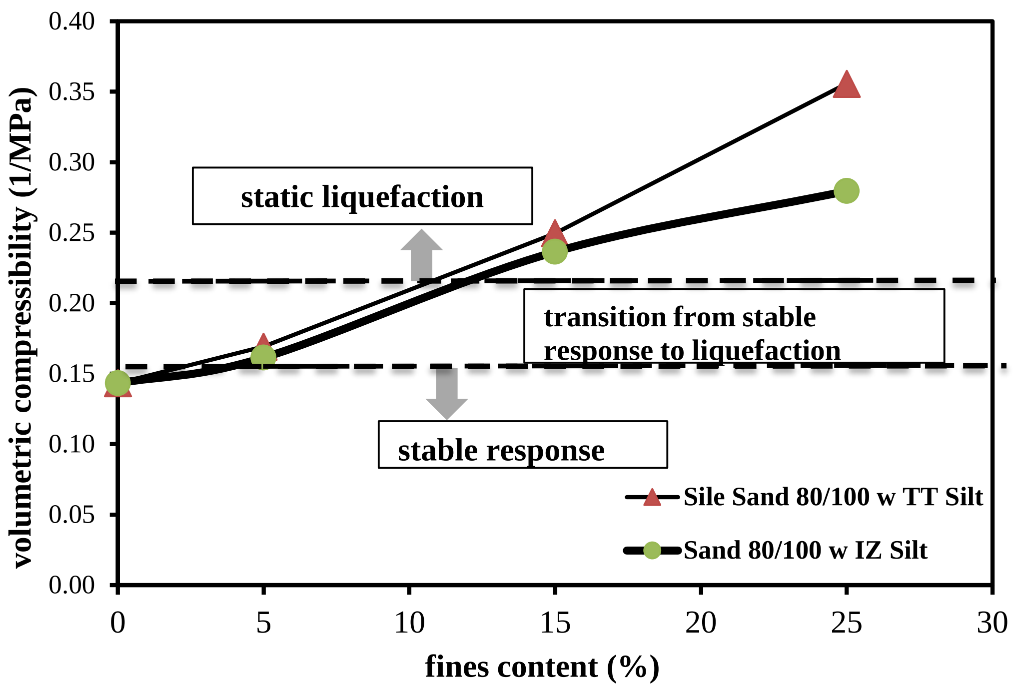

Figure 5.12 : Volumetric compressibility versus liquefaction potential of Sile Sand 80/100 with fines content for two different non-plastic silts.

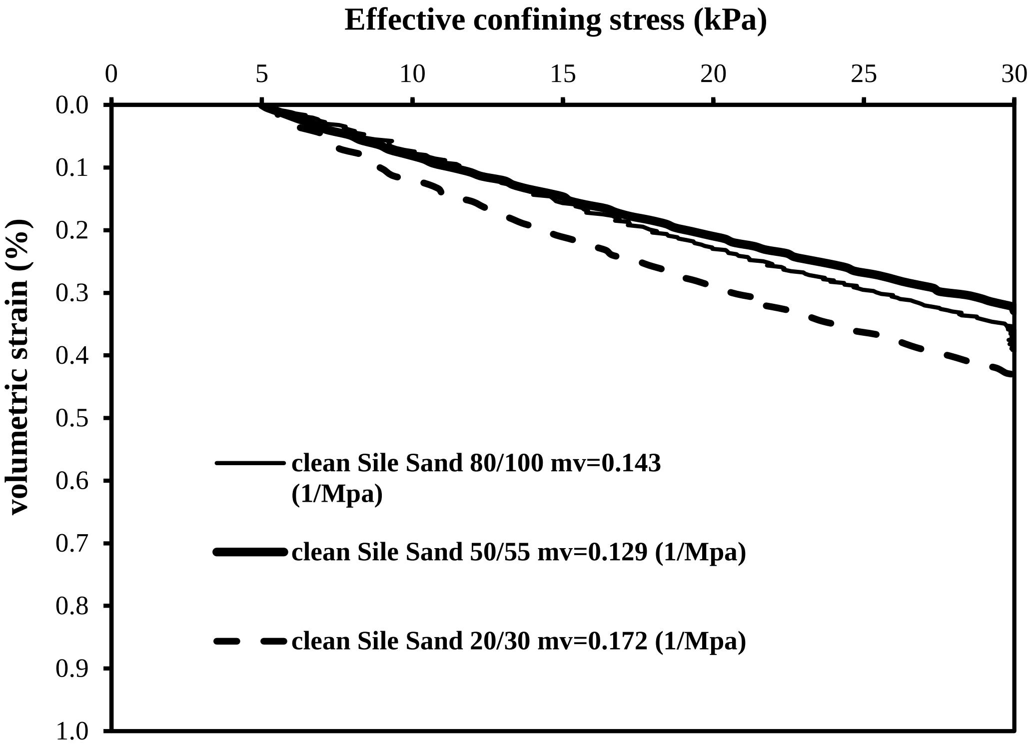

Figure 5.13 : Variation in volumetric strain with effective confining stress and corresponding volumetric compressibilities for clean sands.

6. CONCLUSIONS

The initial step in assessing the liquefaction potential of soils during failures due to static or flow type of liquefaction is to determine the prevalent behavioral characteristics of the soils during undrained static loading. According to the data obtained from case studies, it can be seen that in most cases the very common soil type is sands with silt fractions rather than being clean sands. In fact, the influence of base sand and silt on the liquefaction mechanism is an issue that needs to be further considered.

In this study, influence of fines content, grain size distribution, and shape characteristics of silt grain matrix on static liquefaction behavior of loose sands and the possibility of considering volumetric compressibility (m_v) as an indicator of liquefaction potential for sands and silty sands, were investigated. First, undrained monotonic triaxial compression tests were performed on thirty sands with varying fines contents, which were prepared by mixing three base sands (Sile Sands 20/30, 50/55, 80/100) with same geologic origin but with various gradations and three different non-plastic silts (IZ, SI and TT silts) with different gradations and shape characteristics. Then, available silt shapes investigated using optical and scanning electron microscopes. Finally, isotropic compression test results compared with relevant undrained monotonic triaxial test results, in order to study the possibility of considering the volumetric compressibility (m_v) as an indicator of liquefaction potential of sands and silty sands. It should be noted that, other major factors that could influence the static liquefaction potential of specimens such as initial confining stress (30kPa), sand mineralogy and deposition technique (dry funnel deposition) were kept the same during all experimental program. The experimental outcomes were analyzed based on six main aspects: I) influence of fines content, II) influence of grain size distribution of base sand, III) influence of grain size distribution of silt matrix, IV) influence of silt shape characteristics, V) influence of coefficient of uniformity on static liquefaction of silty sands and finally VI) possibility of conceiving volumetric compressibility (m_v) as an indicator of liquefaction potential. Following is the discussion of the factors mentioned above in detail.

I) Influence of fines content

Concerning to the first aspect, test results showed that liquefaction potential of Sile Sands have systematically increased with increasing fines content in this study (for FC≤25%). The main comparison basis was "loosest possible density after deposition", but several other bases including similar relative density and similar void ratio were also employed during the comparison of static liquefaction behaviors. Accordingly, the trend of increasing liquefaction potential with increasing fines content is verified for three base sands mixed with three different non-plastic silts at four different fines contents (i.e. FC=0%, 5%, 15% and 25%). In fact, the observed trend was in good agreement with the previous studies in literature regarding the influence of non-plastic fines content on liquefaction of sands.

II) Influence of grain size distribution of base sand

Regarding the second aspect, effects of grain size distribution of base sands investigated. It is found that static liquefaction resistance of clean Sile Sands used in this study decreased as they became finer (i.e. $D_{50\text{-}sand}$ decreases) and at the same time more uniform (i.e. CU_{sand} decreases) when similar relative density or loosest possible density (quasi natural void ratio) is used as a comparison basis. On the other hand, when the mentioned sands were mixed with silt, the trend mentioned above was interestingly reversed. In other words, silty sands became more liquefiable as base sand became coarser (i.e. $D_{50\text{-}sand}$ increases) and relatively well graded (i.e. CU_{sand} increases). And this reversed trend was consistently observed for all the three non-plastic silt types. In order to find an explanation for this strange trend, it was hypothesized that the reason for such a reversed trend could be the gap gradation character induced by different base sand gradations. Then, a fourth base sand was specially produced in order to promote further gap gradation and it was experimentally shown that one of the reasons behind the mentioned reversed trend was indeed the gap gradations induced by used Sile Sands. It should be noted that, when natural soils are considered, the above findings imply that most laboratory studies are possibly on the conservative side (i.e. more liquefiable) in terms of static liquefaction potential aspect because laboratory reconstituted sand-silt mixtures are generally prepared substantially gap graded compared to natural sands with silt.

Accordingly, effect of base sand gradation on liquefaction response was found to be dependent on the amount of fines content. It was shown that the effect of base sand gradation was most noticeable at low FC (i.e. 5%) and gradually weakened as FC was increased (e.g. 15%) and almost vanished at FC=25%. It is possible that high excess pore pressure generation and the resulting static liquefaction tendency could have suppressed the influence of different base sand gradations on undrained shearing for loose specimens at relatively higher fines contents (e.g. 25%). However, it is expected that at denser states, such that static liquefaction would not occur, it is also possible that different base sand gradations could still influence the undrained response of samples, even at relatively higher fines contents (e.g. FC=25%).

III) influence of grain size distribution of silt matrix

Regarding the third aspect, when initial stress conditions, mineralogy, fines content and base sand gradation were kept the same, at low fines contents (i.e. $0<FC\leq15\%$), the liquefaction potential of all the three sands used in this study increased with SI, TT and IZ silts, respectively. In fact, the coefficient of uniformities of the silt grain matrixes had surprisingly decreases with the same order as well (i.e. $CU_{SI\text{-}silt} > CU_{TT\text{-}silt} > CU_{IZ\text{-}silt}$). Besides, one can postulate that the relatively well graded nature of SI silt grains might have led to the drop in the static liquefaction due to the potential tendency of more efficient packing of SI silt in between the sand grains compared to the other silts. It was shown that there are several other additional factors beyond CU_{silt} affecting the static liquefaction. One of those additional factors is the size ratio of the sand grains to the silt grains. Monkul and Yamamuro (2011) have proposed a criterion based on mean grain diameter ratio ($D_{50\text{-}sand}/d_{50\text{-}silt}$), which simply states that at the same relative density, FC, initial stress conditions, base sand mineralogy and gradation, the static liquefaction potential of a silty sand increases as the mean grain diameter ratio ($D_{50\text{-}sand}/d_{50\text{-}silt}$) decreases. In fact, this criterion is generally asserted for the silty sands in this study (e.g. IZ silt vs. SI silt and IZ silt vs. TT silt in three base sands with different gradations).

On the other hand, there was an exception for the specimens involving TT silt versus SI silt. In other words, according to data obtained from grain size distribution curves, for the same base sand, $D_{50\text{-}sand}/d_{50\text{-}silt}$ ratio was largest for specimens with TT silt among the three silt types but the static liquefaction resistance of the specimens with TT silt was not the greatest among other tested silts.

IV) influence of silt shape characteristics

With respect to the contrary trend discussed above and with the aim of finding an explanation for it, an extensive grain shape characterization investigation for the three silts was conducted by using both optical and scanning electron microscopes.

Totally, 360 individual silt grains were analyzed based on “Krumbein Scale” (Krumbein and Sloss, 1963) in 2-D and corresponding sphericity and roundness values of the silt grains were determined. With respect to data analysis, TT silt was classified as sub-angular to angular (R=0.26), while SI and IZ silts were classified as sub-rounded with quite close roundness values to each other (R≈0.38). Besides, sphericity (S) values for all the three silts were greater than 0.6, but TT and SI silts were more spherical (S=0.68) than IZ silt (S=0.63).

It was shown that at the same depositional energy, fines content, base sand, and consolidation stress conditions, angular nature of TT silt potentially caused more metastable contacts (i.e. weaker grain contacts that promotes excess pore pressure generation during shearing) within the specimens than sub-rounded SI silt. Accordingly, this resulted in specimens with TT silt to be more liquefiable than their counterparts with SI silt, overruling the mean grain diameter ratio effect for specimens involving those two silt types. Besides, the change in several density index parameters of various specimens such as void ratio and intergranular void ratio also supported that explanation. This finding shows that the samples’ initial fabrics achieved before shearing, and therefore the static liquefaction potentials, were not only influenced by the grain size distribution and the relative size of the silts involved in this study, but can also effected by the shape characteristics of those silt grain matrixes, too.

With respect to all factors mentioned above, it can be inferred that the impact of silt gradation parameters (CU_{silt}, $d_{50\text{-}silt}$) and shape characteristics (R, S) of silt grain matrix on static liquefaction potential of Sile Sands was dependent on the amount of fines content. More explicitly, the influence of silt characteristics (e.g. CU_{silt}, $d_{50\text{-}silt}$, R, S) on static liquefaction behavior of silty sands is coupled with the amount of fines content. Accordingly, for a particular base sand, as the fines content increases from 15% to 25%, stress-strain and the resulting static liquefaction responses of specimens composed of different silts became identical. In other words, the effect of gradation parameters and shape characteristics of silt grain matrix became negligible as fines content was increased towards 25%, and the same trend was observed for all the three

base sands. The concept of transition fines content (FC_t), over which the sand grain matrix loses the domination over undrained behavior was engaged for a possible explanation. In fact, several equations proposed in literature to determine the FC_t were employed and transition fines contents of the corresponding specimens were estimated. However, the estimated FC_t values were deficient to explain why gradation parameters and shape characteristics of silt grain matrix lose their influence on liquefaction behavior beyond a certain fines content (≥15%). What is more interesting is that the effect of silt characteristics (i.e. gradation and shape) on static liquefaction of sands increases with decreasing fines content values below FC_t, unlike the expected behavior, where the role of fines on the engineering response of sandy soils decreases with decreasing fines content (i.e. increasingly sand dominated behavior with decreasing FC is expected). It is thought that high
excess pore pressure generation and resulting static liquefaction could have inhibited the effect of different silt characteristics on undrained shearing and could be the reason why silts characteristics became negligible at higher fines contents for the specimens in this study. On the other hand, had those specimens been tested at denser states such that static liquefaction would not occur, it is possible that mentioned silt characteristics could still influence the undrained response of sands, even at relatively higher fines content (e.g. FC=25%).

V) influence of coefficient of uniformity

Regarding the fifth aspect, relationship between the coefficient of uniformity (C_U) and normalized peak deviator stress (q_{peak}/σ'_{3c}) of all the thirty soils tested was investigated. In spite of the clean sands, in which liquefaction resistance increases with increasing C_U, it was found that liquefaction resistance of silty sands, used in this study, generally decreased with increasing CU. According to the experiments' outcomes, for Sile Sands showing stable and temporary liquefaction responses, sharp decreases in q_{peak}/σ'_{3c} with only minor changes in C_U was observed. On the other hand, for liquefied Sile Sand specimens the decrease in q_{peak}/σ'_{3c} was minor with significant changes in C_U. Besides, two different equations were proposed to show the relationship between q_{peak}/σ'_{3c} with coefficient of uniformity: one for stable and temporarily liquefied specimens and the other one for liquefied specimens based on the mentioned trends of silty sands. Also, three studies in literature were re-visited and it was proved that the proposed equations can also be satisfactorily applied to other sand and silt types.

VI) possibility of conceiving volumetric compressibility (m_v) as an indicator of liquefaction potential

In the final part of investigations, outcomes of isotropic compression tests and undrained triaxial compression tests of three available base sands and also Sile sand 80/100 mixtures with TT silt and IZ silt at three different fines contents each, was investigated. With respect to results of both experiments, it was inferred that there is a strong relationship between volumetric compressibility and liquefaction potential of sandy soils with different fines contents. In fact, the numerical values of m_v appear to enable a general comparison between soils involving different sand and silt types. The approximate boundaries for stable response, transition stage, and liquefaction region are also determined. Consequently, specimens with volumetric compression values smaller than 0.17 (1/MPa) were stable, while all specimens with volumetric compression values greater than 0.23 (1/MPa) liquefied.

Despite the fact that different sands and silts were used in this study, further laboratory and in-situ tests on different sand and silt types are still needed to verify and somewhat tune those volumetric compression boundaries for the benefit of geotechnical engineering practice. It has been expected that if such a verification is successful and approximate boundaries are established, perhaps including categories of different sandy soils, the necessity of the challenging task of obtaining undisturbed samples in silty sands could be avoided. Besides, field tests such as screw plate, pressuremeter and flat dilatometer tests could be used to obtain in-situ equivalent volumetric compressibilities. This would also have the advantage of testing the soil at its original fabric, thus avoiding the problem of appropriate specimen preparation.

Finally, it should be noted that the findings explained above regarding the influence of gradation, fines content, shape characteristics of silt grains and volumetric compressibility of silty sands on undrained shearing are limited to monotonic behavior and resulting static liquefaction. Hence, how and to what extent those coupled factors influence the dynamic behavior and resulting cyclic liquefaction of silty sands seems to be a good field of investigation for future studies.

REFERENCES

ASTM D2487 (2005). Standard practice for classification of soils for engineering purposes, American Society for Testing and Materials, West Conshohocken, PA.

ASTM D422 (2005). Standard test method for particle-size analysis of soils, American Society for Testing and Materials, West Conshohocken, PA.

ASTM D4253-16 (2016). Standard Test Methods for Maximum Index Density and Unit Weight of Soils Using a Vibratory Table, ASTM International, West Conshohocken, PA, www.astm.org.

ASTM D4254-16 (2016). Standard Test Methods for Minimum Index Density and Unit Weight of Soils and Calculation of Relative Density, ASTM International, West Conshohocken, PA, www.astm.org.

ASTM D4318-10e1 (2010). Standard Test Methods for Liquid Limit, Plastic Limit, and Plasticity Index of Soils, ASTM International, West Conshohocken, PA, www.astm.org.

ASTM D4767-11 (2011). Standard Test Method for Consolidated Undrained Triaxial Compression Test for Cohesive Soils, ASTM International, West Conshohocken, PA, www.astm.org.

ASTM D5311 (2005). Standard test method for load controlled cyclic triaxial strength of soil, American Society for Testing and Materials, West Conshohocken, PA.

ASTM D854 (2005). Standard test methods for specific gravity of soil solids by water pycnometer, American Society for Testing and Materials, West Conshohocken, PA.

ASTM D854-14, Standard Test Methods for Specific Gravity of Soil Solids by Water Pycnometer, ASTM International, West Conshohocken, PA, 2014, www.astm.org.

Bahadori, H., Ghalandarzadeh, A., Towhata, I. (2008). Effect of non plastic silt on the anisotropic behavior of sand. Soils and Foundations, JGS, 48(4), 531-545.

Belkhatir, M., Arab, A., Schanz, T., Missoum, H., Della, N. (2011). Laboratory study on the liquefaction resistance of sand-silt mixtures: effect of grading characteristics. Granular Matter, 13, 599-609.

Belkhatir, M., Schanz, T., Arab, A. (2013). Effect of fines content and void ratio on the saturated hydraulic conductivity and undrained shear strength of sand–silt mixtures. Environmental Earth Sciences, 70(6), 2469-2479.

Brandon, T. L., Clough, G. W., Rahardjo, P. P. (1991). Fabrication of silty sand specimens for large and small scale tests. Geotechnical Testing Journal, 14(1), 46-55.

Carraro, J. A. H., Prezzi, M., Salgado, R. (2009). Shear strength and stiffness of sands containing plastic or nonplastic fines. Journal of Geotechnical and Geoenvironmental Engineering, ASCE, 135(9), 1167-1178.

Castro, G. (1969). Liquefaction of sands. (Ph.D. thesis), Harvard University, Cambridge, Massachusetts.

Cho, G.C., Dodds, J., Santamarina, J.C. (2006). Particle shape effects on packing density, stiffness, and strength: natural and crushed sands. Journal of Geotechnical and Geoenvironmental Engineering, ASCE, *132(5)*, 591-602.

Covert, K.M. (1998). Behavior of silty sands under monotonic and cyclic triaxial compression. M.Sc. Thesis, Clarkson University, Potsdam, NY.

Cox, M.R., Budhu, M. (2008). A practical approach to grain shape quantification. Engineering Geology, Elsevier, 96, 1-16.

Cubrinovski, M., Ishihara, K. (2002). Maximum and minimum void ratio characteristics of sands. Soils and Foundations, JGS, (42)6, 65-78.

Dash, H.K., Sitharam, T.G. (2011). Undrained monotonic response of sand-silt mixtures: effect of nonplastic fines. Geomechanics and Geoengineering, *6(1)*, 47-58.

Dash, H.K., Sitharam, T.G. (2011). Undrained monotonic response of sand-silt mixtures: effect of nonplastic fines. Geomechanics and Geoengineering, *6(1)*, 47-58.

Erten, D., and Maher, M. H. (1995). Cyclic undrained behavior of silty sand. Soil Dynamics and Earthquake Engineering, *14*, 115-123.

Fonseca, J., O'Sullivan, C., Coop, M.R., Lee, P.D. (2012). Non-invasive characterization of particle morphology of natural sands. Soils and Foundations, JGS, *52(4)*, 712-722.

Frydman, S., Zeitlen, J. G., and Alpan, I. (1973). The membrane effect in triaxial testing of granular soils. Journal of Testing and Evaluation, ASTM, 1(1), 37-41.

Georgiannou, V.N. (2006). The undrained response of sands with additions of particles of various shapes and sizes. Geotechnique, *56 (9)*, 639–649.

Georgiannou, V.N., Tsomokos, A. (2010). Effect of grain shape and angularity on the undrained response of fine sands. Canadian Geotechnical Journal, *47*, 539-551.

Guo, P., Su, X. (2007). Shear strength, interparticle locking, and dilatancy of granular materials. Canadian Geotechnical Journal, *44*,579-591.

Hazirbaba, K. and Rathje, E.M. (2009). Pore pressure generation of silty sands due to induced cyclic shear strains. Journal of Geotechnical and Geoenvironmental Engineering, ASCE, 135(12), 1892-1905.

Høeg K, Dyvik R, Sandbækken G. (2000). Strength of undisturbed versus reconstituted silt and silty sand specimens. Journal of Geotechnical and Geoenvironmental Engineering, ASCE, *126(7)*:606–617.

Huang, Y.T., Huang, A.B., Kuo, Y.C., Tsai, M.D. (2004). A laboratory study on the undrained strength of a silty sand from Central Western Taiwan. Soil Dynamics and Earthquake Engineering, 24, 733-743.

Igwe, O., Fukuoka, H., Sassa, K. (2012). The effect of relative density and confining stress on shear properties of sands with varying grading. Geotechnical and Geological Engineering, Springer, *30*, 1207-1229.

Igwe, O., Sassa, K., Wang, F. (2007). The influence of grading on the shear strength of loose sands in stress-controlled ring shear tests. Landslides, Springer-Verlag, *4(1)*, 43-51.

Ishihara, K. (1993). Liquefaction and flow failure during earthquakes. Géotechnique, *43(3)*, 351–415.

Kanagalingam, T., Thevanayagam, S. (2005). Discussion to “Contribution of fines to the compressive strength of mixed soils”, Geotechnique, *55(8)*, 627-628.

Koerner, R. M. (1970). Effect of particle characteristics on soil strength. Journal of the Soil Mechanics and Foundations Division, ASCE, SM4, 1221-1234.

Kokusho, T., Hara, T., Hiraoka, R. (2004). Undrained shear strength of granular soils with different particle gradations, Journal of Geotechnical and Geoenvironmental Engineering, ASCE, *130(6)*, 621-629.

Kolbuszewski, J. J., (1948). An Experimental Study of the Maximum and Minimum Porosities of Sands, Proceedings, Second International Conference on Soil Mechanics and Foundation Engineering, Rotterdam, Vol. *1*, pp. 158–165.

Konrad, J.M. (1991). The Nerlerk berm case history: some considerations for the design of hydraulic sand fills. Canadian Geotechnical Journal, *28(4)*, 601-612.

Kramer, S.L. (1996). Geotechnical Earthquake Engineering, Prentice Hall, New Jersey.

Krumbein, W. C., and Sloss, L. L. (1963). Stratigraphy and Sedimentation, Second Ed., Freeman and Company, San Francisco.

Kuerbis, R., Negussey, D., and Vaid, Y.P. (1988). Effect of gradation and fines content on the undrained response of sand. Hydraulic fill structures, ASCE Geotechnical Engineering Division Specialty Publication No. 21, D. J. A. Van Zyl and S. G. Vick, eds., Fort Collins, Colo., 330–345.

Lade, P., Liggio, C., and Yamamuro, J., (1998). Effects of Non-Plastic Fines on Minimum and Maximum Void Ratios of Sand, Geotechnical Testing Journal, Vol. *21*, No. 4, pp. 336-347.

Lade, P.V. (1993) Initiation of static instability in the submarine Nerlerk berm. Canadian Geotechnical Journal, 30(6), 895-904.

Lade, P.V. and Hernandez, S.B. (1977). Membrane penetration effects in undrained tests. Journal of the Geotechnical Engineering Division, 103, GT 2, 109-125.

Lade, P.V. and Yamamuro, J.A. (1997). Effects of nonplastic fines on static liquefaction of sands. Canadian Geotechnical Journal, 34(6), 918-928.

Lade, P.V. and Yamamuro, J.A. 1997. Effects of nonplastic fines on static liquefaction of sands. Canadian Geotechnical Journal, *34(6)*, 918-928.

Lade, P.V., and Yamamuro, J.A. (2011) Evaluation of static liquefaction potential of silty sand slopes. Canadian Geotechnical Journal, 48(2), 247-264.

Lade, P.V., Liggio, C.D. and Yamamuro, J.A. (1998). Effects of nonplastic fines on minimum and maximum void ratios of sand. Geotechnical Testing Journal, *21(4)*, 336-347.

Lade, P.V., Yamamuro, J.A. (2011). Evaluation of static liquefaction potential of silty sand slopes. Canadian Geotechnical Journal, 48, 247-264.

Lade, P.V., Yamamuro, J.A., Liggio, C.D.Jr. (2009) Effects of fines content on void ratio, compressibility, and static liquefaction of silty sand. Geomechanics and Engineering, *1(1)*, 1-15.

Maleki, M., Ezzatkhah, A., Bayat, M., Mousivand, M. (2011). Effect of physical parameters on static undrained resistance of sandy soil with low silt content. Soil Dynamics and Earthquake Engineering, *31*, 1324-1331.

Monkul, M.M. (2006) Stability of loose sandy slopes. Proceedings of Seventh International Congress on Advances in Civil Engineering, Yıldız Technical University, Istanbul, Türkiye, 13 pages (CD-ROM). ISBN: 975-461-416-4.

Monkul, M.M. (2012). On some of the factors influencing the fines' role on liquefaction of silty sands. Geotechnical Special Publication No 225: State of the Art and Practice in Geotechnical Engineering, ASCE, 799-808.

Monkul, M.M. (2013). Influence of gradation on shear strength and volume change behavior of silty sands. Geomechanics and Engineering, 5(5), 401-417.

Monkul, M.M. and Ozden, G. (2007). Compressional behavior of clayey sand and transition fines content. Engineering Geology, *89(3-4)*, 195-205.

Monkul, M.M. and Yamamuro, J.A. (2010). Influence of densification method on some aspects of undrained silty sand behavior. Proceedings of the Fifth International Conference on Recent Advances in Geotechnical Earthquake Engineering and Soil Dynamics, San Diego, California, Paper No: 1.23a, 8 pages (CD-ROM). ISBN: 1-887009-15-9.

Monkul, M.M. and Yamamuro, J.A. (2011). Influence of silt size and content on liquefaction behavior of sands. Canadian Geotechnical Journal, 48, 931-942.

Monkul, M.M., Etminan, E., Senol, A. (2016). Influence of coefficient of uniformity and base sand gradation on static liquefaction of loose sands with silt. Soil Dynamics and Earthquake Engineering (accepted).

Monkul, M.M., Gultekin, C., Gulver, M., Akin, O., Eseller-Bayat, E. (2015). Estimation of liquefaction potential from dry and saturated sandy soils under drained constant volume cyclic simple shear loading. Soil Dynamics and Earthquake Engineering, 75, 27-36.

Monkul, M.M., Lade, P.V., Etminan, E., Senol, A. (2014). Compressibility as an indicator of liquefaction potential. Geotechnical Engineering Journal of the SEAGS & AGSSEA, *45(4)*, 73-77.

Mulilis, J. P., Seed, H. B., Chan, C. K., Mitchell, J. K., and Arulanandan, K., (1977). ''Effects of Sample Preparation on Sand Liquefaction,'' Journal of the Geotechnical Engineering Division, Vol. *103*, No. GT2, pp. 91–108.

Murthy, T. G., Loukidis, D., Carraro, J. A. H., Prezzi, M., Salgado, R. (2007). Undrained monotonic response of clean and silty sands. Geotechnique, *57(3)*, 273–288.

Ng, C. W. W., Fung, W. T., Cheuk, C. Y., Zhang, L. (2004). Influence of stress ratio and stress path on behavior of loose decomposed granite. Journal of Geotechnical and Geoenvironmental Engineering, ASCE, *130(1)*, 36-44.

Ni, Q., Tan, T. S., Dasari, G. R., Hight, D. W. (2004). Contribution of fines to the compressive strength of mixed soils. Geotechnique, *54(9)*, 561–569.

Papadopoulou, A. and Tika, T. (2008). The effect of fines on critical state and liquefaction resistance characteristics of non-plastic silty sands. Soils and Foundations, JGS, *48(5)*, 713-725.

Pitman, T.D., Robertson, P.K., Sego, D.C. (1994). Influence of fines on the collapse of loose sands. Canadian Geotechnical Journal, *31(5)*, 728-739.

Polito, C. P., and Martin II, J. R. (2001). Effects of nonplastic fines on the liquefaction resistance of sands. Journal of Geotechnical and Geoenvironmental Engineering, ASCE, *127(5)*, 408–415.

Polito, C. P., and Martin II, J. R. (2003). A reconciliation of the effects of non-plastic fines on the liquefaction resistance of sands reported in the literature. Earthquake Spectra, EERI, *19(3)*, 635–651.

Powers, M.C. (1953). A new roundness scale for sedimentary particles. Journal of Sedimentary Petrology, *23(2)*, 117-119.

Rahman, M.M., Lo, S.R. (2012). Predicting the onset of static liquefaction of loose sand with fines. Journal of Geotechnical and Geoenvironmental Engineering, ASCE, *138(8)*, 1037-1041.

Rahman, M.M., Lo, S.R. (2014). Undrained behavior of sand-fines mixtures and their state parameter. Journal of Geotechnical and Geoenvironmental Engineering , ASCE, *140(7)*, 04014036.

Rahman, M.M., Lo, S.R., Gnanendran, C.T. (2008). On equivalent granular void ratio and steady state behaviour of loose sand with fines. Canadian Geotechnical Journal, *45*, 1439-1456.

Reimer, M.F. and Seed, R.B. (1997). Factors affecting apparent position of steady-state line. ASCE Journal of Geotechnical Engineering. 123 (3): 281-288.

Rouse, P.C., Fannin, R.J., Shuttle, D.A. (2008). Influence of roundness on the void ratio and strength of uniform sand. Geotechnique, 58(3), 227-231.

Shapiro, S., Yamamuro, J.A. (2003). Effects of silt on three dimensional stress-strain behavior of loose sand. Journal of Geotechnical and Geoenvironmental Engineering , ASCE, *129(1)*, 1-11.

Shen, C.K., Vrymoed, J. L., Uyeno, C.K. (1977). The effect of fines on liquefaction of sands. Proceedings of the 9th International Conference on Soil Mechanics and Foundation Engineering, Tokyo, 2, 381-385.

Sladen, J.A., D'Hollander, R. D., Krahn, J. (1985). Back analysis of the Nerlerk berm liquefaction slides. Canadian Geotechnical Journal, *22(4)*, 579-588.

Thevanayagam, S. (1998). Effect of fines and confining stress on undrained shear strength of silty sands. Journal of Geotechnical and Geoenvironmental Engineering, ASCE, *124(6)*, 479-491.

Thevanayagam, S., Mohan, S. (2000). Intergranular state variables and stress-strain behaviour of silty sands. Geotechnique, 50(1), 1-23.

Thevanayagam, S., Shenthan, T., Mohan, S., Liang, J. (2002). Undrained fragility of clean sands, silty sands, and sandy silts. Journal of Geotechnical and Geoenvironmental Engineering, ASCE, *128(10)*, 849-859.

Troncoso, J.H., Verdugo, R. (1985). Silt content and dynamic behavior of tailing sands. Proceedings of the 11th International Conference on Soil Mechanics and Foundation Engineering, San Francisco, 3, 1311-1314.

Vaid, Y. P. and Negussey, D., (1988). Preparation of Reconstituted Sand Specimens, Advanced Triaxial Testing of Soil and Rock, ASTM STP 977, R. T. Donaghe, R. C. Chaney, and M. L. Silver, Eds., American Society for Testing and Materials, West Conshohocken, PA, pp. 405–417.

Vaid, Y.P. (1994). Liquefaction of silty soils. Ground Failures under Seismic Conditions. Geotechnical Special Publication No 44, ASCE, New York, 1–16.

Vaid, Y.P., Fisher, J.M., Kuerbis, R.H., Negussey, D. (1990). Particle gradation and liquefaction. Journal of Geotechnical Engineering, *116(4)*, 698-703.

Vallejo, L.E. (1995). Fractal analysis of granular materials. Geotechnique, *45(1)*, 159-163.

Vallejo, L.E., Mawby, R., (2000). Porosity influence on the shear strength of granular material–clay mixtures. Engineering Geology, *58*, 125–136.

Wadell, H. (1932). Volume, shape, and roundness of rock particles. Journal of Geology, *40(5)*, 443-451.

Wood, F.M., Yamamuro, J.A., Lade, P.V. (2008). Effect of depositional method on the undrained response of silty sand. Canadian Geotechnical Journal, *45*, 1525-1537.

Yamamuro, J.A., and Lade, P.V. (1997). Static liquefaction of very loose sands. Canadian Geotechnical Journal, *34*, 905–917.

Yamamuro, J.A., and Lade, P.V. (1998). Steady state concepts and static liquefaction of silty sands. Journal of Geotechnical and Geoenvironmental Engineering, ASCE, 124(9), 868–877.

Yamamuro, J.A., Wood, F. M., Lade, P.V. (2008). Effect of depositional method on the microstructure of silty sand. Canadian Geotechnical Journal, *45*, 1538-1555.

Yamamuro, J.A., Wood, F.M. (2004). Effect of depositional method on the undrained behavior and microstructure of sand with silt. Soil Dynamics and Earthquake Engineering 24, 751–760.

Yang, J., Wei, L.M. (2012). Collapse of loose sand with the addition of fines: the role of particle shape. Geotechnique, *62(12)*, 1111-1125.

Yang, S., Lacasse, S., Sandven, R. (2006). Determination of the transitional fines content of mixtures of sand and non-plastic fines. Geotechnical Testing Journal, ASTM, *29(2)*, 1-6.

Yang, S.L., Sandven, R., Grande, L. (2006). Instability of sand-silt mixtures. Soil Dynamics and Earthquake Engineering, *26*, 183-190.

Youd, T.L. (1973). Liquefaction, flow, and associated ground failure. Geological Survey Circular 688.

Zlatovic´, S., Ishihara, K. (1995). On the influence of non-plastic fines on residual strength. Proc. IS-Tokyo'95, First International Conference on Earthquake Geotechnical Engineering,1 ,239–244.

Zlatovic´, S., Ishihara, K. (1997). Normalized behavior of very loose non-plastic soils: effects of fabric. Soils and Foundations, *37(4)*, 47-56.

Zuo, L., Baudet, B.A. (2015). Determination of the transitional fines content of sand-non plastic fines mixtures. Soils and Foundations, *55(1)*, 213-219.

APPENDICES

APPENDIX A: Principle stress ratio (σ'_1/ σ'_3) versus axial strain (ε_a) graphs.

APPENDIX A: Principle stress ratio (σ'_1/ σ'_3) versus axial strain (ε_a) graphs.

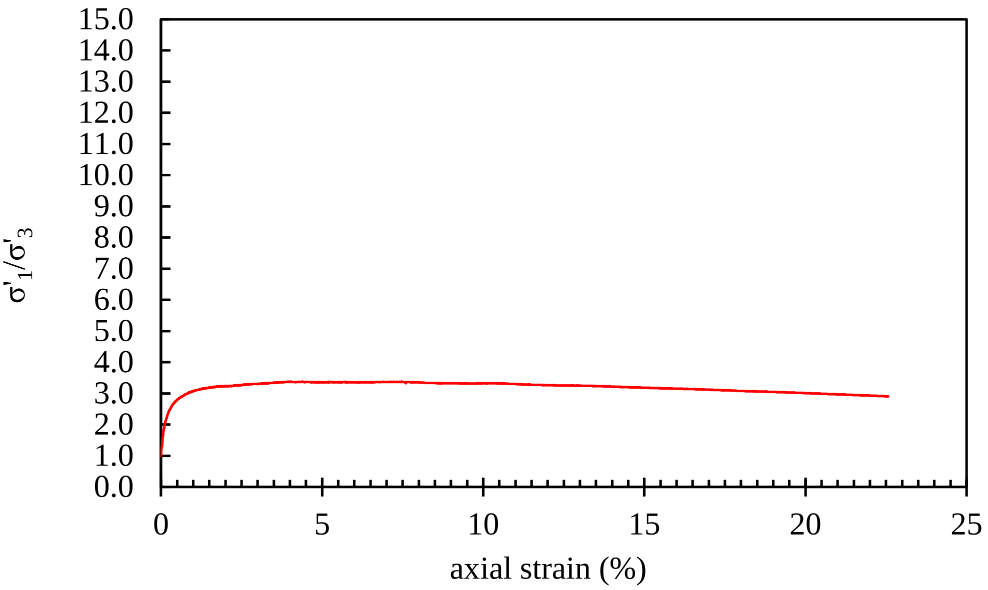

Figure A.1 : Sile Sand 80/100.

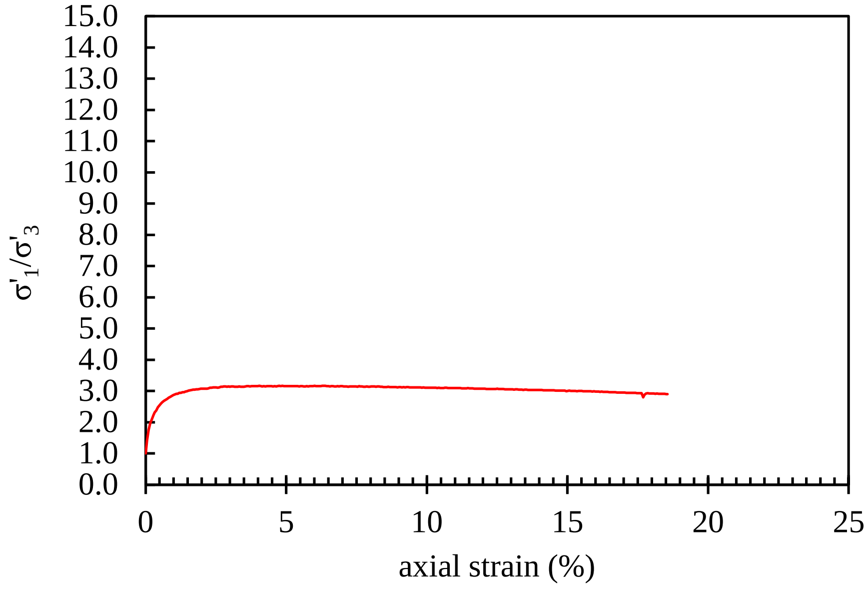

Figure A.2 : 95 % Sile Sand 80/100 + 5% TT Silt.

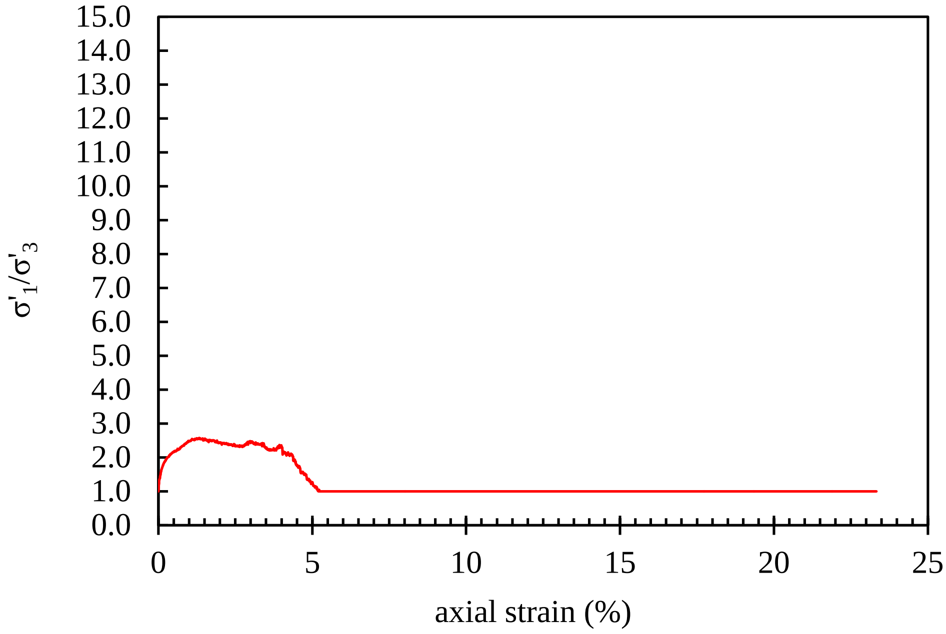

Figure A.3 : 85 % Sile Sand 80/100 + 15% TT Silt.

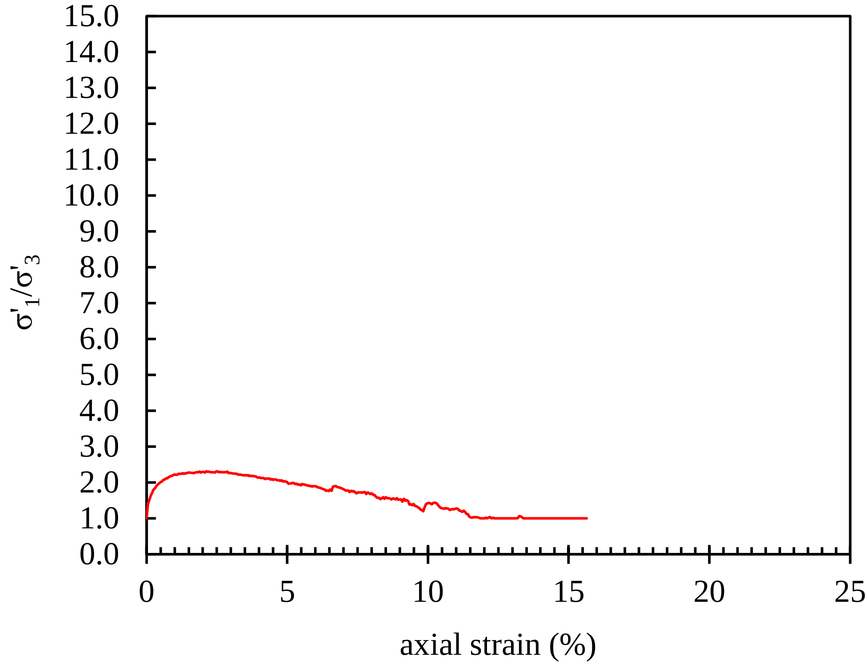

Figure A.4 : 75 % Sile Sand 80/100 + 25% TT Silt.

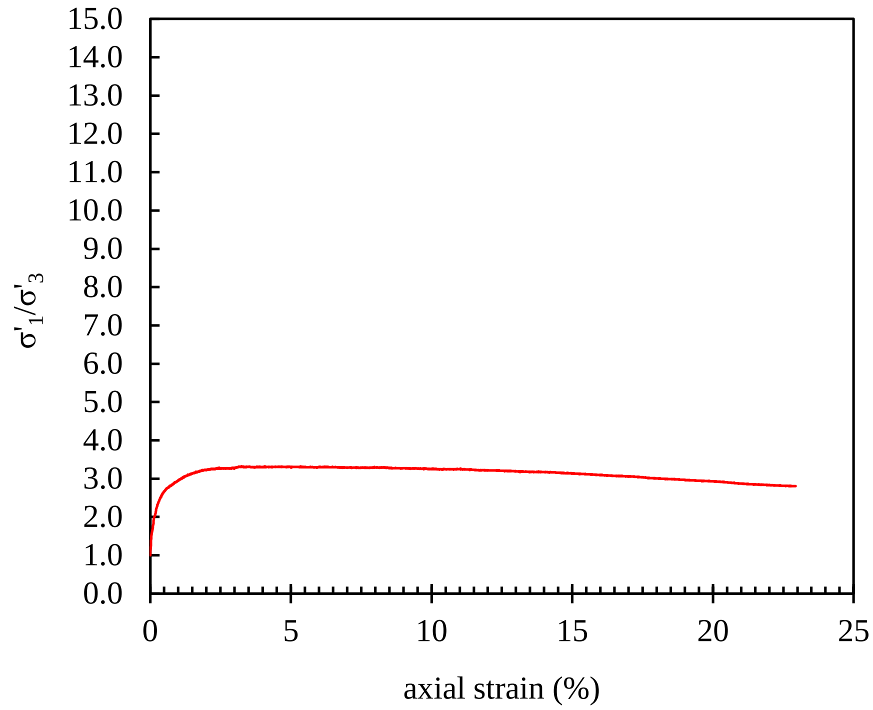

Figure A.5 : 95 % Sile Sand 80/100 + 5% SI Silt.

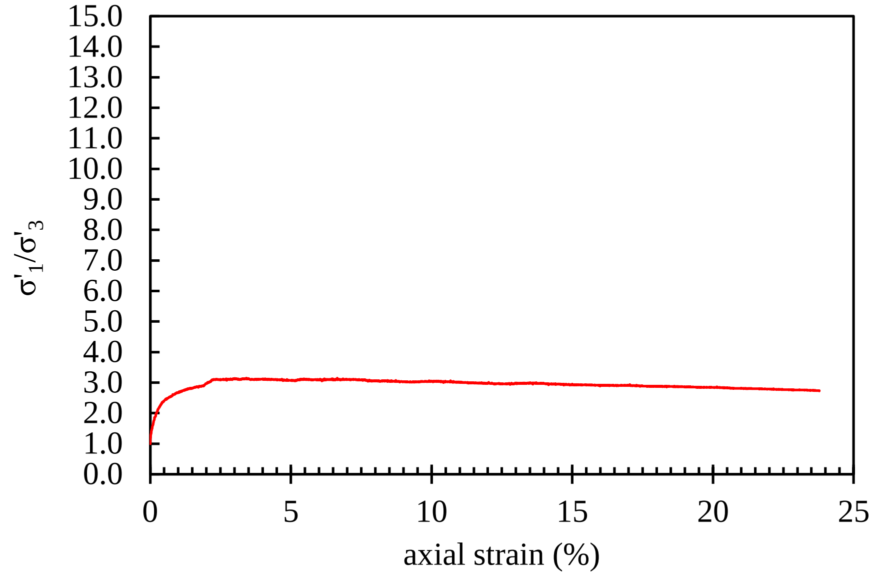

Figure A.6 : 85 % Sile Sand 80/100 + 15% SI Silt.

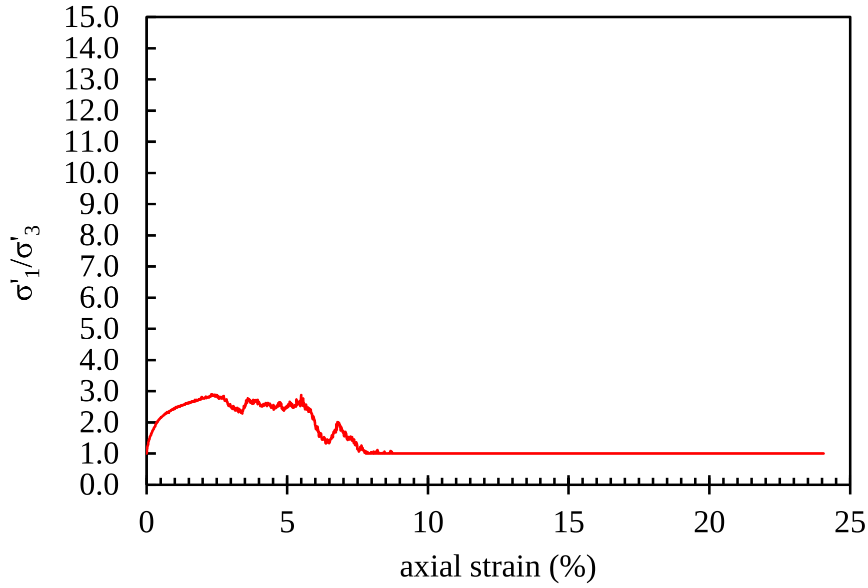

Figure A.7 : 75 % Sile Sand 80/100 + 25% SI Silt.

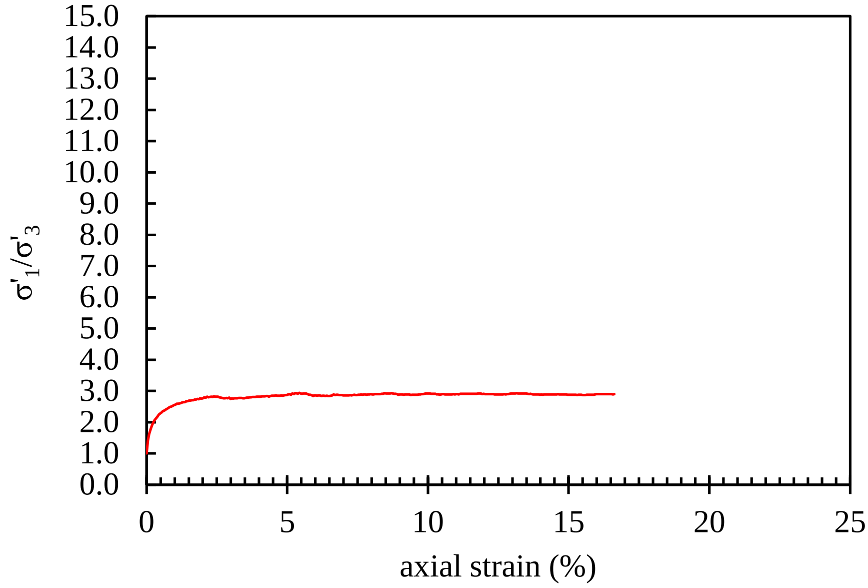

Figure A.8 : 95 % Sile Sand 80/100 + 5% IZ Silt.

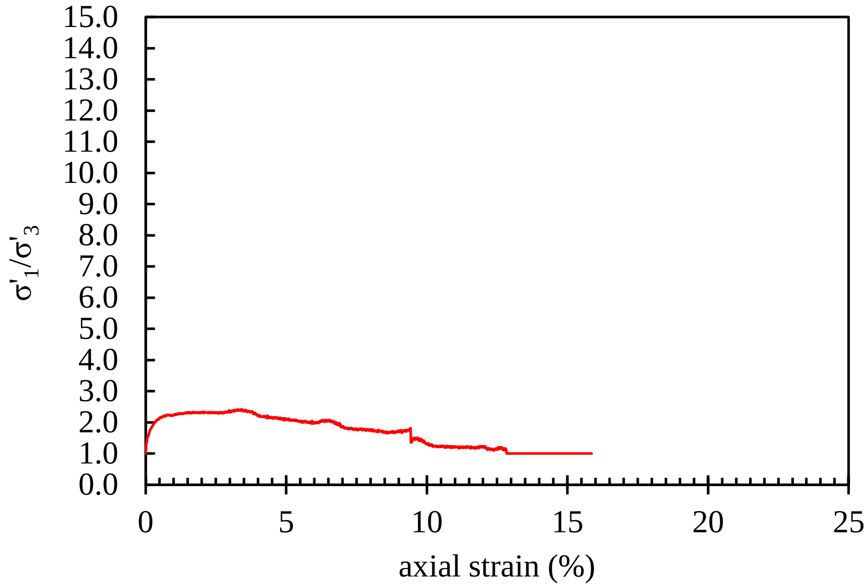

Figure A.9 : 85 % Sile Sand 80/100 + 15% IZ Silt.

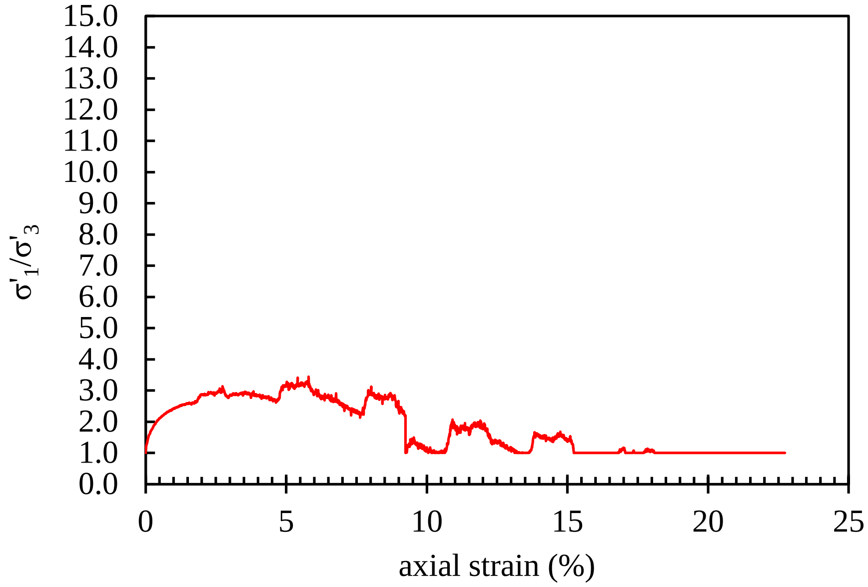

Figure A.10 : 75 % Sile Sand 80/100 + 25% IZ Silt.

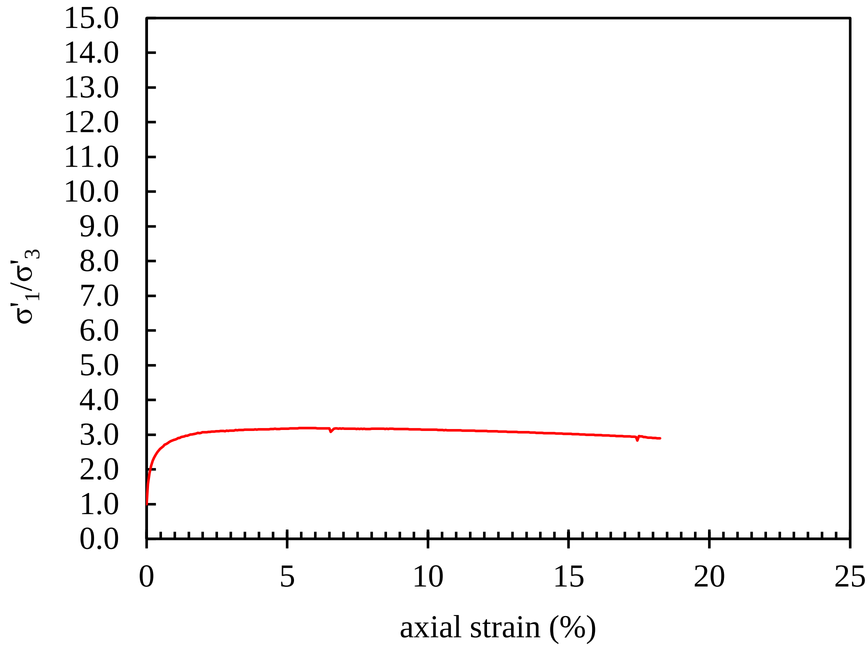

Figure A.11 : Sile Sand 50/55.

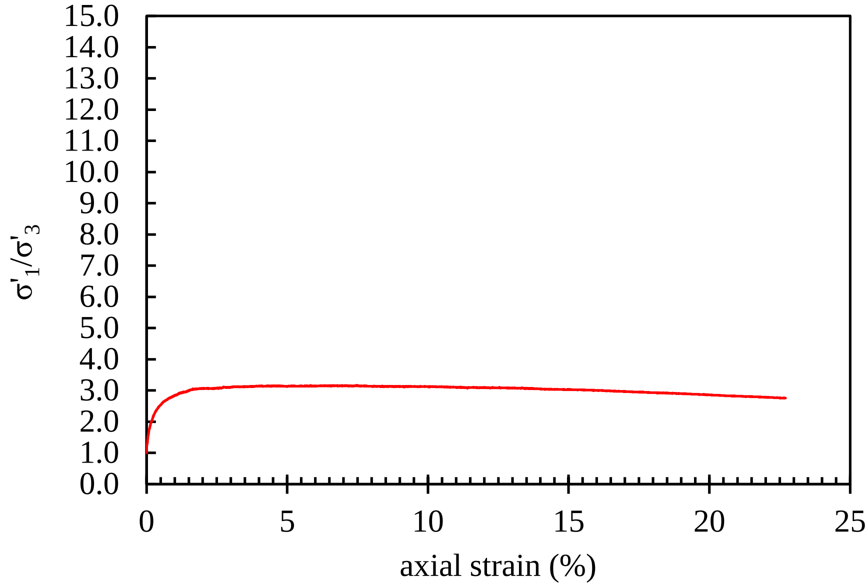

Figure A.12 : 95 % Sile Sand 50/55 + 5% TT Silt.

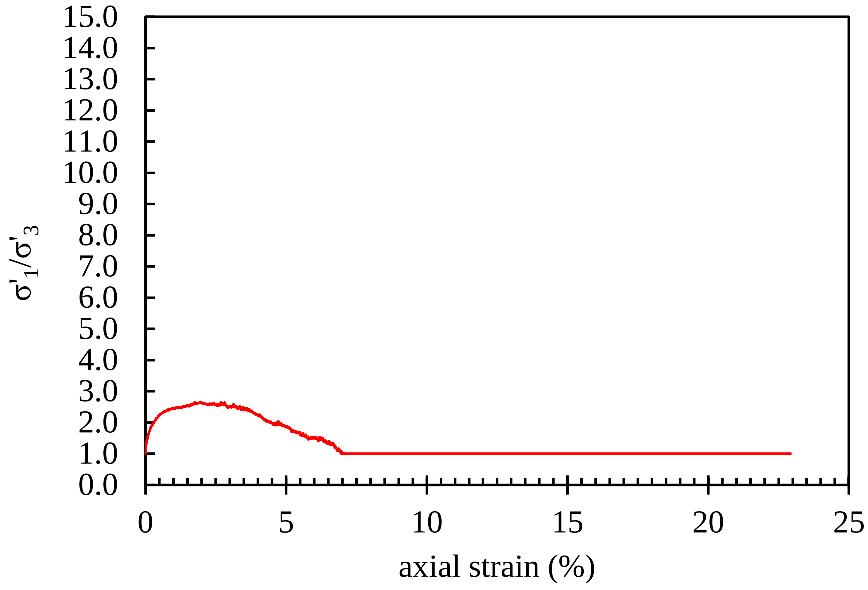

Figure A.13 : 85 % Sile Sand 50/55 + 15% TT Silt.

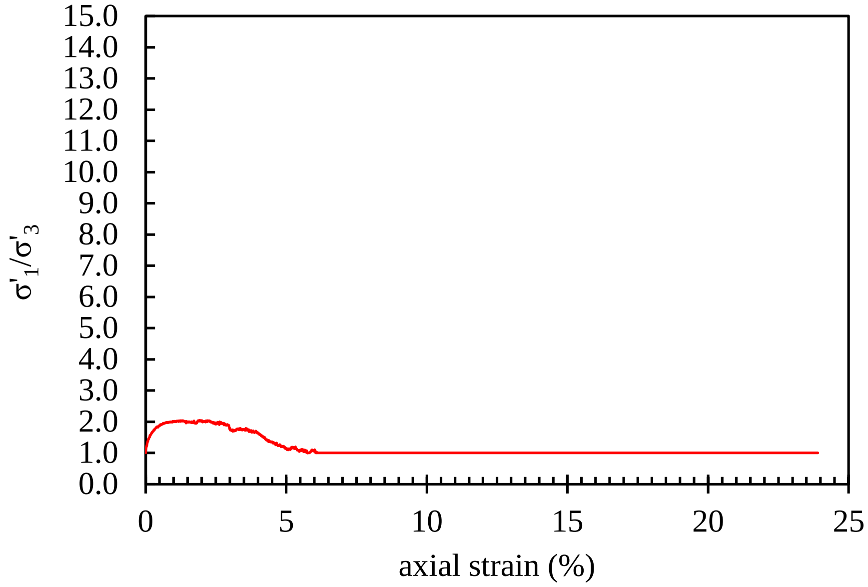

Figure A.14 : 75 % Sile Sand 50/55 + 25% TT Silt.

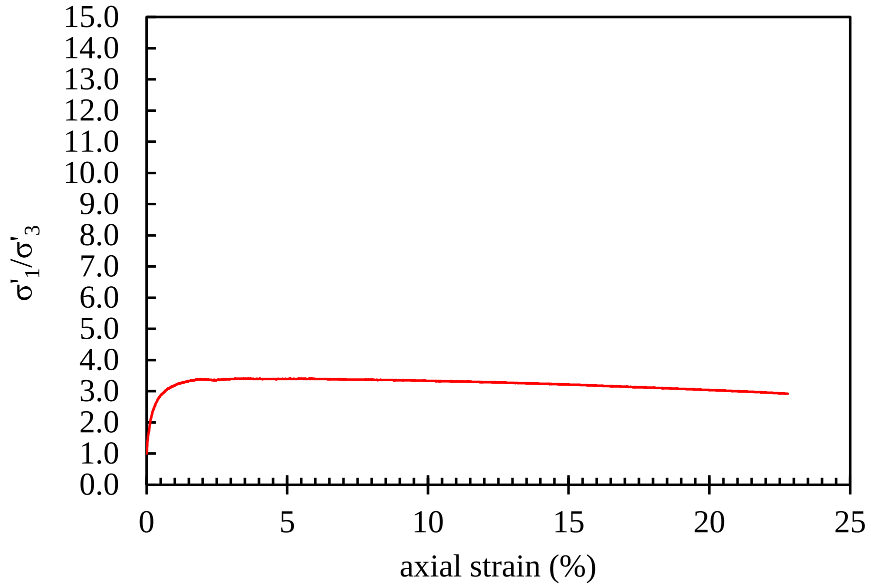

Figure A.15 : 95 % Sile Sand 50/55 + 5% SI Silt.

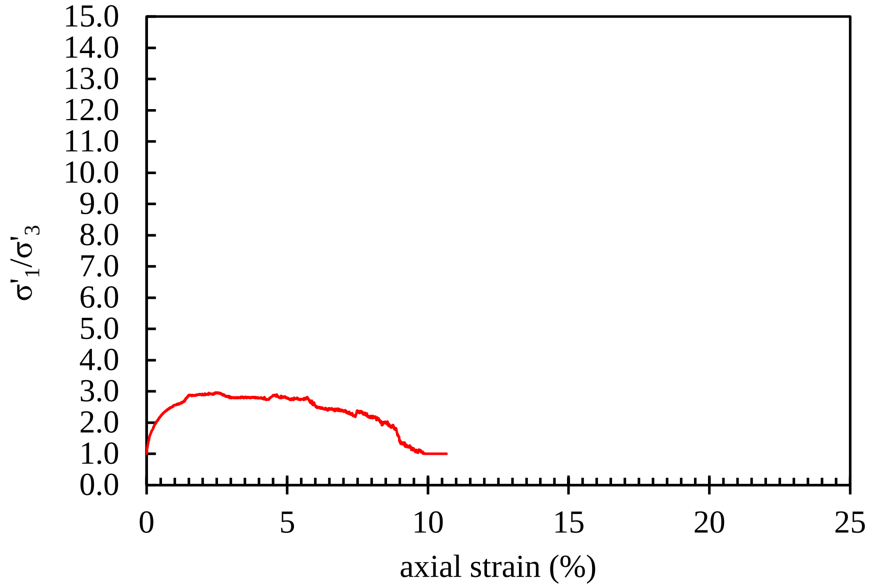

Figure A.16 : 85 % Sile Sand 50/55 + 15% SI Silt.

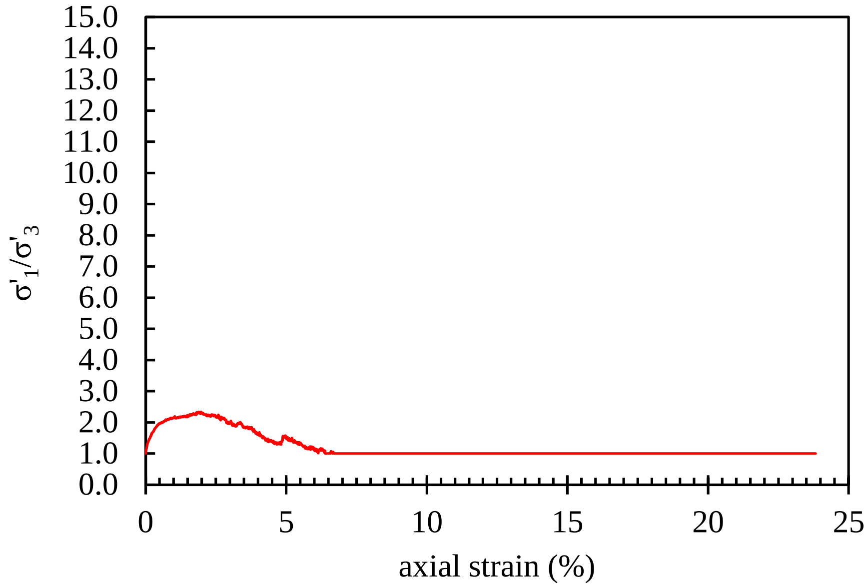

Figure A.17 : 75 % Sile Sand 50/55 + 25% SI Silt.

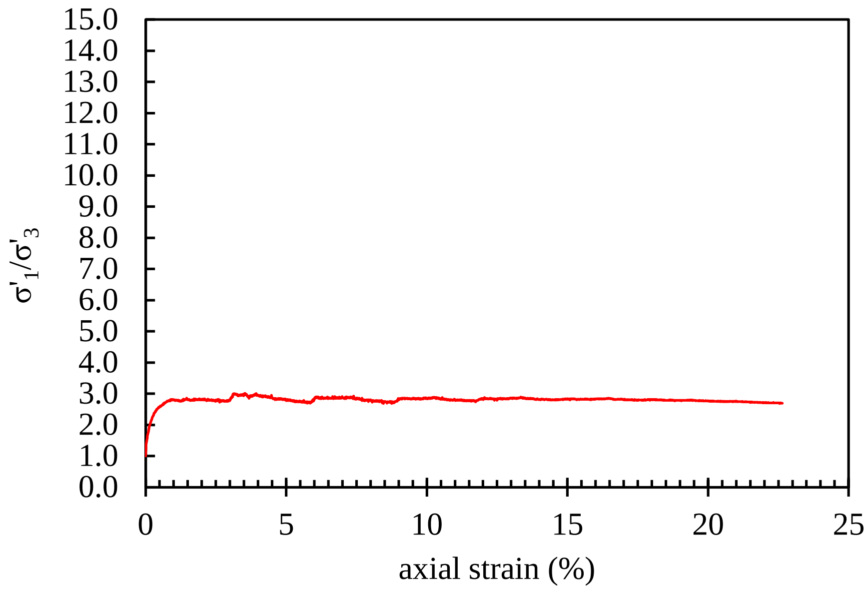

Figure A.18 : 95 % Sile Sand 50/55 + 5% IZ Silt.

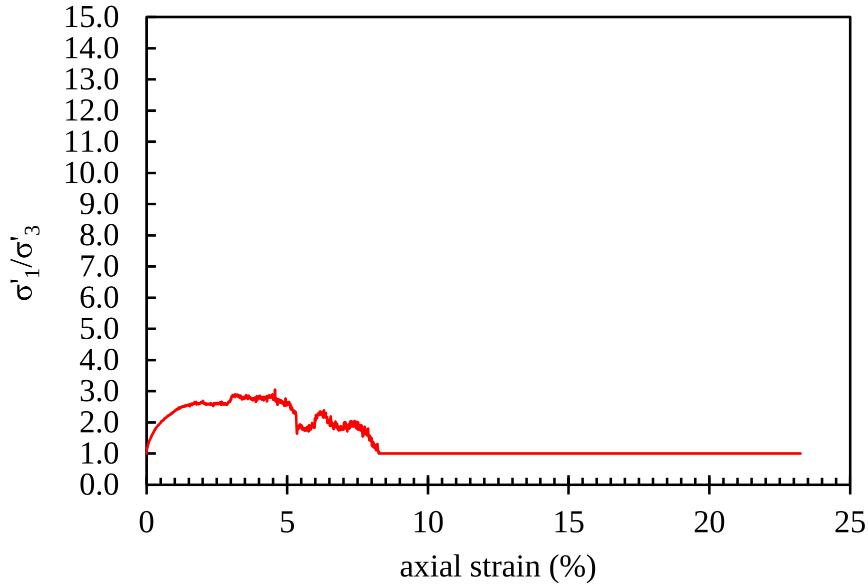

Figure A.19 : 85 % Sile Sand 50/55 + 15% IZ Silt.

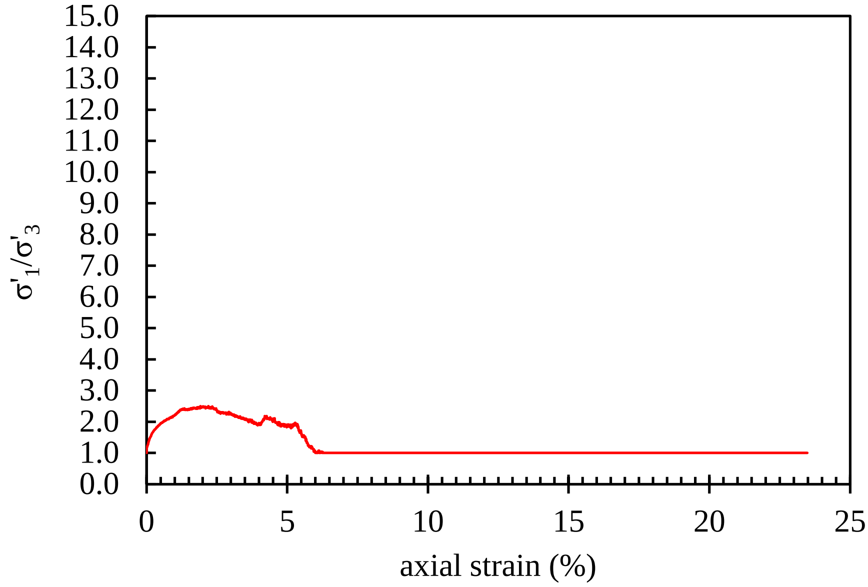

Figure A.20 : 75 % Sile Sand 50/55 + 25% IZ Silt.

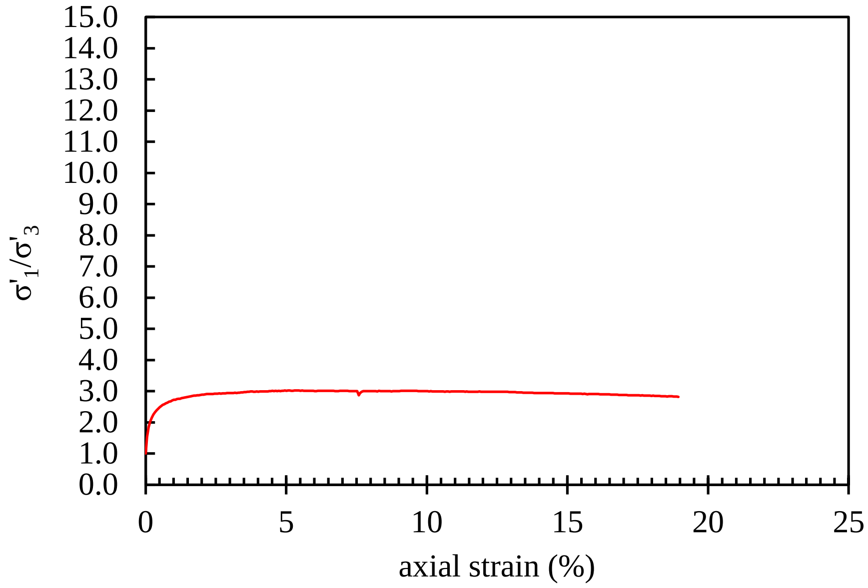

Figure A.21 : Sile Sand 80/100.

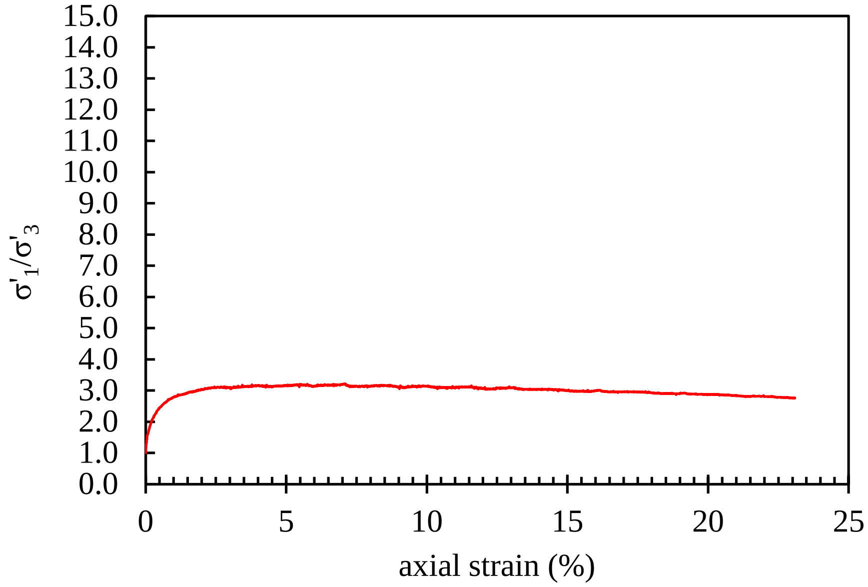

Figure A.22 : 95 % Sile Sand 50/55 + 5% TT Silt.

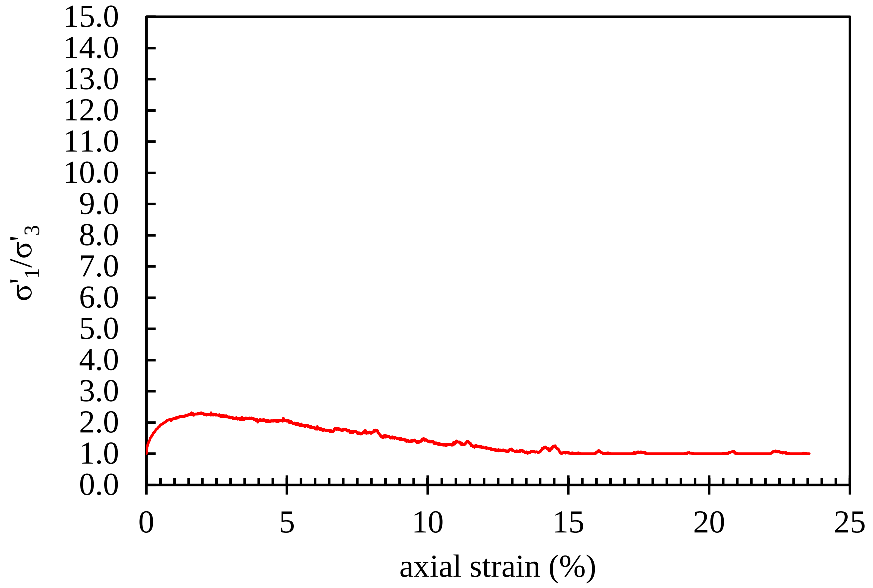

Figure A.23 : 85 % Sile Sand 50/55 + 15% TT Silt.

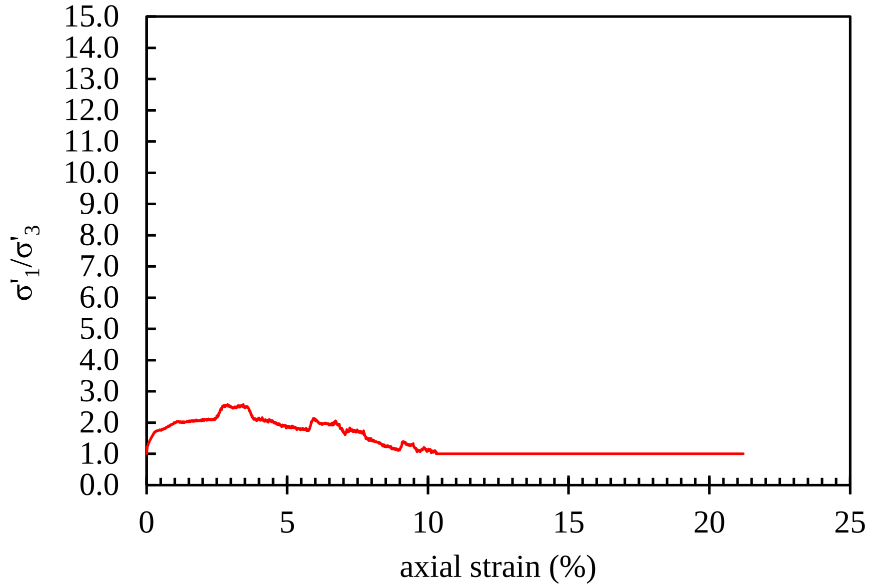

Figure A.24 : 75 % Sile Sand 50/55 + 25% TT Silt.

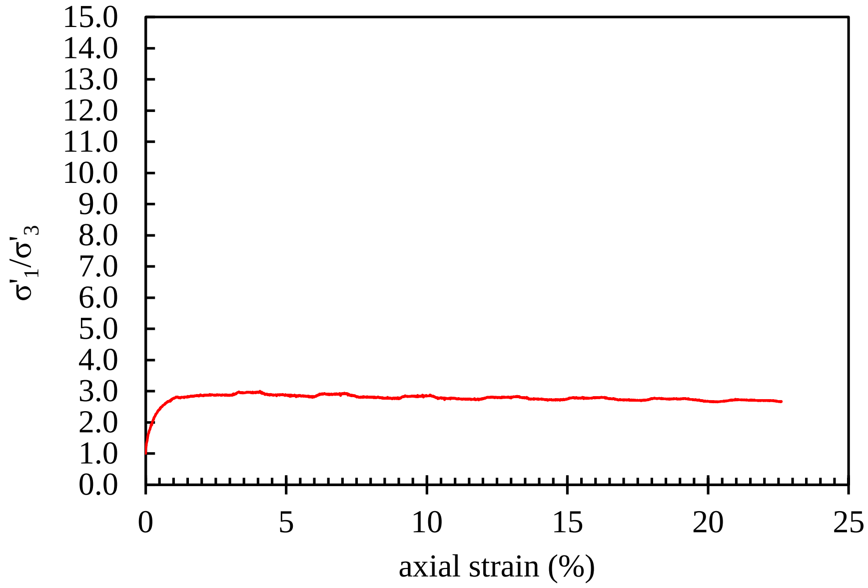

Figure A.25 : 95 % Sile Sand 50/55 + 5% SI Silt.

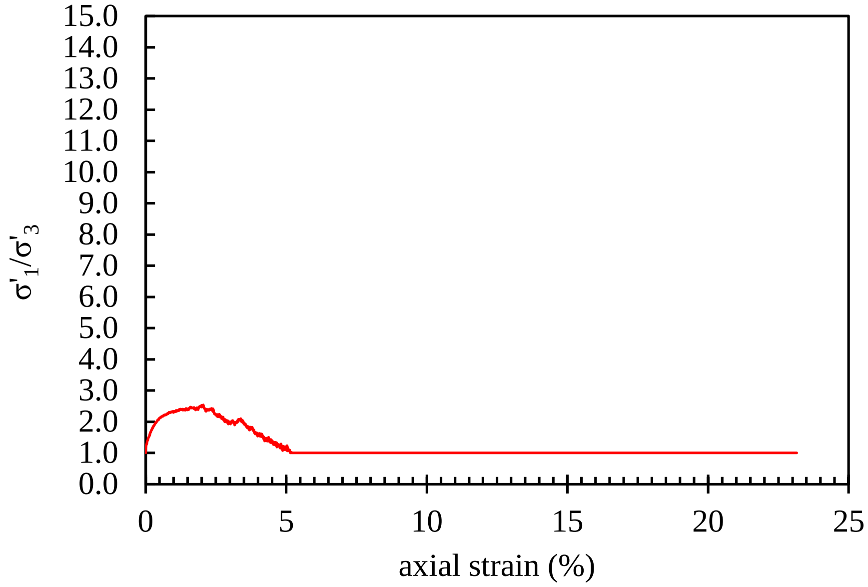

Figure A.26 : 85 % Sile Sand 50/55 + 15% SI Silt.

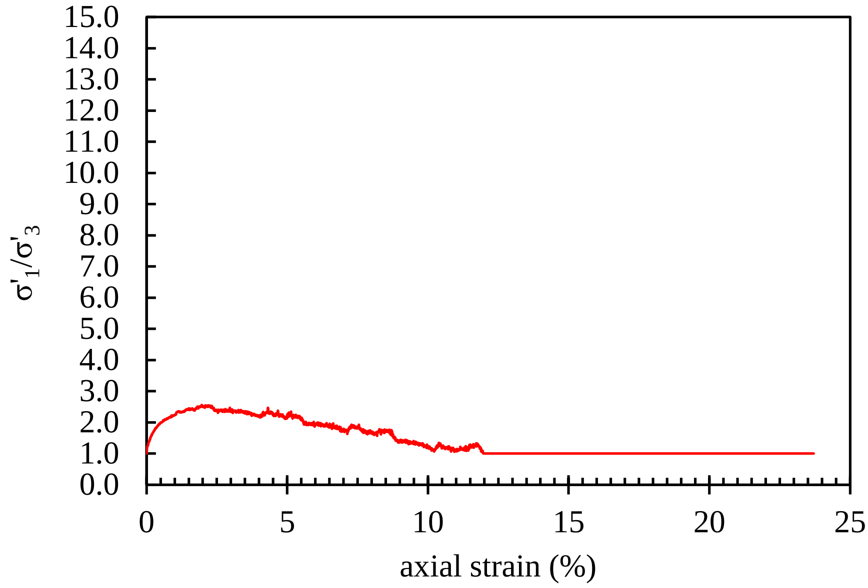

Figure A.27 : 75 % Sile Sand 50/55 + 25% SI Silt.

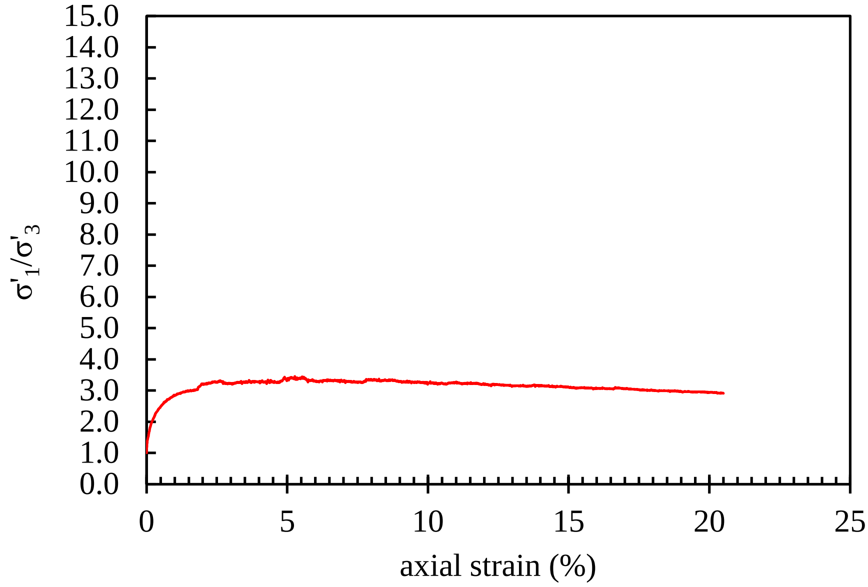

Figure A.28 : 95 % Sile Sand 50/55 + 5% IZ Silt.

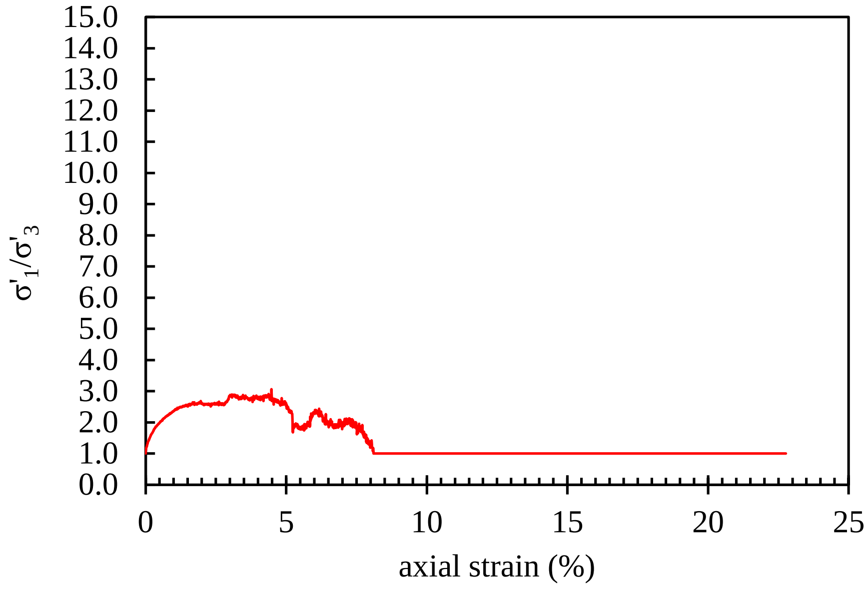

Figure A.29 : 85 % Sile Sand 50/55 + 15% IZ Silt.

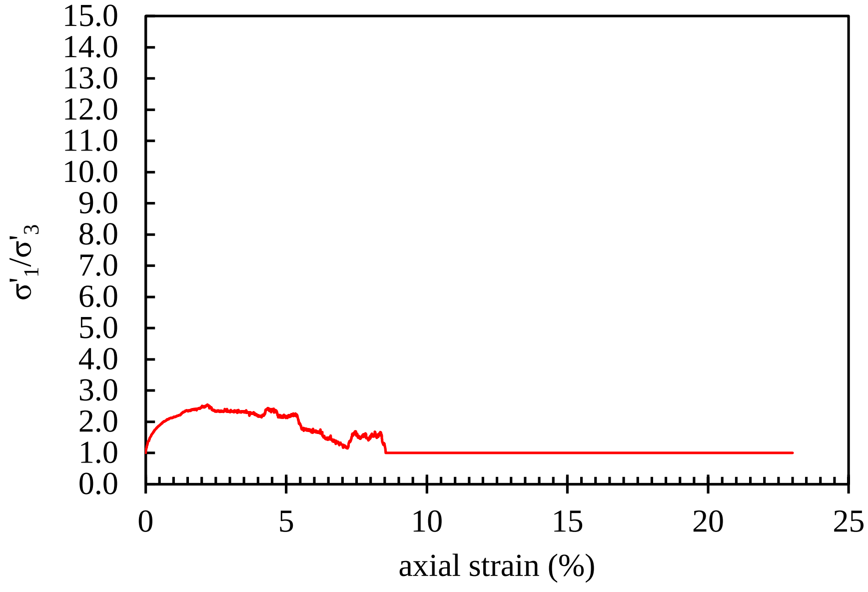

Figure A.30 : 75 % Sile Sand 50/55 + 25% IZ Silt.

CURRICULUM VITAE

Name Surname : Ehsan ETMINAN

Place and Date of Birth : URMIA/ 24, November, 1984

E-Mail : etminan2002@itu.edu.tr

etminan2002@yahoo.com

EDUCATION :

- **B.Sc.** : 2009, Urmia University, Civil Engineering
- **M.Sc.** : 2012, ITU, Soil Mechanics and Geotechnical Eng.

PUBLICATIONS, PRESENTATIONS AND PATENTS ON THE THESIS:

- Monkul, M.M., **Etminan, E.**, Senol, A. (2016). "Influence of Coefficient of Uniformity and Base Sand Gradation on Static Liquefaction of Loose Sands with Silt", Soil Dynamics and Earthquake Engineering, Vol. 86, 185-197. SCI.
- Monkul, M.M., Lade, P.V., **Etminan, E.,** Senol, A. (2014). "Compressibility as an indicator of liquefaction potential", Geotechnical Engineering Journal of SEAGS-AGSSEA, 45 (4), 73-77.
- Monkul, M.M., **Etminan, E.,** Senol, A. (2016) "Coupled Influence of Content, Gradation and Shape Characteristics of Silts on Static Liquefaction of Loose Sands with Silt'' (Under Review).
- **Etminan, E.,** Monkul, M.M., Senol, A. (2015). "Silt influence on static liquefaction of sands". Proceedings of the XVI European Conference on Soil Mechanics and Geotechnical Engineering, Edinburgh, U.K.; DOI:10.1680/ecsmge.60678; ISBN 978-0-7277-6067-8.
- Monkul, M.M., **Etminan, E.,** Senol, A., Lade, P.V. (2014). "Statik Yükleme Etkisinde Sıvılaşma ve Hacimsel Sıkışma Katsayısı". ZM 15: Zemin Mekaniği ve Temel Mühendisliği 15. Ulusal Kongresi, ZM15, ODTÜ, Ankara, Türkiye, syf. 215-222.